



2807712953

ROYAL FREE THESIS 1994

MEMBRANE CURRENTS OF CULTURED RAT  
NEOSTRIATAL NEURONES.

Andrew J. Doyle.  
September, 1993.

Academic Supervisor: Dr. C.D. Richards.

Head of Department: Prof. K.M. Spyer.

Physiology Department, The Royal Free Hospital  
School of Medicine, Rowland Hill Street,  
London NW3 2PF.

Industrial Supervisor: Dr. C.M. Stubbs.

Glaxo Group Research, Park Road, Ware, Herts.

This thesis has been submitted for the award of Ph.D.  
from the University of London, Science Faculty.

MEDICAL LIBRARY,  
ROYAL FREE HOSPITAL  
HAMPSTEAD.

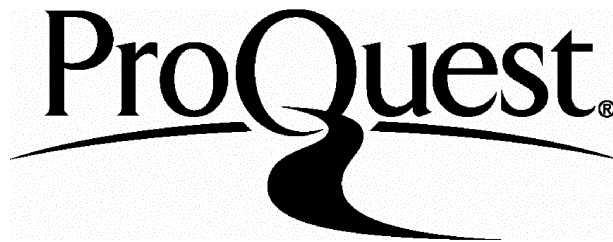
ProQuest Number: U555318

All rights reserved

INFORMATION TO ALL USERS

The quality of this reproduction is dependent upon the quality of the copy submitted.

In the unlikely event that the author did not send a complete manuscript and there are missing pages, these will be noted. Also, if material had to be removed, a note will indicate the deletion.



ProQuest U555318

Published by ProQuest LLC(2016). Copyright of the Dissertation is held by the Author.

All rights reserved.

This work is protected against unauthorized copying under Title 17, United States Code.  
Microform Edition © ProQuest LLC.

ProQuest LLC  
789 East Eisenhower Parkway  
P.O. Box 1346  
Ann Arbor, MI 48106-1346



## ABSTRACT.

This thesis describes an electrophysiological study of cultured neurones from the rat neostriatum using the patch clamp technique. The aims of the study were to investigate the voltage-activated currents which play a role in determining the activity patterns of these neurones and to examine individual  $K^+$  channels responsible for the resting conductance.

The neurones displayed highly negative resting membrane potentials ( $\approx -90$  mV) and a "leak" conductance which showed inward rectification. They expressed an assortment of voltage-activated macroscopic currents. Transient outward currents, which activated rapidly on depolarization, were especially prominent. Such currents were progressively inactivated by sub-threshold depolarization.

The three most prevalent potassium-conductive channels in these neurones have been identified and partially characterized. Comparable channels were observed in cell-attached and outside-out configurations. In cell-attached patches, small and intermediate conductance channels (27 pS and 130 pS in symmetrical 140 mM  $K^+$ ) were active over a wide range of potentials including the resting membrane potential. Large conductance "maxi" channels (200-275 pS) were also present and were strongly activated by depolarization.

Maxi channel activity varied considerably from patch to patch, sometimes being appreciable at the resting potential. Activity could often be permanently elevated by depolarization. Such a "priming" effect on maxi channel activity has not previously been reported.

The novel small and intermediate channels were considerably active at the resting potential. It has been estimated that each channel type would contribute, on average, 2-3 nS to the resting conductance under physiological conditions. The resting input conductance measured in whole cell experiments was of a similar order of magnitude (mean  $\approx$  3 nS). Thus, these channels could account for the bulk of the resting conductance.

The possible roles of the whole cell and single channel  $K^+$  currents recorded in this study, and the consequences of their activation with regard to cell excitability are discussed.

<b>CONTENTS:</b>	<u>Page</u>
i. ABSTRACT.	2
ii. CONTENTS.	4
iii. LIST OF FIGURES.	8
iv. LIST OF TABLES.	9
v. ABBREVIATIONS AND SYMBOLS.	10
vi. ACKNOWLEDGEMENTS.	13

Part I. INTRODUCTION

Section 1. Introduction.	14
1.1. Aims and rationale.	14
1.2. Intercellular communication in the nervous system.	15
1.2.1. Resting potential.	15
1.2.2. Action potentials.	16
1.2.3. Neural networks.	16
1.2.4. Somatic and dendritic conductances.	17
1.2.4.1. Calcium conductances.	17
1.2.4.2. Macroscopic potassium conductances in vertebrate central neurones.	18
1.2.4.2.1. Delayed rectifiers.	19
1.2.4.2.2. Calcium-activated K <sup>+</sup> currents.	19
1.2.4.2.3. Transient K <sup>+</sup> currents.	20
1.2.4.2.4. The M-current.	21
1.2.4.2.5. Inwardly-rectifying currents.	22
1.2.4.2.6. Resting conductances.	23
1.3. The patch clamp technique.	23
1.4. Anatomy of the basal ganglia.	25
1.5. Cell culture.	27
1.6. Electrophysiological properties of neostriatal neurones.	29
1.6.1. Firing patterns of medium spiny output neurones.	29
1.6.2. Electrophysiological properties of giant aspiny neurones.	30
1.6.3. Neurotransmitters and neuromodulators.	31
1.6.3.1. Excitatory amino acids (EAAs).	31

1.6.3.2. Dopamine (DA).	32
1.6.3.3. Acetylcholine (ACh).	32
1.6.3.4. The significance of DA-ACh interactions.	33
1.6.3.5. Other transmitters/modulators.	34
1.6.3.6. Synaptic transmission vs. modulation.	35
1.6.4. Intrinsic membrane properties are responsible for the low level of spontaneous activity of medium spiny neurones.	36
1.6.4.1. Passive membrane properties.	36
1.6.4.2. Active currents contributing to the firing patterns of medium spiny neurones.	36
1.6.4.3. Whole cell currents revealed by voltage clamp studies.	37
1.7. Single channel investigations.	39
1.7.1. Ion channels: a brief description.	39
1.7.1.1. Conductance.	39
1.7.1.2. Ionic selectivity.	40
1.7.1.3. Gating.	40
1.7.1.4. Structure.	41
1.7.2. Types of potassium channel characterized at the single channel level.	43
1.7.2.1. Delayed rectifiers.	43
1.7.2.2. Calcium-activated K <sup>+</sup> channels.	44
1.7.2.3. Inward rectifiers.	45
1.7.2.4. ATP K <sup>+</sup> channels.	47
1.7.2.5. Agonist-activated K <sup>+</sup> channels.	48
1.7.2.6. Non-specific channels.	48
1.7.3. Individual potassium channels in neurones.	48
1.7.4. Dopamine-activated potassium channels.	50
1.7.5. Potassium channels active at the resting potential.	51

Part II. METHODS.

Section 2. Culture methods.	53
Section 3. Patch clamp methods.	54
3.1. Cells.	54

3.2. Electrodes.	55
3.3. Components of the patch clamp apparatus.	55
3.4. Seals.	56
3.5. Recording.	57
3.5.1. Cell-attached.	57
3.5.2. Whole cell.	57
3.5.3. Outside-out.	58
3.6. Perfusion.	59
Section 4. Analysis.	61
4.1. Whole cell currents.	61
4.2. Single channel currents.	61
4.3. Statistics.	63
 Part III. RESULTS.	
 Section 5. Culture results.	65
5.1. Development of the neurones.	65
5.2. Appearance of the neurones.	66
5.3. Suitability for patching.	67
Section 6. Whole cell patch clamp results.	73
6.1. Whole cell parameters.	73
6.2. Whole cell currents.	75
6.2.1. Inward and outward rectification.	76
6.2.2. Sodium current.	77
6.2.3. Voltage-dependent, sustained potassium current.	78
6.2.4. Voltage-dependent, transient potassium currents.	79
6.3. Instability of the recordings.	81
Section 7. Single channel patch clamp results.	95
7.1. Formation of seals.	95
7.2. Resolution and noise.	96
7.3. Appearance of the channels.	96
7.4. Cell-attached recordings.	96
7.5. Outside-out recordings.	98
7.6. A small conductance channel.	100
7.7. A large conductance "maxi" channel.	101
7.8. An intermediate conductance channel.	103
7.9. Channels active at RMP.	104

7.10. Other channels.	105
7.11. Dopamine and quinpirole.	105

Part IV. DISCUSSION AND CONCLUSIONS.

Section 8. Discussion.	116
8.1. Suitability of the protocol.	116
8.1.1. Culture.	116
8.1.2. Electrophysiology.	117
8.2. Resting potential and whole cell capacitance.	118
8.3. Inward rectification and input resistance.	120
8.4. Whole cell currents.	121
8.4.1. Types of current.	121
8.4.2. Comparison with the currents recorded by others.	122
8.4.3. Summary of whole cell current properties.	125
8.5. Single channel currents.	126
8.5.1. Selectivity.	126
8.5.2. Maxi channel properties.	129
8.5.2.1. Conductance and selectivity.	129
8.5.2.2. Activity.	130
8.5.2.3. What could account for different activity levels?	130
8.5.2.4. Priming.	131
8.5.2.5. Functions.	131
8.5.3. Properties of the small and intermediate channels.	133
8.5.3.1. Description.	133
8.5.3.2. Comparison with other channels.	134
8.5.4. Resting channels.	135
8.6. What phenotype do cultured neurones express?	138
8.7. Actions of ACh and DA on neuronal currents.	139
8.8. Differences between the results of the present study and those of Freedman & Weight (1988 & 1989).	140
8.9. Questions.	141
Section 9. Conclusions.	141

Part V. REFERENCES.	144
---------------------	-----

## LIST OF FIGURES.

<u>Figure</u>	<u>Page</u>
5.1. Photographs: neostriatal cells in culture (day 1).	68
5.2. Photographs: neostriatal cells (day 7).	69
5.3. Photographs: neostriatal cells (day 11).	70
5.4. Photographs: neostriatal cells (day 14).	71
5.5. Photographs: "mature" neurones & glia in culture.	72
6.1. Distribution of resting potentials.	83
6.2. Whole cell currents: steps from resting potential.	84
6.3. Inwardly rectifying currents in symmetrical [K <sup>+</sup> ].	85
6.4. Sodium currents.	86
6.5. Sustained outward currents.	87
6.6. The effects of TEA on voltage-activated and leak currents.	88
6.7. Varying degrees of transient outward current in different cells.	89
6.8. Inactivation of the transient outward current.	90
6.9. Different activation and inactivation parameters for transient outward currents in different cells.	91
6.10. A component of outward current which is refractory to re-activation.	92
6.11. Blockade of transient outward currents by 4-AP.	93
6.12. Deterioration of resting potential and whole cell currents with time.	94
7.1. Single channels active at the resting potential.	106
7.2. Small and maxi channels in cell-attached patches.	107
7.3. Small and maxi channels in O/O patches.	108
7.4. Some properties of the small channels.	109
7.5. Openings and closures of a small channel.	110
7.6. Voltage-dependent activity of the maxi channel.	111
7.7. Priming and mode-switching of the maxi channel.	112
7.8. Some properties of an intermediate channel.	113
7.9. Activity of the intermediate channel.	114
7.10. Intermediate channels exhibiting low and high activity levels.	115

## LIST OF TABLES.

<u>Table</u>	<u>Page</u>
3.1. Composition of the recording solutions.	60
6.1. Whole cell parameters.	74
6.2. Conductances at the beginning and end of an experiment.	82
8.1. Comparison of striatal neurone sodium currents in different studies.	123
8.2. Characteristics of the small and intermediate channels.	133

## ABBREVIATIONS AND SYMBOLS.

ANGII	- angiotensin II
ACh	- acetylcholine
aCSF	- artificial cerebro-spinal fluid
A-D	- analogue to digital (converter)
AHP	- afterhyperpolarization
4-AP	- 4-aminopyridine
Ba <sup>2+</sup>	- barium ion
BK	- big (maxi) K <sup>+</sup> channel
cAMP	- cyclic adenosine monophosphate
CED	- Cambridge Electronic Design
Cs <sup>+</sup>	- caesium ion
D <sub>1</sub>	- dopamine receptor D <sub>1</sub> -subtype
D <sub>2</sub>	- dopamine receptor D <sub>2</sub> -subtype
DA	- dopamine
D-A	- digital to analogue (converter)
DAT	- digital audio tape
DMEM	- Dulbecco's modified Eagle medium
DNA	- deoxyribonucleic acid
DRG	- dorsal root ganglion (sensory) neurone
EAA	- excitatory amino acid (glutamate etc.)
EGTA	- ethylene glycol-O,O'-bis(2-aminoethyl)-N,N,N',N'-tetraacetic acid
E <sub>K</sub>	- reversal potential for K <sup>+</sup> ions
E <sub>Na</sub>	- reversal potential for Na <sup>+</sup> ions
EPSP	- excitatory post-synaptic potential
f	- frequency
F	- Faraday's constant (96500 C.mol <sup>-1</sup> )
G	- conductance
GABA	- Γ-aminobutyric acid
GH <sub>3</sub>	- pituitary cell line
G-H-K	- Goldman-Hodgkin-Katz (current equation)
GTP	- guanosine triphosphate
G <sub>sc</sub>	- single channel conductance
HEPES	- N-2-hydroxyethylpiperazine-N'-2-ethanesulfonic acid

5-HT	- 5-hydroxytryptamine (serotonin)
HVA	- high-voltage-activated (transient K <sup>+</sup> current)
IPSP	- inhibitory post-synaptic potential
i	- unitary current amplitude
I	- current
I	- mean patch current
I <sub>A</sub>	- A-current
I <sub>D</sub>	- D-current
I <sub>H</sub> or I <sub>Q</sub>	- slow inwardly rectifying mixed current
I <sub>M</sub>	- M-current
I <sub>Na</sub>	- sodium current
I-V	- current-voltage (relationship)
K <sup>+</sup>	- potassium ion
K <sub>IR</sub>	- rapid inwardly rectifying potassium current
K <sub>S</sub>	- sustained potassium current
K <sub>t</sub>	- transient potassium current
L-DOPA	- L-dihydroxyphenylalanine
Leu	- leucine
LHRH	- luteinizing hormone releasing hormone
LVA	- low-voltage-activated (transient K <sup>+</sup> current)
n	- sample size
N	- number of channels in a patch
NA	- noradrenaline
NMDA	- N-methyl-D-aspartate
N.P <sub>o</sub>	- open probability (of a patch)
N <sub>TOT</sub>	- number of channels per cell
O/O	- outside-out (patch)
P <sub>2</sub>	- subtype of purinoceptor
P <sub>o</sub>	- open probability (of a channel)
P <sub>open</sub>	- open probability (of a channel)
P <sub>x</sub>	- permeability to x
R	- universal gas constant (8.314 J.mol <sup>-1</sup> .K <sup>-1</sup> )
RMP	- resting membrane potential
r.p.m.	- revolutions per minute
SK	- small K <sup>+</sup> channel
SEM	- standard error (of the means)
T	- absolute temperature (K)

- $\tau$  - time constant ( $\tau$ ) for an exponential function
  - TEA - tetraethylammonium ion
  - TTX - tetrodotoxin
  - V - voltage/potential
  - z - gating charge valency or slope factor (in the Boltzmann equation)
- 
- [x] - concentration of x
  - [x]<sub>in</sub> - concentration of x inside a cell
  - [x]<sub>out</sub> - concentration of x outside a cell

## **ACKNOWLEDGEMENTS.**

I gratefully acknowledge the assistance of the SERC and my industrial sponsors, Glaxo Group Research. I am indebted to all my colleagues at the Royal Free who have helped me during my time in London. I would particularly like to thank Ken Wann and Brian Amos for their friendship and support. You have been great fun to work with, guys!

## **Part I. INTRODUCTION.**

### **Section 1. Introduction.**

#### **1.1. Aims and rationale.**

The neostriatum is a constituent of the basal ganglia, which are a group of sub-cortical nuclei involved in the control of movement. Basal ganglia disease is common and gives rise to motor disorders such as Parkinsonism and Huntington's chorea. Considerable research has been directed towards understanding the pathologies which underly these debilitating and distressing conditions. Knowledge of the normal functioning of the basal ganglia is the starting point for the rational development of successful therapies. Much is known about the anatomy of the basal ganglia, their connections with related structures and the transmitters involved in communication between the different elements. There is also considerable information regarding the electrophysiological properties of individual neurones in various basal ganglia regions. However, there are still many aspects of neuronal behaviour that remain to be elucidated.

The aim of the present study was to investigate the membrane properties which determine the excitability of neurones in the neostriatum. The patch clamp technique was used to measure whole cell and single channel currents in cultured neostriatal neurones. The initial part of the study was directed towards examining the whole cell currents in this preparation to ascertain which voltage-activated currents are expressed by neostriatal neurones in culture. The primary objective of the study was to identify and characterize individual potassium channels. Particular attention was paid to those active at the resting membrane potential which would contribute to the resting conductance and therefore be important in determining the degree of neuronal polarization.

## **1.2. Intercellular communication in the nervous system.**

Elements of the nervous system communicate electrically via chemical synapses. Most cells are polarized. In excitable cells changes in the degree of membrane polarization serve as a signalling mechanism.

### **1.2.1. Resting potential.**

Healthy neurones are polarized at rest. The resting membrane potential is negative i.e. the inside of the cell is negatively charged with respect to the outside. The magnitude of the resting potential varies between neuronal types.

Potentials differences arise because of the existence of ionic gradients across the cell membrane and the differential permeability of the membrane to various ions. The permeability of the membrane is due to the presence of channels which conduct different ionic species. Cells have a high concentration of potassium ions and a low concentration of sodium ions intracellularly. Extracellularly, the situation is reversed. The cell membrane is selectively permeable to potassium at rest (Bernstein, 1902 & 1912). The high ratio of potassium to sodium permeability dictates that the resting potential is close to the negative equilibrium potential for potassium ( $E_K \approx -97$  mV at body temperature) rather than the positive equilibrium potential for sodium ( $E_{Na} \approx +75$  mV at body temperature). During an action potential, the membrane briefly becomes more permeable to sodium than potassium and the membrane potential approaches that of the sodium equilibrium potential. (Nernst, 1888; Goldman, 1943; Hodgkin & Katz, 1949)

### **1.2.2. Action potentials.**

An action potential is an "all or nothing", stereotyped sequence of changes in membrane potential which is activated by a supra-threshold depolarization. Such a depolarization is normally caused in the somatic membrane of central neurones by the temporal and spatial summation of excitatory synaptic potentials. Action potentials are initiated in the axon hillock and are transmitted forward along the axon. The neuronal action potential consists of a regenerative increase in sodium conductance which results in depolarization, followed by a delayed increase in potassium conductance in conjunction with a delayed decrease in the sodium conductance which together cause membrane repolarization. Action potentials elicit other action potentials downstream by local current flow which causes sufficient depolarization to exceed threshold (Hermann, 1872; Hodgkin, 1937). Action potentials are not elicited upstream because the membrane is temporarily refractory to action potential generation. Thus, the action potential is propagated without decrement to the axon terminals. (Hodgkin and Katz, 1949; Hodgkin & Huxley, 1952).

### **1.2.3. Neural networks.**

Neurones influence their target cells (e.g. other neurones) by sending trains of action potentials down their branching axons. Action potentials invading axon terminals initiate the release of transmitter molecules which traverse the synapses and act upon post-synaptic cells.

Each neurone receives excitatory and inhibitory inputs from many sources and sends outputs to a multitude of other neurones. Such massive convergence and divergence gives rise to complicated networks. The pattern of action potential firing in a particular neurone depends on the integration of excitatory and inhibitory inputs. The firing pattern of that neurone in turn influences

the excitability changes of its targets by the release of excitatory or inhibitory transmitters.

#### **1.2.4. Somatic and dendritic conductances.**

Somatic and dendritic membranes possess a wider variety of conductances than those of axons. This reflects the fact that they are involved in the integration of synaptic inputs as well as the generation of action potentials. Like axons, they possess resting potassium conductances, and sodium and potassium conductances responsible for action potential generation. Calcium conductances and a diverse range of additional potassium conductances are also present.

##### **1.2.4.1. Calcium conductances.**

Extracellular calcium concentration is in the low millimolar range and intracellular calcium is buffered to nanomolar levels. This means that there is an even larger trans-membrane electrochemical gradient for calcium than for sodium. Voltage-activated calcium channels are opened by depolarization, resulting in further depolarization. L-type calcium channels inactivate slowly and incompletely; their activation results in sustained calcium influx. T-type and N-type channels are rapidly inactivating. The consequences of  $\text{Ca}^{2+}$  influx are two-fold. Firstly, calcium channel activation can give rise to prolonged action potentials or depolarizing plateaux. Secondly, calcium influx provides a coupling mechanism between electrical signals and intracellular events. Numerous enzymes and proteins effecting intracellular or membrane-bound processes are regulated by calcium, their activity being highly sensitive to the prevailing intracellular calcium concentration. Important  $\text{K}^+$  conductances are also activated by increases in intracellular  $[\text{Ca}^{2+}]$ .

#### **1.2.4.2. Macroscopic potassium conductances in vertebrate central neurones.**

Halliwell (1990) reviewed the types of potassium conductances that have been demonstrated in central neurones. The diversity of potassium currents that can be recorded in voltage-clamp experiments reflects the variety of functions that these conductances subserve. Potassium currents fall into the following categories: voltage-dependent, calcium-dependent, agonist-dependent and leak or resting currents. Some voltage-dependent currents are also  $\text{Ca}^{2+}$ - or agonist-sensitive. In general,  $\text{K}^+$  currents act to restrain the excitatory influence of  $\text{Na}^+$  and  $\text{Ca}^{2+}$  currents.

The functions of  $\text{K}^+$  currents are manifold. They are involved in repolarization of action potentials; various  $\text{K}^+$  currents help determine their shape and duration. The propensity of a neurone to fire is also controlled by  $\text{K}^+$  currents. The nature of the firing depends upon the interplay between different currents responsible for AHPs and inter-spike ramps. Certain  $\text{K}^+$  currents play a role in synaptic integration whereas others define the resting membrane potential. A subset of  $\text{K}^+$  currents mediates the excitability changes caused by agonists.

#### **1.2.4.2.1. Delayed rectifiers.**

Delayed rectifier potassium channels were described in giant axons of the squid, *Loligo*, by Hodgkin and Huxley (1952). These channels contribute to the repolarization phase of an action potential. As the name suggests, they are activated after some delay by depolarization and give the impression that the membrane passes outward current more easily than inward current. Classical delayed rectifier currents are sensitive to TEA and relatively insensitive to 4-AP. Their activation threshold is similar to that of the fast sodium current and they remain activated throughout the duration of a suprathreshold depolarizing step.

The role of Hodgkin & Huxley-type delayed rectifiers in vertebrate central neurones is less clear. Their activation is too slow to be able to account for action potential repolarization. Activation of other channel types also gives rise to outward rectification.  $\text{Ca}^{2+}$ -activated  $\text{K}^+$  currents and rapidly-activating transient  $\text{K}^+$  currents are probably responsible for repolarization in vertebrate central neurones (Zbicz & Weight, 1985; Storm, 1987; Rudy, 1988; Halliwell, 1990).

#### **1.2.4.2.2. Calcium-activated $\text{K}^+$ currents.**

Potassium currents which are activated by calcium influx are known to exist. A fast,  $\text{Ca}^{2+}$ -dependent current is partly responsible for action potential repolarization in somatic and dendritic membranes. It is also voltage-dependent and sensitive to TEA and charybdotoxin. (Miller *et al*, 1985; Zbicz & Weight, 1985; Fox *et al*, 1987; Numann *et al*, 1987; Storm, 1987).

Neuronal AHPs can be blocked by inhibitors of calcium influx. Two distinct  $\text{Ca}^{2+}$ -dependent  $\text{K}^+$  currents are responsible for short-duration and longer-lasting AHPs. The first is voltage-dependent and TEA-sensitive; its role is thought to be

to limit calcium influx through voltage-activated channels by causing hyperpolarization and hence inactivation. The second is a voltage-independent, apamin-sensitive current which is responsible for spike accommodation. It is subject to modulation, being suppressed by numerous transmitters including acetylcholine, noradrenaline and dopamine. (Lang & Ritchie, 1988 & 1990; Halliwell, 1990).

#### 1.2.4.2.3. Transient $K^+$ currents.

The A-current (Hagiwara *et al*, 1961; Connor and Stevens, 1971; Neher, 1971) is expressed by a wide range of vertebrate neurones (see Rogawski, 1985). It is a transient potassium current which is rapidly activated by depolarization (threshold  $\approx -60$  mV) and decays with a time constant ( $\tau$ ) that is less than 100 ms. It is completely inactivated at membrane potentials positive to  $-40$  mV; inactivation is removed by hyperpolarization. The current is blocked by millimolar concentrations of 4-AP (Thompson, 1977) and nanomolar concentrations of dendrotoxin (Dolly *et al*, 1984; Halliwell *et al*, 1986).

Another rapidly-activating transient current, the D-current ( $I_D$ ) was first described in hippocampal neurones by Storm (1988). It has since been reported in other neuronal types. Its properties differ from that of  $I_A$  in a number of respects. It is characterized by a much slower decay ( $\tau > 1$  s). Its activation threshold ( $\approx -75$  mV) and threshold for relief of inactivation ( $\approx -55$  mV) are more negative than those of  $I_A$ . It is more sensitive to blockade by 4-AP ( $K_i \approx 30 \mu M$ ).  $I_D$  also remains inactivated for much longer (time constant  $\approx 5$  s) than  $I_A$ .

An important role of rapidly-activating transient currents is the regulation of sub-threshold behaviour.  $I_A$  and  $I_D$  are activated at sub-threshold potentials and therefore act to delay or prevent the attainment of threshold. The amount of transient

outward current available to oppose depolarizing inputs will depend upon the level of current inactivation. This, in turn depends upon the degree of membrane polarization prior to the depolarizing input. Thus, the willingness of a neurone to fire will be determined by its voltage history.

Since the D-current remains inactivated for long periods of time following activation, successive excitatory inputs will cause progressively greater depolarizations. Thus, the D-current acts to effect temporal synaptic integration over a time scale of seconds. Repetitive sub-threshold depolarizations could therefore summate to initiate firing.

The availability of transient currents also controls the pattern of spike discharge (accommodation vs. repetitive firing) once it has been initiated. The inter-spike voltage trajectory will be steep if  $I_A$  and  $I_D$  are inactivated and shallow if they are not. The degree of inactivation will be influenced by the magnitude of the AHP. Transient currents themselves may contribute to fast AHPs.

Transient currents (particularly  $I_D$ ) are probably involved in spike repolarization since 4-AP causes spike broadening.

(Reviewed by Halliwell, 1990)

#### **1.2.4.2.4. The M-current.**

The M-current ( $I_M$ ) is a voltage-activated, non-inactivating current which is switched on at potentials positive to -60 mV. It acts to oppose steady depolarizing inputs and, because it activates and de-activates slowly, is responsible for accommodation of spike trains. It is suppressed by muscarinic agonists (Brown and Adams, 1980), luteinizing hormone-releasing hormone (LHRH) and angiotensin II (ANGII). Somatostatin enhances this current (Jacquin *et al*, 1988; Moore *et al*, 1988). Thus,

various transmitters can influence the sensitivity of neurones to afferent input and their accommodative behaviour via modulation of  $I_M$ .

(Reviewed by Brown, 1988; Halliwell, 1990)

#### 1.2.4.2.5. Inwardly-rectifying currents.

Some membranes rectify inwardly or "anomalously" (i.e. they pass current more readily in the inward direction, counter to the predictions of the constant field theory, Hodgkin & Katz, 1949). This property is advantageous in cells, such as those of heart muscle, which exhibit long depolarized plateau potentials. A surprisingly wide range of neurones also exhibit inward rectification. This property has been demonstrated in neurones from olfactory cortex (Constanti & Galvan, 1983), globus pallidus (Stanfield *et al*, 1985), locus coeruleus (Inoue *et al*, 1988), raphe nucleus (Williams *et al*, 1988), hippocampus (Halliwell & Adams, 1982), nucleus accumbens (Uchimura *et al*, 1989) and neostriatum (Calabresi *et al*, 1987a).

Two types of inwardly rectifying currents can be demonstrated. The first ( $K_{IR}$ ) is a relatively pure  $K^+$  current which activates rapidly at potentials negative to  $E_K$  and is blocked by internal  $Cs^+$  or external  $Ba^{2+}$ . The second ( $I_H$  or  $I_Q$ ) is a mixed  $Na^+$  and  $K^+$  current which activates slowly at negative potentials and reverses positive to  $E_K$ . It is distinguished from  $K_{IR}$  by its lack of sensitivity to  $Ba^{2+}$ . The function of inwardly rectifying currents in neurones is not entirely clear. It has been suggested that one role may be to limit the degree of hyperpolarization that can be caused by electrogenic pumps. Another suggestion is that the inwardly-rectifying conductances contribute to resting permeability and help determine RMP. This would seem to be borne out by the fact that both inward rectification and resting conductance are decreased in certain neurones by substance P (Stanfield *et al*, 1985).

#### **1.2.4.2.6. Resting conductances.**

Neurones and other excitable cells have negative resting potentials. Their membranes must, therefore, be selectively permeable to potassium. A component of the resting conductance can be modified by transmitters like acetylcholine (ACh), noradrenaline (NA) and 5-HT (5-hydroxytryptamine). (Halliwell, 1990). Astonishingly little is known about the channels responsible for this important conductance.

#### **1.3. The patch clamp technique.**

Patch clamp is an electrophysiological technique which can be used to record membrane currents arising from the opening and closure of single ion channels. The technique entails pressing the tip of a fire-polished glass microelectrode against the cell membrane to form a high resistance seal. The small patch of membrane enclosed by the pipette tip can then be voltage clamped. The high resistance of the seal ensures that most of the current passing through the patch flows into the pipette and can be measured by appropriate circuitry. (Neher and Sakmann, 1976; Neher *et al*, 1978; Horn and Patlak, 1980; Sigworth and Neher, 1980; Hamill and Sakmann, 1981; Hamill *et al*, 1981; Neher, 1981; Sakmann and Neher, 1983a).

Hamill *et al* (1981) described improvements to the technique which greatly enhanced its efficacy. They showed that seals could be improved (G $\Omega$ s rather than M $\Omega$ s) by applying gentle suction to the pipette. High resistance seals permit low noise recordings. Improved signal to noise ratio provided better resolution of channel openings. Single channel recordings can be performed in three different configurations; cell-attached, excised inside-out and excised outside out. In addition, the whole cell configuration can be used to record macroscopic currents flowing across the entire membrane. Tight seal whole cell recording has certain advantages compared with conventional

intracellular recording using sharp electrodes.

The simplest patch clamp configuration is the cell-attached configuration. After seal formation, currents are recorded in a patch of membrane which remains attached to the cell. The intracellular surface of the patch continues to be in contact with the normal intracellular environment and is therefore exposed to relatively "physiological" conditions.

By contrast, excised patch configurations are extremely useful because the solutions on both sides of a patch can be controlled by the experimenter and the reversal potential for the various ions can be specified. The inside-out configuration is achieved by pulling the electrode away from the cell whilst in cell-attached mode and tearing off the membrane patch, the seal between membrane and patch remaining intact. The solution bathing the exposed "intracellular" surface can be manipulated.

The whole cell configuration is attained from the cell-attached mode by applying further suction to rupture the patch of membrane at the electrode tip, creating a low resistance pathway between the electrode and cell interior. This allows the entire membrane to be clamped and current flow across it to be measured. Whole cell recording is advantageous since it usually inflicts less membrane damage than intracellular recording. It is also applicable to smaller cells than can be examined using conventional techniques. An additional advantage is that lower resistance recording electrodes can be used; 1-10 M $\Omega$  in the case of whole cell recording compared with in excess of 100 M $\Omega$  for conventional recording. This leads to less distortion and better voltage clamping. In whole cell recording, the intracellular contents are dialysed by the solution in the recording electrode. This can be an advantage or disadvantage. It means that the experimenter can alter the intracellular environment and assess the effects of this alteration on electrophysiological parameters. However, vital regulatory factors can also be "washed away" so that normal functioning is impaired.

The outside-out configuration can be attained from the whole cell configuration by withdrawing the electrode from the cell in much the same way as inside-out patches are formed from cell-attached ones. A patch of membrane detaches from the cell and re-seals, leaving the "extracellular" surface exposed. Drugs and transmitters can be applied to the medium bathing this surface.

In the present study, whole cell recording was used to investigate voltage-activated macroscopic currents. Single channel recordings were performed using high potassium solutions in the patch electrode. Cell-attached and outside-out configurations were employed to investigate potassium channels active at potentials, corresponding to the resting potential in intact cells.

#### **1.4. Anatomy of the basal ganglia.**

The basal ganglia consist of the substantia nigra, corpus striatum, and globus pallidus. Other brainstem structures and parts of the thalamus are closely associated. The corpus striatum in mammals has two major, functionally distinct divisions. The dorsal striatum includes the nucleus accumbens and parts of the olfactory tubercle. It has connections with the limbic system and is thought to be involved in emotional and motivational processes. The ventral striatum or neostriatum consists of the caudate nucleus and putamen which in the rat are combined. This part of the striatum has sensorimotor functions. (Groves, 1983; Stoof *et al*, 1992). The present study has been confined to neurones isolated predominantly from the ventral region.

The neostriatum has efferent connections with the corticospinal and reticulospinal motor systems. Its major output pathways are to the globus pallidus and substantia nigra (Freund *et al*, 1984; Walters *et al*, 1987). Impulses are transmitted through the corticospinal system via the globus pallidus to the

thalamus and motor cortex. The reticulospinal system is accessed via the globus pallidus, sub-thalamic nucleus and substantia nigra.

The most important afferent connections to the neostriatum come from the cerebral cortex, thalamus and substantia nigra. Inputs also arise from brainstem areas including the ventral tegmental area and midline raphe nucleus. (Example references: Lynch *et al*, 1973; Nauta *et al*, 1974; Robertson and Travers, 1975; Vandermaelen *et al*, 1978; Groves, 1983; Misgeld *et al*, 1984; Stoof *et al*, 1992). The nigro-striatal pathway is of particular clinical importance. Dopamine is the classical transmitter of this pathway. Decreased dopaminergic input to the striatum due to cell death in the substantia nigra is responsible for the movement disorder, Parkinsonism, which is characterized by hypokinesia, rigidity and tremor (Calne & Langston, 1984). Huntington's chorea results from degeneration of neurones within the neostriatum itself.

The neostriatum contains a diversity of neuronal types (see e.g. Bishop *et al*, 1982; Chang *et al*, 1982; Lehman & Langer, 1983). The majority (95%) are medium-sized with characteristically spiny dendrites. Medium spiny neurones are the projection neurones of the neostriatum, relaying directly to the globus pallidus and substantia nigra. They receive inputs from cortex, nigra and thalamus, and also from neostriatal interneurones. Medium spiny output neurones are GABAergic and inhibit their nigral and pallidal targets (Groves, 1983; Lehman & Langer, 1983). Because axon collaterals feed back to the neostriatum, activation of output neurones also results in recurrent inhibition (Park *et al*, 1980).

The remaining 5% are interneurones of various classes; some are GABAergic, some somatostatinergic and others cholinergic. Giant aspiny cholinergic interneurones are the most conspicuous by virtue of their size. They constitute 1-2% of the neuronal population and receive inputs from the same areas as medium spiny

neurones. Interaction between these neurones and the output neurones plays a crucial role in determining normal motor behaviour. (Reviewed by Lehman & Langer, 1983; Stoof *et al*, 1992).

### **1.5. Cell culture.**

*In vitro* preparations are suitable for electrophysiological studies. Stable recordings are much more difficult to obtain *in vivo* due to movement. *In vitro* preparations are useful because neurones can be studied in isolation. In addition, it is easy to specify the extracellular environment by manipulating the composition of the bathing solutions. Patch clamp studies have previously been performed using acutely isolated cells, cells maintained in long term culture or cells remaining within tissue slices.

The present study employed cultured neurones which have certain advantages. Neurones in culture possess clean membranes which are necessary for the formation of high resistance seals between patch electrode and cell. They adhere well to glass cover slips on which they are grown, which makes sealing easier and is essential if isolated patches are required. Cultured neurones of the appropriate age remain electrically compact and can be satisfactorily space clamped but have developed sufficient processes to permit identification. "In primary striatal cell culture, neurons do not appear to produce spines characteristic of those found in mature striatum...Nevertheless, striatal neurons in culture do exhibit differentiated morphologies and can be grouped into relatively distinct classes" (Surmeier *et al*, 1988b). These authors found that neurones could be easily distinguished from glial cells. Squamous glia grew across the glass slips on which they were plated to form a mat. Neurones and astroglia/microglia growing in spaces in the mat could be distinguished morphologically. Most neurones had ovoid cell bodies with one process emerging from either end. Triangular

neurones had three major processes. The cell bodies of astroglia or microglia were round or irregularly shaped; four or more processes emerged from different parts of the cell body and subdivided more proximally than neuronal processes.

The neurones were divided into four groups on the basis of the size and shape of the soma and nuclear position. Type I neurones with ovoid somata accounted for about 80% of the neurones in culture, whilst type II, triangular neurones accounted for nearly 20%. The authors suggested that both these neuronal types in culture correspond to medium spiny neurones *in vivo*. A disadvantage of using cultured neurones is that immature cells must be used; adult neurones do not survive in culture.

The advantage of an acutely dissociated preparation is that adult neurones can be used. However, identification of acutely isolated neurones is difficult since most processes are lost during the dissociation procedure. In addition, dissociation usually involves the use of proteolytic enzymes which may damage membrane constituents such as receptors or channels.

An advantage of patching in slices is that neurones remain in an environment closer to that encountered physiologically. One disadvantage is that patching is carried out "blind"; the neurones cannot be visualized before an experiment. Another disadvantage is that extensive dendritic arborization remains and the neurones cannot be voltage clamped in their entirety.

## **1.6. Electrophysiological properties of neostriatal neurones.**

There have been numerous electrophysiological investigations of neurones from the neostriatum. The majority have employed extracellular or intracellular recording techniques to measure membrane potential changes in response to various stimuli. Far fewer investigations have used voltage clamp techniques to directly observe membrane currents. Most is known about medium spiny neurones because they are so prevalent.

### **1.6.1. Firing patterns of medium spiny output neurones.**

*In vivo* studies in mammals have revealed that these neurones exhibit remarkably low levels of spontaneous activity, a phenomenon that Purpura and Malliani (1967) aptly described as "slothfulness". Three activity patterns were observed; occasional bursting, low level tonic firing or silence (Hull *et al*, 1970; Niki *et al*, 1972; De Long, 1972 & 1973; Sugimori *et al*, 1978; Wilson and Groves, 1981; Mercuri *et al*, 1985; Calabresi *et al*, 1987a, 1990a). According to Wilson and Groves (1981) medium spiny neurones *in vivo* are capable of encoding information both in terms of burst duration and firing frequency.

Many investigators have employed *in vitro* preparations. Intracellular recordings of neurones in neostriatal slices have revealed a total absence of spontaneous spiking, presumably due to the lack of tonic synaptic input (Cherubini *et al*, 1988; Calabresi *et al*, 1987a & 1990b). Neurones in slices can be induced to fire action potentials in a number of different ways. This can be achieved by direct depolarizing current injection, by electrical stimulation of excitatory afferents, by intra-striatal stimulation or by application of excitatory transmitters (e.g. Kita *et al*, 1984 & 1985a,b; Cherubini *et al*, 1988;argas *et al*, 1988 & 1989; Galarraga *et al*, 1989; Kawaguchi *et al*, 1989; Calabresi *et al* 1987a,b & 1990b).

Artificial stimulation of medium spiny neurones can be achieved directly or trans-synaptically. Trans-synaptic stimulation gives rise to a mixture of excitatory and inhibitory post synaptic potentials (EPSPs and IPSPs respectively). Summation of sufficient EPSPs results in action potential firing. The number and frequency of spikes elicited in the post-synaptic neurone depends on the frequency and intensity of the stimulus. (Frigyesi and Purpura, 1967; Purpura and Malliani, 1967; Hull et al, 1970a & b, 1973; Buchwald et al, 1973; Marco et al, 1973; Kitai et al, 1976; Kocsis and Kitai, 1977a & b; Sugimori et al, 1978).

Studies both *in vivo* and *in vitro* have shown that depolarizing current injection stimulates action potential firing to a degree which is dependent upon the magnitude of the current. Direct injection of a small current just sufficient to bring a neurone to threshold results in the firing of a single action potential which has a long latency and is followed by a short afterhyperpolarization (AHP). Injection of a larger current stimulates spiking at a rate which is linearly related to the intensity of the depolarizing current. Repetitive firing shows little or no accommodation and does not result in the generation of long-lasting hyperpolarizations. This is an interesting finding since it suggests that small conductance,  $Ca^{2+}$ -activated  $K^+$  channels may be absent from medium spiny neurones. (Galarraga et al, 1985 & 1989; Kita et al, 1985a; Calabresi et al, 1987a & b; Bargas et al, 1988 & 1989; Kawaguchi et al, 1989; Calabresi et al, 1990b).

#### **1.6.2. Electrophysiological properties of giant aspiny neurones (cholinergic interneurones).**

Bishop et al (1982) and Wilson et al (1990) recorded from identified giant aspiny cholinergic interneurones *in vivo*. These neurones were tonically active, firing slowly and irregularly. EPSPs were elicited by stimulation of afferents from cortex, thalamus and nigra. Depolarizing current injection stimulated

an initial increase in firing which rapidly accommodated. Repetitive firing could not be induced due to the presence of large, long-lasting AHPs. Thus, the electrophysiological properties of these neurones contrasted markedly with those of medium spiny neurones.

### **1.6.3. Neurotransmitters and neuromodulators.**

Medium spiny neurones are inherently languid and appear not to fire in the absence of synaptic input. *In vivo*, the neurones are subjected to both excitatory and inhibitory bombardment. Activity in excitatory afferents gives rise to excitatory post synaptic potentials (EPSPs) which bring the neurones closer to threshold. Conversely, inhibitory post synaptic potentials (IPSPs) move them further from threshold and lessen the likelihood that it will be reached. Inhibitory inputs are more efficacious than excitatory ones since they are located more proximally on dendrites and spines (see Groves, 1983; Kita *et al*, 1984). This means that medium spiny neurones can only be provoked into firing by temporally and spatially correlated inputs.

#### **1.6.3.1. Excitatory amino acids (EAAs).**

Glutamate or related transmitters mediate the excitatory signals which emanate from cortex and thalamus prior to initiation of a movement (see Groves, 1983). Stimulation of cortical and thalamic afferents produces large EPSPs in the medium spiny neurones and less frequently a combination of EPSPs and IPSPs (Buchwald *et al*, 1973; Fuller *et al*, 1975; Wilson *et al*, 1983a; Calabresi *et al*, 1990a). There is evidence that the EPSPs result from activation of N-methyl-D-aspartate (NMDA) and non-NMDA receptor-channels (Cherubini *et al*, 1988). The IPSP component appears to be mediated via GABA ( $\Gamma$ -aminobutyric acid) and is thought to be due to recurrent inhibition (Wilson *et al*,

1982, 1983a & b; Calabresi et al, 1990a).

#### **1.6.3.2. Dopamine (DA).**

The substantia nigra plays a vital role in regulating the activity of the neostriatum. As has already been mentioned, breakdown of this regulation has devastating effects. Dopamine exerts postsynaptic effects on the medium spiny neurones. Stimulation of nigral afferents produces both EPSPs and IPSPs. There is controversy as to whether the net effects of dopamine are excitatory or inhibitory (see Groves, 1983). Calabresi et al (1990a) showed that repetitive stimulation of nigral afferents decreased firing in the postsynaptic neurone; this effect being the opposite of that seen by cortical afferent stimulation.

The mechanism by which nigral neurones influence the activity of neostriatal output neurones is not entirely clear. Mercuri et al (1985) have demonstrated postsynaptic reductions by dopamine of both glutamatergic excitation and GABAergic inhibition. Calabresi et al (1987a) have shown that dopamine, acting via D<sub>1</sub> receptors has a direct inhibitory effect by reduction of a tetrodotoxin-sensitive (TTX-sensitive) inward current.

Dopamine also has well documented presynaptic effects. It inhibits release of glutamate and acetylcholine via a diffuse neuromodulatory action on D<sub>2</sub> receptors. It also regulates its own release by acting on autoreceptors. (Brown and Arbuthnott, 1983; Lehman and Langer, 1983; Mercuri et al, 1985).

#### **1.6.3.3. Acetylcholine (ACh).**

The neostriatum contains a high concentration of acetylcholine (Feldberg & Vogt, 1948). ACh in this region originates entirely from intrinsic neurones (McGeer et al, 1971;

Butcher & Butcher, 1974; Kimura *et al*, 1980; Woolf & Butcher, 1981; Lehman & Langer, 1983; Bolam *et al*, 1984). The major cholinergic neurones within the neostriatum are large, aspiny interneurones (Lehman & Langer, 1983; Bolam *et al*, 1984; Phelps *et al*, 1985). Acetylcholine release is stimulated by EAAs acting synaptically on the dendrites of cholinergic interneurones. Release is inhibited by DA acting on the pre-synaptic terminals of these neurones. (Lehman & Langer, 1983)

ACh released by cholinergic interneurones apparently exerts post-synaptic and pre-synaptic effects (Dodt & Misgeld, 1986). In some studies application of ACh led to direct muscarinic or nicotinic excitation of medium spiny neurones, increasing the firing rate, but firing induced by application of glutamate was diminished (Bloom *et al*, 1965; McLennan & York, 1966; Spehlmann, 1975; Bernardi *et al*, 1976; Misgeld *et al*, 1984; Dodt & Misgeld, 1986). In other studies, the predominant effect of ACh was inhibitory (e.g. Tagaki & Yamamoto, 1978). The inhibition was attributed to pre-synaptic mechanisms (e.g. Akaike *et al*, 1988). Malenka & Kocsis (1988) showed that ACh inhibits the release of EAAs. Nabatame *et al* (1988) demonstrated cholinergic inhibition of the excitatory actions of DA.

#### **1.6.3.4. The significance of DA-ACh interactions.**

It was shown in the sixties and seventies that muscarinic receptor antagonists and dopamine receptor agonists ameliorate Parkinsonian symptoms. These observations suggested that ACh/DA balance is vital for normal striatal function (McGeer *et al*, 1961; Barbeau, 1962; Duvoisin, 1967; Hornykiewicz, 1966 & 1973). It has since been established that excess cholinergic tone gives rise to hypokinetic disorders (e.g. Parkinsonism) whereas hyperkinetic conditions (e.g. Huntington's chorea) arise from an excess of dopaminergic tone (Aquilonius and Sjostrom, 1971).

Release of ACh from giant cholinergic interneurons is under the tonic inhibitory influence of dopamine (Lehmann and Langer, 1983). Dopaminergic tone is diminished in Parkinsonism due to death of nigral neurons. This leads to an increase in ACh release. Both dopaminomimetics and anticholinergic agents tend to counter the neostriatal ACh/DA imbalance responsible for Parkinsonism.

DA/ACh interaction can be partly explained by proposing that medium spiny neurons receive parallel inputs from DAergic and cholinergic neurons (Lehman & Langer, 1983). There is anatomical evidence to support such a proposition (Freund *et al*, 1984; Chang, 1988; Izzo & Bolam, 1988).

#### **1.6.3.5. Other transmitters/modulators.**

A multitude of other chemicals is implicated in synaptic transmission within the basal ganglia system. GABA is the primary transmitter of medium spiny output neurons (Kita & Kitai, 1984). It influences the extra-striatal target neurons and, by recurrent inhibition, neurons of the neostriatum itself. Certain interneurons are also GABAergic (Bolam *et al*, 1985). Others are somatostatinergic (DiFiglia & Aronin, 1982).

A small proportion of spiny output neurons (probably projecting to the substantia nigra) contains substance P which excites target cells (Groves, 1983; Lehman & Langer, 1983). In addition to GABA, medium spiny neurons projecting to the globus pallidus contain Leu-enkephalin. GABAergic neurons projecting to the substantia nigra also contain dynorphin.

Axon collaterals feed back to the neostriatum, so it is unsurprising that opioids affect transmission within this structure. Jiang & North (1992) demonstrated that  $\mu$ - and  $\delta$ -opioids pre-synaptically inhibited EAA-mediated excitation.  $\delta$ -opioids pre-synaptically inhibited GABA-mediated inhibition and

had a direct hyperpolarizing effect on unidentified interneurons. Adenosine is another compound which has been shown to pre-synaptically inhibit EAA-mediated excitation (Malenka & Kocsis, 1988). In addition, it directly activated a  $K^+$  current in medium spiny neurons (Trussel & Jackson, 1985).

There is known to be a tryptaminergic (5-HT) projection from the dorsal raphe nucleus to the striatum (Miller *et al*, 1975). 5-HT has been reported to have direct excitatory and inhibitory effects on medium spiny neurons. The inhibition was apparently due to activation of an inwardly-rectifying  $K^+$  current (Yakel *et al*, 1988) and the excitation was due to the suppression of a voltage-activated sub-threshold  $K^+$  current (Stefani *et al*, 1990b).

#### **1.6.3.6. Synaptic transmission vs. modulation.**

Chemicals released by neurons can exert their effects across synapses (consisting of specialized and closely apposed structures) or can act diffusely at some distance from their release site. The former action is true neurotransmission whereas the latter is more appropriately described as neuromodulation.

Therapeutic regimes which alter the prevailing levels of DA (such as replacement by L-DOPA) or ACh are effective in Parkinsonism. This implies that neuromodulation accounts for a large part of the chemical communication within the basal ganglia.

#### **1.6.4. Intrinsic membrane properties are responsible for the low level of spontaneous activity of medium spiny neurones.**

The unusually low spontaneous firing rate of medium spiny neurones obviously has some functional significance for the operation of the neostriatum. Powerful evidence has emerged that the characteristic firing behaviour is determined by the intrinsic membrane properties of these neurones rather than by tonic inhibitory input (Calabresi *et al* 1987b, 1990a & b). Passive membrane properties and voltage-activated currents are important in determining the response to synaptic input.

##### **1.6.4.1. Passive membrane properties.**

Medium spiny neurones are noticeably polarized compared with other neuronal types including giant aspiny neurones. Wilson *et al* (1990) observed that medium spiny neurones *in vivo* had resting potentials "far from the action potential threshold" whereas giant aspiny neurones had potentials "within a few millivolts of the spike threshold".

Medium spiny neurones also exhibit prominent inward rectification around the resting potential (Yakel *et al*, 1988; Bargas *et al*, 1988; Calabresi *et al*, 1987a; Stefani *et al*, 1990a). In contrast, giant aspiny neurones do not exhibit appreciable inward rectification (Wilson *et al*, 1990). The significance of the inwardly-rectifying current in medium spiny neurones is not clear.

##### **1.6.4.2. Active currents contributing to the firing patterns of medium spiny neurones.**

The considerable delay between the application of a depolarizing stimulus and initiation of firing is a conspicuous feature of medium spiny neurones. One possible explanation for

the "reluctance" of these cells to fire action potentials is the presence of a potassium current activated by sub-threshold depolarizations which would tend to counteract the depolarizations. Indirect evidence for such a current was obtained by Bargas *et al* (1989) from intracellular voltage recordings. They observed that hyperpolarization prior to depolarizing current injection increased spike latency and decreased action potential frequency. Prior depolarization had opposite effects. These phenomena could be explained by the inactivation of a potassium current by depolarization and its relief by hyperpolarization. Such characteristics are typical of an A-type transient potassium current (see e.g. Hille, 1984; Rudy, 1988).

Depolarizing current injection gives rise to a ramp-like depolarizing pre-potential which, if it reaches threshold, initiates a train of spikes (Galarraga *et al*, 1985; Kita *et al*, 1985a; Calabresi *et al*, 1987a; Bargas *et al*, 1989). It has been proposed that the pre-potential results from the interplay between a rapidly-activating A-type potassium current and a slow, TTX-sensitive sodium current. (Calabresi *et al*, 1987a; Bargas *et al*, 1989)

The repetitive, non-adaptive firing behaviour in response to supra-threshold depolarizations has been attributed to calcium-activated and voltage-activated potassium currents (Bargas *et al*, 1989; Galarraga *et al*, 1989).

#### **1.6.4.3. Whole cell currents revealed by voltage-clamp studies.**

Before the present study, membrane currents in medium spiny neurones had been investigated directly in only a handful of voltage clamp studies.

In their paper describing single channel potassium currents in acutely dissociated, unidentified rat striatal neurones Freedman and Weight (1988) also presented a brief account of some whole cell currents which could be elicited by depolarization. They reported a rapidly activating and inactivating inward current and a delayed, sustained outward current.

Ogata and Tatebayashi (1990) provided a detailed description of the fast sodium current, which underlies action potential firing, in acutely dissociated guinea pig neostriatal neurones.

Surmeier's group have reported voltage-activated potassium currents in acutely dissociated and cultured medium spiny neurones of the rat (Surmeier *et al*, 1988a & 1989; Akins *et al*, 1990; Stefani *et al*, 1990b). The neurones appear to express a complicated mixture of currents and the precise nature of the individual current components remains unclear. Surmeier *et al* (1988a & 1989) confirmed the existence of a depolarization-activated, TEA-sensitive sustained potassium current in cultured rat neostriatal neurones. They also described two depolarization-activated transient potassium currents. The first had characteristics very similar to those of the classical A-current; they termed this the low-voltage-activated (LVA) current. The second had characteristics akin to the *Drosophila* "Shaker" channel (Salkoff and Wyman, 1981; Sole *et al*, 1987), activating at more depolarized potentials; this was designated the high-voltage-activated (HVA) current. Both currents activated and inactivated rapidly, were blocked by millimolar concentrations of 4-AP and were progressively inactivated by depolarization. Neurones were found to express one current or the other, never both. The type of transient current expressed was dependent upon the recording conditions. With high potassium concentration in the patch pipette HVA currents predominated.

Thus, neostriatal neurones in different preparations have been shown to exhibit the inward currents necessary for EPSP and

action potential generation. However, these currents are normally offset by pronounced potassium currents which render the neurones comparatively inexcitable.

### **1.7. Single channel investigations.**

#### **1.7.1. Ion channels: a brief description.**

Only small molecules (such as water or urea), with sufficient kinetic energy, or fat-soluble molecules are able to penetrate the lipid portion of the cell membrane. Ions are highly impermeant due to their charge. Excitable cells depend upon differential permeability to ionic species in order to generate the membrane potentials necessary for signalling. Selective permeability is conferred by ion channels.

##### **1.7.1.1. Conductance.**

Movement of ions through channels is speedy ( $10^6$ - $10^8$  ions  $s^{-1}$ ). Conductance shows relatively little temperature dependence and the throughput is much higher than can be accounted for by carrier-mediated processes. Channels are narrow, water-filled glycoprotein pores which span the membrane and permit the passage of specific ions.

A feature of channels is their selectivity. The minute dimensions of channel pores mean that they can pass substances of ionic proportions but not molecules much larger than water. They also discriminate between anions and cations. Cation channels are generally highly impermeable to anions and vice versa. Channels can even distinguish different types of positively or negatively charged ions. There are, for example, specific channels for sodium and potassium.

The permeance of an ion depends not only on its ability to enter the channel but also its mobility once inside. Ions enter water-lined pores more easily than they enter pure lipid but there is still an energy barrier to be overcome because the channel radius is such that part of the hydration shell must first be removed. Once inside the channel there are no counterions to balance the charge, so ions must be stabilized by charges on the channel protein itself.

Ions do not diffuse freely within a channel but hop between discrete saturable binding sites. The mobility of an ion depends upon the presence of water molecules and other ions. When an ion pauses, following ions must wait.

#### **1.7.1.2. Ionic selectivity.**

What is the basis for ionic specificity? Charges within the channel pore are important in differentiating between positive and negative ions. The selectivity amongst ions with the same charge cannot be accounted for by filtering in terms of size alone since some channels are more permeable to larger ions than smaller ones. Selectivity filters must employ specific binding of "desirable" ions. The filters consist of a narrowing of the channel aperture such that ions come into direct contact with the channel protein with no intervening water layers. The mobility of an ion through this constriction depends upon the energy balance between removing water from the ion and interaction of the selectivity filter with the partly dehydrated ion.

#### **1.7.1.3. Gating.**

Channels exist in conducting and non-conducting states. To switch between the two states requires a conformational change in the channel protein. They can therefore be considered to have gates which are open or closed.

Gating characteristics of voltage-dependent channels are altered by changes in membrane polarization. Activity of other channels is influenced by the binding of extracellular ligands (hormones, transmitters, drugs etc.) to membrane receptors. Changes in channel kinetics can be mediated by direct interaction of the channel with G-proteins or via intracellular messenger cascades. Intracellular messengers such as  $\text{Ca}^{2+}$ , cAMP or ATP can bind to channels and modulate their behaviour. Channels can also be regulated by chemical modification e.g. phosphorylation and dephosphorylation of intracellular sites.

#### **1.7.1.4. Structure.**

The molecular structure of channels is gradually being mapped. Sodium channels were the first to have their structures elucidated. This was because of their relative abundance and ease of purification with specific probes such as TTX. A high degree of structural homology exists between voltage-activated sodium, potassium and calcium channels. Much less is known about the structures of ligand-gated channels.

The main protein of the voltage-gated sodium channel is an  $\alpha$ -subunit in the region of 250-300 kD. The pore and gating regions reside in this sub-unit. Associated sub-units are not necessary to produce a functioning channel and their role is yet to be determined. The  $\alpha$ -subunit consists of four repeated amino acid sequences (I-IV). Within each of these repeats there are thought to be six lipophilic membrane-spanning domains (S1-S6) connected by hydrophilic intracellular and extracellular segments. It is thought that the four repeats are aligned in the membrane rather like the staves of a barrel with the central domains S5 and S6 of each repeat forming the pore. Voltage-gated potassium channels exhibit structural similarities with sodium channels. Each  $K^+$  channel sub-unit corresponds to one of the four repeats of the  $Na^+$  channel. Four sub-units are required to form a functional channel. The sub-units each contain six membrane-spanning domains analogous to those of the  $Na^+$  channel.

The amino acid sequences of toxin-binding sites within the protein and those segments responsible for ionic selectivity vary between different channel types.

The S4 domain is highly conserved between voltage-gated channel types. It contains an abundance of positively charged amino acids and is believed to constitute the voltage-sensing gate which changes conformation under the influence of an electrical field. Channels which inactivate also possess an inactivation gate. This resides in an intracellular segment and can be envisaged as a "ball" which is tethered to the channel and can block it from the inside by simply plugging the pore.

(Reviewed by Hille, 1984; Wann, 1993)

### **1.7.2. Types of potassium channel characterized at the single channel level.**

A striking attribute of potassium channels is their enormous diversity. Many of the numerous macroscopic  $K^+$  currents that have been described result from the activity of more than one channel type.

#### **1.7.2.1. Delayed rectifiers.**

Channels responsible for delayed outward rectification in the squid giant axon were identified at the single channel level by Conti & Neher in 1980. Delayed rectifier channels have since been demonstrated in a variety of non-neuronal preparations including rabbit smooth muscle (Benham & Bolton, 1983) chick heart (Clapham & De Felice, 1984) and frog skeletal muscle (Standen et al, 1985).

The properties of delayed rectifier channels vary from preparation to preparation. Conductance, as for other channel types, depends very much upon the recording conditions employed. Larger conductances are recorded when the extracellular faces of the channels are exposed to higher  $[K^+]$ . Delayed rectifier channels are almost invariably of low conductance (ranging from 2 pS in low  $[K^+]$  to  $\approx 50$  pS in high  $[K^+]$ ; see Adams & Nonner, 1990 for details). They are activated by depolarization and elevated activity persists for the duration of the depolarization. They are blocked by appropriate concentrations of TEA and are insensitive to 4-AP. Voltage-sensitive, calcium-activated channels also impart the property of delayed rectification. Hodgkin & Huxley-type delayed rectifier channels, however, are  $Ca^{2+}$ -insensitive.

#### 1.7.2.2. Calcium-activated K<sup>+</sup> channels.

Calcium-activated K<sup>+</sup> channels are present in many different cell types. They are involved in glandular secretion and the shaping of action potential firing in muscle and nerve. There is some confusion over the terminology used to categorize these channels. They are traditionally divided into small and large conductance types, but a whole spectrum of conductances has been observed.

"Maxi" or BK channels have been most extensively studied because their large conductance makes them conspicuous and easy to record. They are the largest channels to have been encountered. Their conductance of 200-300 pS in symmetrical (140 mM) K<sup>+</sup> solution is close to the theoretical maximum for a pore. Conductance in physiological K<sup>+</sup> gradients is in the region of 100 pS. They combine high conductance with high selectivity; a typical permeability ratio for K<sup>+</sup>:Na<sup>+</sup> being 100:1. Maxi channels are activated by the calcium entering a cell during depolarization. They are also strongly activated by depolarization per se, displaying sigmoidal voltage-dependence. They exhibit varying degrees of voltage-dependence and sensitivity to Ca<sup>2+</sup> between tissues. They have been recorded in tissues as diverse as chromaffin cells (Marty, 1981), skeletal muscle (Barrett *et al*, 1982; McManus & Magleby, 1988), smooth muscle (Benham *et al*, 1985) pancreatic  $\beta$ -cells (Cook & Hales, 1984), GH<sub>3</sub> pituitary cells (Wong *et al*, 1982) and neurones (section 1.7.3.). Maxi channels are relatively sensitive to blockade by TEA and charybdotoxin but are insensitive to apamin. Using these blockers it has been shown that the fast Ca<sup>2+</sup>-dependent K<sup>+</sup> current in neurones is attributable to maxi channel activity (Miller *et al*, 1985; Storm, 1987).

Small conductance (SK) channels are also strongly activated by Ca<sup>2+</sup> influx. Their conductance is below 20 pS (symmetrical K<sup>+</sup>) in many cells. They are less sensitive than the maxi channel to voltage but are subject to modulation by numerous

transmitters. Substances such as neurotensin, ATP (acting via  $P_2$  receptors) and adrenaline activate these channels (e.g. in intestinal smooth muscle causing hyperpolarization and inhibition of contraction). The channels underly certain neuronal AHPs and are blocked by apamin but not by low concentrations of charybdotoxin. They have been observed, for example, in skeletal muscle (Blatz & Magleby, 1986), hepatocytes (Capiod & Ogden, 1987), anterior pituitary cells (Lang & Ritchie, 1988), smooth muscle cells (Bülbring & Tomita, 1987) as well as neurones.

Voltage-dependent and independent  $Ca^{2+}$ -activated channels of intermediate conductance have been reported. The voltage-independent type have been demonstrated in red corpuscles (Grygorzyk & Schwarz, 1983) and are involved in volume regulation. Their conductance is in the region of 40 pS in symmetrical  $K^+$ . Like the maxi channel, these channels are blocked by low concentrations of charybdotoxin. Depolarization-activated intermediate channels are found in invertebrate neurones (Ewald *et al*, 1985), mammalian olfactory neurones (Maue & Dionne, 1987) and  $GH_3$  pituitary cells (Lang & Ritchie, 1990). Conductance is  $\approx$  35-60 pS in symmetrical  $K^+$ . They are thought to be responsible for spike accommodation and are blocked by different toxins in different preparations.

(Reviewed by Latorre *et al*, 1989; Haylett & Jenkinson, 1990.)

#### **1.7.2.3. Inward rectifiers.**

Inward rectification can be caused by gated channels which activate on hyperpolarization and inactivate on depolarization. Alternatively, macroscopic rectification can result from rectification at the single channel level.

Single channels responsible for inward rectification were first recorded in tunicate egg cells (Fukushima, 1981), heart cells (Trube *et al*, 1981), and skeletal muscle cells (Ohmori *et*

al, 1981). The channels exhibit both voltage-dependent gating and single channel rectification. Like other  $K^+$  channels their conductance is dependent upon extracellular  $[K^+]$ . A unique property is that their gating is also dependent upon extracellular  $[K^+]$ . Channel conductance is usually substantially less than 40 pS in symmetrical ( $\approx 150$  mM)  $K^+$ .

The function of inward rectifiers in egg and muscle is to permit long depolarizing plateaux with minimum energy expenditure. They are active at negative potentials, so may contribute to resting conductance, but are switched off during depolarization to minimize antagonistic current flow.

Anomalous rectifiers are blocked by external  $Cs^+$  (mM concentrations) and external  $Ba^{2+}$  ( $\mu$ M concentrations). When held at negative potentials, where the channels were fully activated, no open to closed channel transitions were detected with solely KCl in the recording electrode. Channels were perpetually in the open state unless blocking ions such as  $Na^+$  or  $Ba^{2+}$  were included (Ohmori et al, 1981).

Matsuda (1988) demonstrated that the rectification of single inwardly-rectifying  $K^+$  channels in guinea-pig heart cells was partly due to blockade by intracellular  $Mg^{2+}$  and partly to voltage-dependent gating. In cell-attached patches only outward current was detectable through these channels. When cells were permeabilized and the inner surface of the patch exposed to low  $Mg^{2+}$  solution, the channels also passed inward current and had an ohmic conductance of 22 pS (in symmetrical, 150 mM  $K^+$ ). Intracellular  $Mg^{2+}$  did not block inward current through the channels.

A salient feature of inward rectifiers is that they exhibit sub-conductance states. The channels are thought to consist of pore clusters which have a common gate but can also be individually blocked by internal ions such as  $Mg^{2+}$  (Matsuda, 1988).

#### 1.7.2.4. ATP K<sup>+</sup> channels.

ATP K channels were initially recorded in mammalian cardiac muscle fibres (Noma, 1983). They are also present in the  $\beta$ -cells of pancreatic islets (Ashcroft *et al*, 1984; Cook & Hales, 1984; Sturgess *et al*, 1985; Trube *et al*, 1986), skeletal muscle cells (Spruce *et al*, 1985), arterial smooth muscle cells (Standen *et al*, 1989) and neurones (Ashford *et al*, 1988). They are blocked by intracellular ATP at millimolar (i.e. physiological) concentrations.

Single channel conductance is in the region of 50-65 pS at negative potentials (symmetrical 150 mM K<sup>+</sup>). There is pronounced inward rectification due to blockade of outward currents by internal Na<sup>+</sup>, Mg<sup>2+</sup> and Ca<sup>2+</sup> (Findlay, 1987; Horie *et al*, 1987).

The channels play an important physiological role in the regulation of insulin secretion by pancreatic  $\beta$ -cells. The normal stimulus for insulin release is raised blood glucose concentration. Glucose easily crosses  $\beta$ -cell membranes. Once inside the cell it is metabolized, raising intracellular ATP levels. ATP blocks the K<sup>+</sup> channels, decreases the K<sup>+</sup>:Na<sup>+</sup> permeability ratio and causes depolarization. This, in turn, leads to Ca<sup>2+</sup> influx through voltage-gated channels and Ca<sup>2+</sup>-dependent insulin release is instigated. Sulphonylurea drugs selectively block ATP K<sup>+</sup> channels and are clinically useful in type II diabetes where insulin secretion is defective.

The role of ATP K<sup>+</sup> channels in other cells is less clear. In muscle fibres, they could serve a protective function by causing hyperpolarization and inhibition of contraction under conditions of fatigue when ATP is depleted.

ATP K<sup>+</sup> channels are opened by a class of drugs which includes cromakalim, pinacidil and minoxidil sulphate. The antihypertensive effects of these drugs could be due to their activation of ATP K<sup>+</sup> channels in arteriolar smooth muscle.

#### **1.7.2.5. Agonist-activated K<sup>+</sup> channels.**

Hormones, transmitters and drugs can act to modify cell excitability by activating K<sup>+</sup> channels. Some channels are activated indirectly by intracellular messengers. Ca<sup>2+</sup>-activated channels, for example, are stimulated by agonist-induced [Ca<sup>2+</sup>] rises. This type of activation can be invoked by applying agonists to the outside of the cell.

Other channel types are activated more directly via interaction with G proteins. Such activation can only be recorded by including agonists in the patch pipette. Agonist-activated channels of this type are inactive in the absence of agonists. Typical of this class of channels are those activated by muscarinic agonists which were recorded in heart cells by Sakmann *et al* (1983) and Soejima & Noma (1984). Kurachi *et al* (1986) showed that adenosine activated the same channel. Activation of a common channel by different agonists is a frequent finding. Another example of agonist-activated channels are those found in GH<sub>3</sub> cells (Yatani *et al*, 1987) which inwardly rectify ( $G \approx 55$  pS at negative potentials). They are activated by carbachol and somatostatin.

#### **1.7.2.6. Non-specific channels.**

Potassium also permeates non-selective cation channels including those gated by NMDA, kainate or ACh. Non-selective channels can be distinguished from specific K<sup>+</sup> channels by measuring their reversal potential in asymmetrical solutions.

#### **1.7.3. Individual potassium channels in neurones.**

There have been relatively few single channel studies in neurones but the major types of potassium channel have been shown to exist.

Delayed rectifiers, with properties similar to those found in axons, have been demonstrated in the somatic membranes of hippocampal (Rogawski, 1986) and hypothalamic (McLarnon, 1989) neurones.

The channels which underly A-currents were recorded in nodose (Cooper & Shrier, 1985) and DRG (Kasai *et al*, 1986) sensory neurones. Depolarization rapidly activated bursts of channel openings. The bursting decayed within tens of milliseconds. The channels were sensitive to 4-AP and could only be activated after inactivation had been relieved by hyperpolarization. Single channel conductance was in the region of 20 pS in physiological  $[K^+]$  gradients and  $\approx$  40 pS in symmetrical 150 mM  $K^+$ .

Maxi  $K^+$  channels are widely distributed in the nervous system. They are known to exist in nodose (Cooper & Shrier, 1985), sympathetic (Smart, 1987), hippocampal (Franciolini, 1988), DRG (Simonneau *et al*, 1987) neurones.

Simonneau *et al* (1987) discovered two distinct inwardly-rectifying  $K^+$  channels with intermediate conductances in DRG neurones.

Two types of ATP  $K^+$  channel are present in the membranes of neocortical (Ashford *et al*, 1988) and glucose-sensing ventromedial hypothalamic neurones (Ashford *et al*, 1990a & b). The first is similar to the  $\beta$ -cell ATP channel in that it is blocked by intracellular ATP. However, it differs from non-neuronal ATP  $K^+$  channels, being less sensitive to ATP, having a larger conductance and displaying outward rectification. The second channel has a conductance of maxi channel proportions and rather than being inhibited, it is activated by ATP.

Hippocampal neurones possess  $K^+$  channels which are activated by 5-HT (Van Dongen *et al*, 1988) and GABA (Premkumar, 1990). A 45 pS channel in locus coeruleus neurones is opened by opioids and  $\alpha_2$ -agonists (Miyake *et al*, 1989).

#### **1.7.4. Dopamine-activated potassium channels.**

Dopamine-activated macroscopic  $K^+$  conductances have been observed in rat substantia nigra neurones (Lacey *et al*, 1987; Roeper *et al*, 1990) and lactotrophs (Israel *et al*, 1985 & 1987). The channels responsible for the hyperpolarizing effect of DA-agonists had not been identified at the beginning of the present study.

Freedman and Weight (1988 & 1989) reported dopamine-activated potassium channels in acutely dissociated adult rat striatal neurones of unidentified type. The channels had a conductance of 85 pS and were potently blocked by quinine. They were activated by DA and the  $D_2$  agonist, quinpirole, and the activation was antagonized by  $D_2$  antagonists.  $D_1$  agonists did not cause activation.

The activation by  $D_2$  agonists in these cells is perplexing because other investigators have not found  $D_2$  agonists to have any effect on the firing patterns of identified medium spiny neurones. In contrast,  $D_1$  agonists have been shown to inhibit firing (section 1.6.3.2.). This (and other evidence) suggests that the neurones studied by Freedman and Weight may not have been medium spiny ones. In order to try and clarify the situation, some of the experiments by Freedman and Weight involving dopamine agonists were repeated in the present study using cultured cells which could be more easily identified as medium spiny neurones.

### 1.7.5. Potassium channels active at the resting membrane potential.

There is very little information regarding channels responsible for the resting potassium conductance in any cell type. Resting conductance in highly polarized cells is sometimes theoretically attributed to "the inward rectifier" (e.g. Uchimura *et al*, 1989) but the channels responsible for inward rectification have been examined in very few studies.

Ohmori *et al* (1981) described inwardly rectifying channels active at the resting potential in the presence of external  $Ba^{2+}$  in rat myotubes. The channels exhibited long openings and closures and had a conductance of  $\approx 10$  pS at negative potentials (symmetrical 155 mM  $K^+$ ). Sakmann & Trube (1984) also reported inwardly rectifying channels ( $G \approx 27$  pS; symmetrical 145 mM  $K^+$ ) in cell-attached patches from heart ventricular cells. They concluded that these channels were responsible for the resting conductance but that current flow through them at depolarized potentials was too small to resolve. Simonneau *et al* (1987) recorded two types of inward rectifiers in DRG neurones (cell-attached, symmetrical 140 mM  $K^+$ ). The first did not pass outward current and its kinetics were similar to the 27 pS channel in heart cells (Sakmann & Trube, 1984) but the conductance was much larger at 90 pS. The second had a conductance of  $\approx 120$  pS at negative potentials. It rectified strongly but was able to pass outward current.

The only channels so far recorded in striatal neurones are those activated by dopamine and quinpirole. Freedman and Weight reported that "no channel openings were seen at the resting membrane potential" in the absence of  $D_2$  agonists. This is a rather puzzling finding since there must be potassium-selective channels active at rest to account for the negative resting potential. Equally mysteriously, opioid-activated  $K^+$  channels were reported in locus coeruleus neurones but no channel activity was seen at RMP in the absence of agonists (Miyake *et al*, 1989).

The inward rectifiers described by Simonneau et al (1987) in DRG cells were active at potentials corresponding to the RMP and were therefore likely to have contributed to resting conductance of these sensory neurones. To the author's knowledge this was the only report of "resting"  $K^+$  channels in neurones before commencement of the present study. Prior to this study, resting K channels had not been described in central neurones. The major aim, therefore, was to seek out channels responsible for the resting potassium conductance and to characterize them as fully as possible.

## Part II. METHODS

### Section 2. Cell culture

Cultures were prepared using cells from neonatal rats aged between 3 and 6 days. A rat pup of either sex was sacrificed by cervical dislocation. All subsequent procedures were performed under sterile conditions to prevent microbial contamination. The brain was quickly removed, placed on a dissecting table and washed with ice-cold dissection medium (DMEM with Earle's salts, buffered to pH 7.4 with 25 mM HEPES; obtained from Gibco). It was then hemi-sected and blocks of neostriatal tissue removed. The blocks were transferred to a small petri dish containing dissection medium and minced with a fine pair of scissors. The tissue was next transferred to a centrifuge tube containing the same cold medium and gently dissociated by trituration with Pasteur pipettes of progressively finer bore.

The resulting suspension was centrifuged at 500 r.p.m. for 5 minutes to separate dissociated cells from the sub-cellular fraction. The supernatant was removed and the cells re-suspended in fresh medium. Cells were counted using a haemocytometer, diluted to an appropriate concentration and seeded into sterile petri dishes at a density of  $5 \times 10^5$  cells per dish. Tissue from one animal was sufficient for 3 or 4 dishes. Each petri dish contained 5 ml of culture medium and eight glass slips (16 mm diameter, from Raymond Lamb) which had previously been acid washed and coated with poly-L-lysine (molecular mass 70 000 to 150 000, Sigma) to facilitate cell adhesion. The culture medium contained DMEM and 10% foetal calf serum (Gibco) or 10% heat-inactivated horse serum (Gibco). It was buffered with 16 mM bicarbonate and included 1 mM glutamine (Sigma), 10 mg/ml streptomycin (Sigma) and 10000 units/ml penicillin (Sigma). When using horse serum-enriched medium an addition of 3  $\mu$ g/ml insulin from bovine pancreas (Sigma) was required. Cells were incubated at 37°C in 5% CO<sub>2</sub> which buffered the medium at pH 7.4. The medium was replaced by fresh medium every seven days thereafter.

## Section 3. Patch clamp methods.

### 3.1. Cells.

Patch clamp recordings were performed on neurones which had been grown in culture for at least two weeks. A glass slip containing cells was removed from a culture dish and transferred to the plastic recording chamber. The slip was attached to the glass base of the chamber using tiny blobs of grease. The slip was then immersed in bathing solution (composition shown in table 3.1.). Most of the whole cell and single channel experiments were carried out with the cells bathed in aCSF. In a few cases, the cells were bathed in the same high potassium solution which was used in the recording electrode (table 3.1.). High  $K^+$  bathing solution was occasionally used for cell-attached recordings to depolarize the cells so that their resting potential could be specified at 0 mV. High  $K^+$  bathing solution was also used when examining O/O patches under symmetrical conditions and in some whole cell recordings. All experiments were carried out at room temperature (18-25°C). Cells survived for a matter of hours if left in aCSF. When bathed in high  $K^+$  medium they remained healthy for 15-30 minutes, after which time they became decidedly swollen and granular.

Slips were viewed from below using a phase-contrast light microscope. Neurones were distinguished from glial cells by morphological criteria. Two types of neurone were selected for patching. Those with ovoid somata, and having two major processes, were the most frequently patched. Neurones with a triangular appearance, having three main processes were also patched. The selection procedure was fairly rigid. Neurones had to be phase-bright, of medium size (diameter of cell body  $\approx$  12-20  $\mu$ m) with clean membranes and agranular cytoplasm. Neurones possessing long ( $>$  75  $\mu$ m) or highly branched processes were excluded.

### **3.2. Electrodes.**

Patch (recording) electrodes were fabricated from thick-walled, filamented borosilicate glass capillaries (Clarke Electromedical, GC150F) by a two-stage pulling procedure. A List L/M-3P-A vertical electrode puller was used. The first pull on a high heat setting thinned the glass. The capillary was then re-centred and pulled on a lower setting to yield two electrodes with similar dimensions. The settings were carefully chosen to produce electrodes with a steep taper and inside tip diameter of 1-2  $\mu\text{m}$ . Electrodes with resistances in the 3-14  $\text{M}\Omega$  range could be reproducibly pulled. Sufficient fire-polishing was achieved during the pulling process and further polishing was not required for the formation of stable seals. The electrodes were back-filled with the high  $\text{K}^+$  solution using a fine syringe needle. Solutions were filtered to reduce the likelihood of electrode blockage.

Reference electrodes were pulled from thin-walled electrode glass (GC150TF) and were filled with the same solution as that bathing the cells. The resistance of these electrodes was rendered much smaller than that of the patch electrodes by gently touching them on the base of the recording chamber to break their tips.

### **3.3. Components of the patch clamp apparatus.**

Current recordings were carried out inside an earthed cage to minimise interference from external electromagnetic sources. The high fidelity voltage-clamp apparatus (Axon Instruments Axopatch 200) consisted of a headstage and main amplifier. The headstage, containing a current to voltage converter was mounted on a micromanipulator inside the cage. Inside the headstage, an operational amplifier passed current and sensed voltage. The circuitry of the main amplifier boosted and scaled the signal and eliminated artefacts. The holding (clamp) potential could be

adjusted manually or by computer. The headstage contained a pipette holder with an Ag/AgCl wire. The unit was sealed so that when fitted with a glass microelectrode suction or positive pressure could be applied to the interior of the pipette.

The set-up included a digital storage oscilloscope (Tektronix 2201) to view the currents, an A-D & D-A converter (CED 1401 Interface) and logging devices. For whole cell experiments, voltage-stepping protocols were generated by computer and the resulting currents were digitized and stored on disk (Tandon 286, CED voltage-clamp software). Single channel currents were logged to digital audio tape using a Sony DAT deck (modified by HHb Communications Ltd). Current records were routinely low-pass filtered at 5 kHz (-3 dB level, 4-pole low-pass Bessel filter) prior to logging.

#### 3.4. Seals.

To form a seal, a microelectrode was attached to the headstage and manoeuvred into position using the micromanipulator. Before passing through the air-water interface positive pressure was applied to prevent the pipette tip from accumulating detritus. Once the electrode tip was in solution, any standing potential was cancelled using the pipette offset control. The Axopatch was switched to "track" mode and a 5 mV test pulse applied to assess the pipette resistance. With the aid of the microscope, the tip was lowered on to the cell surface and the pressure released. Gentle suction was applied, usually resulting in the formation of an acceptable seal (resistance > 1 G $\Omega$ ). The magnitude of the seal resistance could be assessed by measuring the current deflection elicited by the test pulse.

### **3.5. Recording.**

After accomplishing a cell-attached seal, the voltage clamp circuit was switched on. Electrode capacitance was nullified using the Axopatch controls. Recordings could then be made in cell-attached mode or other configurations could be entered.

#### **3.5.1. Cell-attached.**

Channels were observed in the cell-attached mode over a wide range of holding potentials from hyperpolarized to depolarized (up to RMP  $\pm$  120 mV; larger imposed potentials caused seal breakdown). Segments of record at different holding potentials were amplified (50-fold or 100-fold) and logged to DAT for subsequent analysis. At the end of each cell-attached experiment, a whole cell seal was attempted in order to determine the resting potential. This could be achieved by measuring the potential at which the holding current was zero. In this way, absolute patch potential could be specified. As has been previously mentioned, the alternative method of specifying the patch potential in the cell-attached configuration was to zero the membrane potential by bathing the cells in high K<sup>+</sup> solution.

#### **3.5.2. Whole cell.**

The whole cell mode was achieved by applying reasonably strong pulses of negative pressure whilst in the cell-attached mode. This resulted in the rupture of the patch of membrane beneath the electrode tip and led to the formation of a low resistance pathway between the electrode and cell interior. Attainment of the whole cell mode could be recognized by the appearance of large capacitance transients and by an increase in the current generated by the test pulse. The magnitude of this current was used to calculate the input resistance at the RMP. A fast component of the capacitance transient could be eliminated

by adjusting the whole cell capacitance and series resistance controls to the appropriate settings. A slower component (presumably due to capacitance of neuronal processes which could not be adequately space clamped) was uncancellable using the Axopatch controls.

The Axopatch series resistance compensation procedure required complete cancellation of capacitance transients. Compensation could not, therefore be employed in these experiments. However, this was not found to be a problem. The whole cell currents generated by cultured neostriatal neurones were small. Clamping errors of only a few millivolts would occur even with the largest currents. The rate of attainment of the clamp potential would not be unduly retarded (the rise time constant being typically 200  $\mu$ s). Macroscopic currents were elicited by voltage steps of different magnitudes and durations from a variety of holding potentials. Signals were amplified (2-fold or 5-fold) and logged to disk. Sampling frequency ranged between 500 Hz and 25 kHz.

### **3.5.3. Outside-out.**

Outside-out patches were obtained by delicately removing the electrode from the cell body whilst in whole cell mode. A long strand of membrane was pulled with the electrode. As the electrode was moved further away the strand eventually broke and a new patch sealed across the tip. Activity in O/O patches was recorded in asymmetrical solutions, with aCSF bathing the outer face and high  $K^+$  solution bathing the inner face, or symmetrical high  $K^+$  solutions. Segments of record were amplified and logged to DAT.

### **3.6. Perfusion.**

Neurones patched in whole cell mode were often too unstable to withstand perfusion with drug-containing solutions. Nevertheless, perfusion was attempted on several occasions. Perfusion was via a gravity-driven system. Syringe barrel reservoirs were connected to an outflow pipe made from a DNA spotting tube (0.18 mm, outside diameter) which protruded from the end of a 10  $\mu$ l Gilson pipette tip. A six-way tap was used to direct flow through the system from one barrel at a time. The outflow pipe was positioned 50-100  $\mu$ m diagonally above the test cell so that solution flowed over it.

**Table 3.1.**

**Composition of the recording solutions (mM).** The recording electrode contained 140 mM KCl solution (A) in almost all experiments. A 40 mM KCl solution (C) was used on a few occasions. In Cl<sup>-</sup> substitution experiments, the 140 mM KCl was replaced by potassium aspartate solution (D). The cells were most often bathed in aCSF (B) but were sometimes bathed with the high K<sup>+</sup> solution (A). For measurement of whole cell sodium currents the KCl in the pipette was replaced with CsCl.

<u>Constituent</u>	<u>Solution</u>		
	<u>High K<sup>+</sup> (A)</u>	<u>aCSF (B)</u>	<u>40 mM K<sup>+</sup> (C)</u>
KCl	140	3	40
NaCl	5	150	105
MgCl <sub>2</sub>	1	2	1
CaCl <sub>2</sub>	1	2	1
EGTA	11	0	11
HEPES	10	10	10
D-glucose	0	10	0
pH	7.4 (KOH)	7.2 (NaOH)	7.4 (KOH)

Drugs and blockers were included in the pipette solution for some cell-attached recordings. In whole cell experiments drugs were added to the bathing solution.

An 11:1 [EGTA]:[Ca<sup>2+</sup>] ratio produced a free [Ca<sup>2+</sup>] of the order of 10<sup>-8</sup> M (measured using a calcium electrode; Orion Research Inc.).

## **Section 4. Analysis.**

### **4.1. Whole cell currents.**

The CED voltage clamp software was used to visualize macroscopic current records and to measure net currents at various points during a voltage step, for current-voltage (I-V) plots and conductance calculations. Current records could also be exported to a graphics package (Fig.P, Biosoft).

### **4.2. Single channel currents.**

Segments of record (30-90 s) were re-played, amplified (Digitimer Neurolog DC Amplifier), low-pass filtered at 1 kHz or 2 kHz (-3 dB level, 4-pole Bessel) and imported into the "PAT" single channel analysis program at a sampling rate of 10 kHz. The program (supplied by J. Dempster, University of Strathclyde) was used to plot current records, construct current amplitude distribution histograms and detect channel transitions between the open and closed states.

Unitary current amplitude was determined, at different holding potentials, from the distribution histograms and current-voltage relationships plotted. The gradient of the regression through the I-V plot gave channel conductance.

The automated transition detection routine was employed to calculate  $P_{\text{open}}$  and to compute open and closed time distributions for a channel. Open probability for a particular channel could be determined if there was only one present in a patch. The detection threshold for channel opening or closure was set at 50% of the unitary current amplitude. After automatic detection the transition record was inspected visually. Transitions resulting from obvious noise artefacts were re-classified or the section of record containing them was rejected. When filtering at 1 kHz, it took  $\approx 500 \mu\text{s}$  for currents to attain their full amplitude.

Therefore, short openings and closures were not fully resolved. When fitting curves to open or closed time distributions, bins containing events which lasted for less than 2 ms were excluded.

Average noise levels could be calculated by the program after sweeping a cursor over a representative section of the data in which the channel was closed. Mean current for the total recording segment could be obtained by a similar procedure. When carrying out mean current measurements records were digitized at 200 Hz on playback. Such measurements were useful for determining the open probability of a patch in which more than one channel was active. Patch open probability ( $N \cdot P_o$ ) is given by the following equation:

$$N \cdot P_o = I/i$$

$N$  = number of channels in the patch

$P_o$  = open probability for a single channel

$I$  = mean patch current

$i$  = unitary current amplitude

### 4.3. Statistics.

Data are generally presented as mean and standard error (SEM) values with the sample size (n) indicated. Modal values are also presented in some cases where a distribution is obviously skewed. Curves were fitted to data using P.Fit (Biosoft). Conductance vs. voltage and open probability vs. voltage relationships were fitted with the Boltzmann equation:

$$x = 1 / (1 + \exp((V - V_h) \cdot z \cdot F / R \cdot T))$$

$x = G/G_{\max}$  = relative conductance

or

$x = P_o$  = open probability

$V$  = voltage

$V_h$  = voltage at which  $x$  is half its maximal value

$z$  = slope factor/relative gating valency

$F$  = Faraday's constant = 96500 C.mol<sup>-1</sup>

$R$  = universal gas constant = 8.314 J.mol<sup>-1</sup>.K<sup>-1</sup>

$T$  = absolute temperature = 295 K

The I-V relationship for a maxi channel recorded in an O/O patch bathed in asymmetrical [K<sup>+</sup>] was fitted with the Goldman-Hodgkin-Katz (G-H-K) current equation:

$$I_K = P_K \cdot k \cdot z \cdot F \cdot V \cdot ([K]_i - [K]_o \cdot \exp(-V \cdot k) / (1 - \exp(-V \cdot k)))$$

$I_K$  = single channel K<sup>+</sup> current

$P_K$  = channel K<sup>+</sup> permeability

$k = z \cdot F / R \cdot T$

$z$  = valency of K<sup>+</sup> = 1

$$\begin{aligned} [K]_i - [K]_o &= K^+ \text{ gradient across the patch} \\ &= 1.37 \times 10^{-4} \text{ mol.cm}^{-3} \end{aligned}$$

Other symbols are as defined for the previous equation.

Comparisons between different currents were made using two-tailed, unpaired t-tests for small, unpaired samples (ie. using pooled variance estimates). The sign test for paired samples was used to assess the significance of membrane potential changes during an experiment.

## **Part III. RESULTS.**

### **Section 5. Cell culture.**

#### **5.1. Development of the neurones.**

During the dissociation procedure neurones were completely stripped of their processes. Figure 5.1. shows low and high power phase contrast photomicrographs of neostriatal cells 3 hours after dissociation and plating. The round, phase-bright somata of viable cells can just be distinguished from cellular debris and undissociated cell masses. A small proportion of the cells adhered to the poly-lysine-coated slips and grew. The degree of survival was variable. The yield of suitable neurones ranged between half a dozen and several dozen per slip. This was sufficient for patch experiments; no more than five seals were attempted per slip.

Culturing was more successful with horse serum-enriched medium than with that containing calf serum. In calf serum, growth was more rapid but glial proliferation and overgrowth of the neurones was a problem. Neurones sprouted more extensively in calf serum and were more difficult to identify. Horse serum is less nutritious and is deficient in growth factors. For this reason, an insulin supplement was required to permit adequate neuronal growth. The sluggish maturation in horse serum was not necessarily disadvantageous. Neonatal neurones grown for a longer time in culture may develop a phenotype closer to that of adult neurones. Because cultures were less contaminated by glia and neurones were more easily identifiable, horse serum-containing medium was routinely used. Cultures were grown for a number of weeks so antibiotics were required to prevent infection.

Figure 5.2. shows that 7 days after plating the cells bodies had enlarged greatly but the cells remained as unidentifiable globules.

Figure 5.3. illustrates the appearance of the cells after 11 days in culture. During the second week neurones developed ovoid or triangular somata and a small amount of sprouting occurred. Recognizable cell types began to emerge. In photograph 5.3.A. a triangular neurone is clearly distinguishable from an astroglial/microglial cell. Squamous glia are also visible.

Figure 5.4. shows cultures 14 days after plating. By this stage many of the neurones had been overgrown by squamous glia. Healthy-looking neurones, suitable for patching, occupied lacunae in the glial mat.

If maintained for longer than three or four weeks, neurones sprouted secondary and tertiary processes. Extensive arborization occurred and the cell membranes started to bleb. Processes of adjacent neurones became entangled and appeared to form contacts. Glia continued to spread. The slips eventually degenerated into a tangled mass of processes and glia by which the cell bodies were totally obscured.

## **5.2. Appearance of the neurones.**

With appropriate plating density (initially  $5 \times 10^5$  dissociated cells per dish) neurones were relatively easy to distinguish morphologically from glia and sufficient neurones were not overgrown.

Figure 5.5.A. illustrates mature medium-sized neurones suitable for patching. The long axis of the cell body ranged between  $\approx 12-20 \mu\text{m}$ . The types of neurone observed were comparable to those described by Surmeier *et al* (1988) for embryonic neostriatal cultures. The middle neurone is an archetypal bipolar, ovoid neurone designated type I by Surmeier *et al*. This was by far the most common type of neurone; the majority of patch recordings were made from this kind of cell.

The lower cell is a triangular, type II neurone; these neurones constituted about one fifth of the cells patched. The upper neurone has three main processes and an irregular cell body; it would be classed as a "triangular" neurone in the present study. Neurones with more than three main processes were not patched as they were not sufficiently distinguishable from glia. Figure 5.5.B. shows a typical astroglial/microglial cell for comparison.

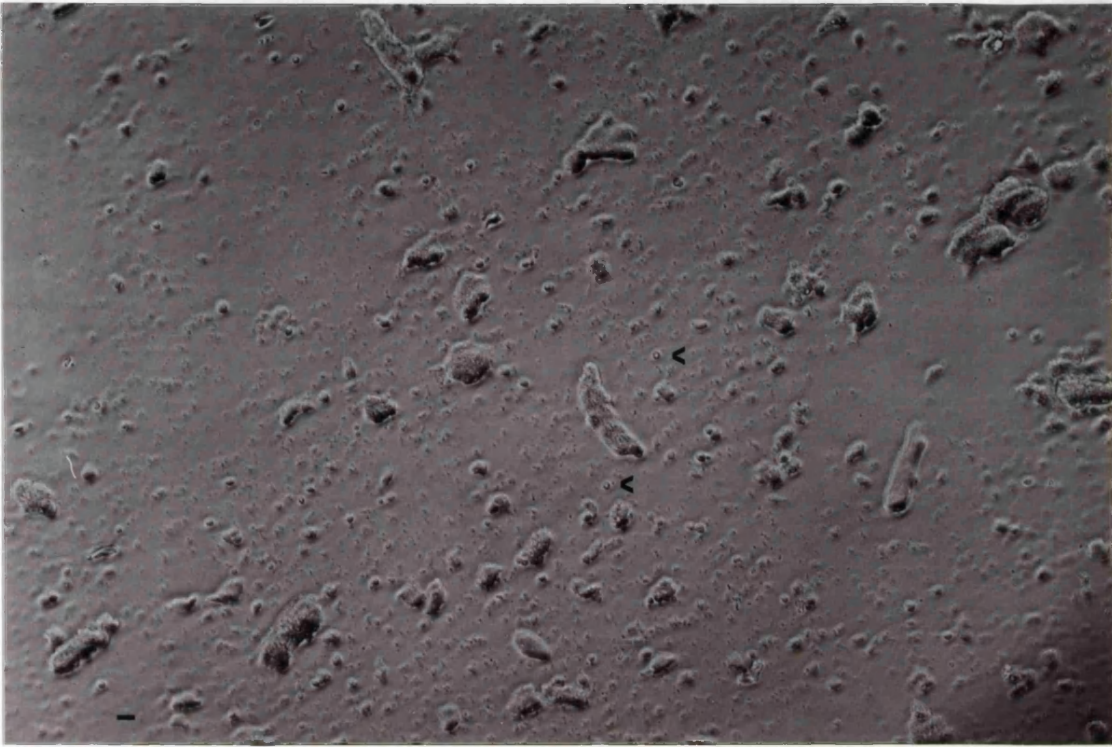
### **5.3. Suitability for patching.**

Neurones were most suitable for patching after 2-3 weeks in culture. At this stage they were relatively compact but sufficiently differentiated to allow them to be distinguished from glia. They were better stuck to the underlying glass slips than younger cells, allowing outside-out patches to be pulled. They were more robust than older cells and had cleaner somatic membranes. Smooth, clean and bleb-free membranes were an absolute requirement for satisfactory seal formation.

**Figure 5.1.**

**Photomicrographs of neostriatal cells 3 hours after dissociation and plating.** (A) Low power view (x 100 magnification; air objective; the scale bar is 25  $\mu\text{m}$ ). Viable, phase-bright, round cells (examples indicated by arrow heads) can just be discerned amongst the undissociated cell clusters and sub-cellular debris. (B) High power view (x 400 magnification; oil immersion objective; the scale bar is 6  $\mu\text{m}$ ). A single dissociated cell (indicated by an arrow head), surrounded by cellular fragments, is shown in the centre of the field.

**A**



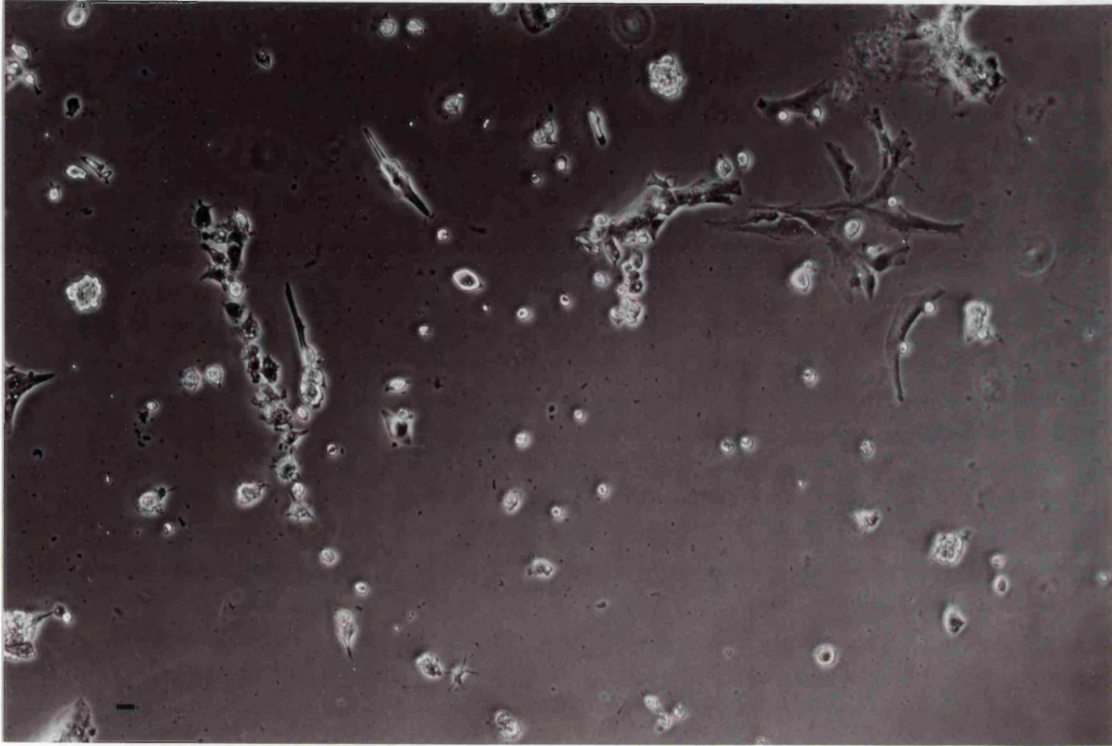
**B**



**Figure 5.2.**

**Photomicrographs of neostriatal cells after 7 days in culture (horse serum-enriched medium). (A) Low power view (x 100, air objective). (B) High power view (x 400, oil objective). The cells have enlarged since plating but show no sign of sprouting and remain indistinguishable.**

**A**



**B**

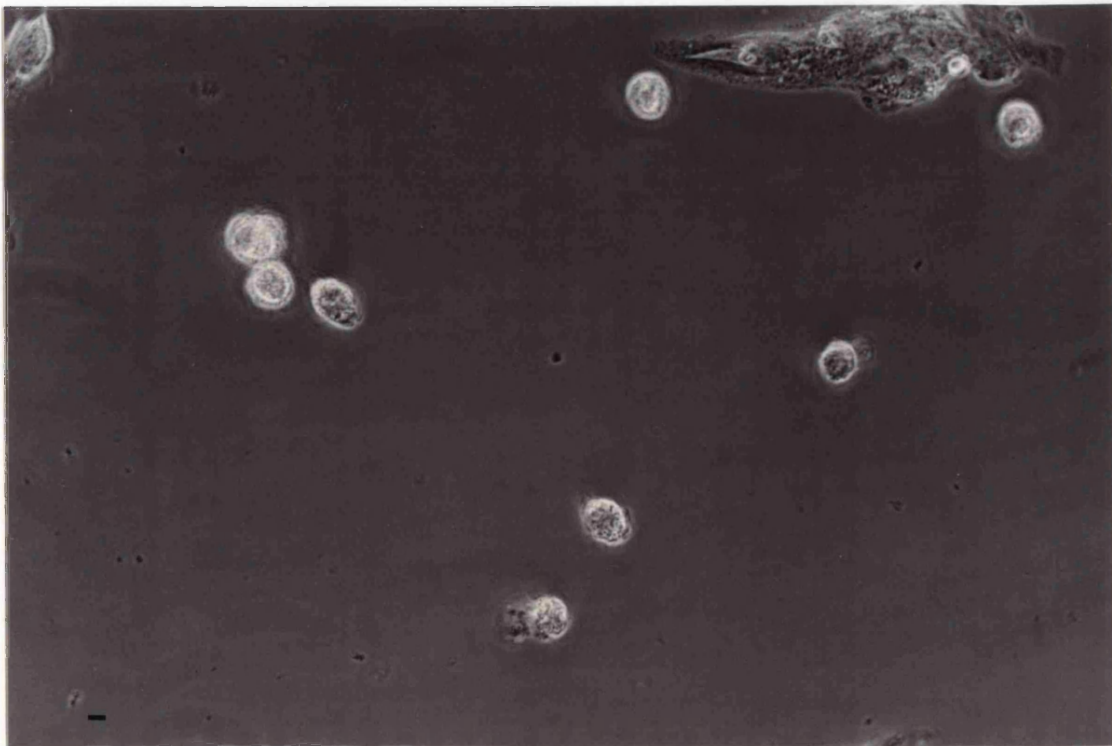
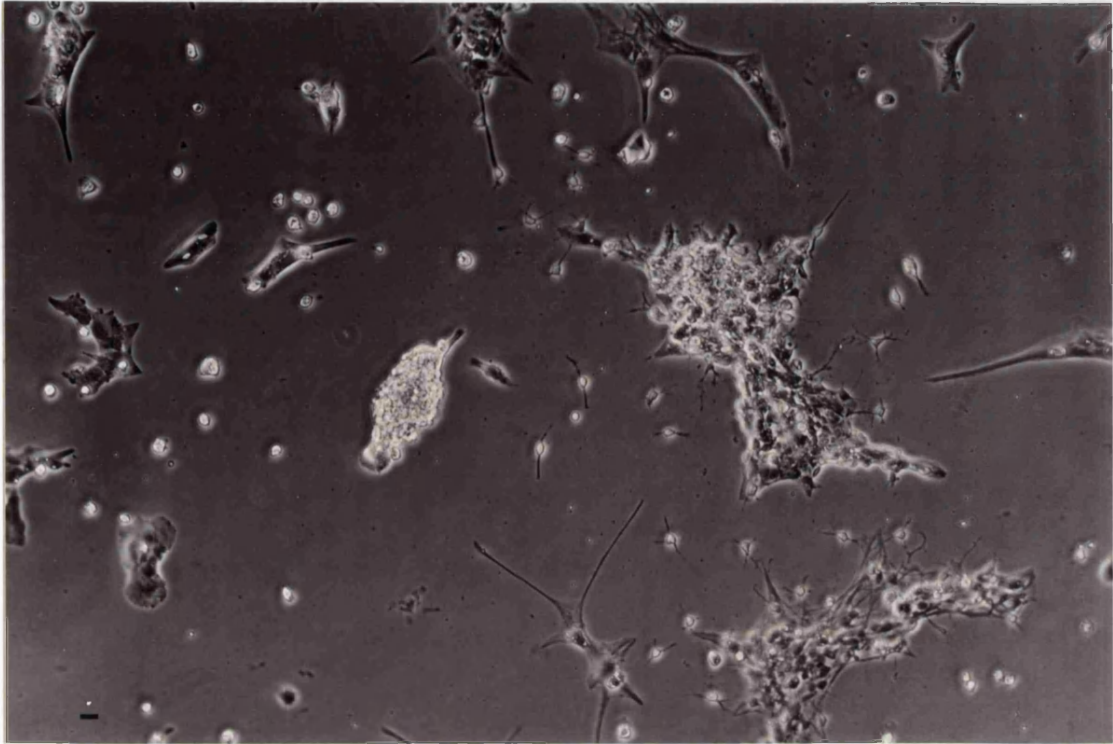


**Figure 5.3.**

**Photomicrographs of neostriatal cells after 11 days in culture.** (A) Low power view (x 100). At this stage neurones and astroglia/microglia have begun to sprout, and possess short processes. Squamous glia have proliferated and spread to form mats. (B) High power view (x 400). This photograph shows that different cell types can start to be distinguished in cultures of this age. The lower central cell (a) is clearly a triangular neurone with three processes. The upper central cell (b) is an astroglial or microglial cell with branching processes emanating from the soma. The bottom right cell (c) is a squamous glial cell.

**A**



**B**

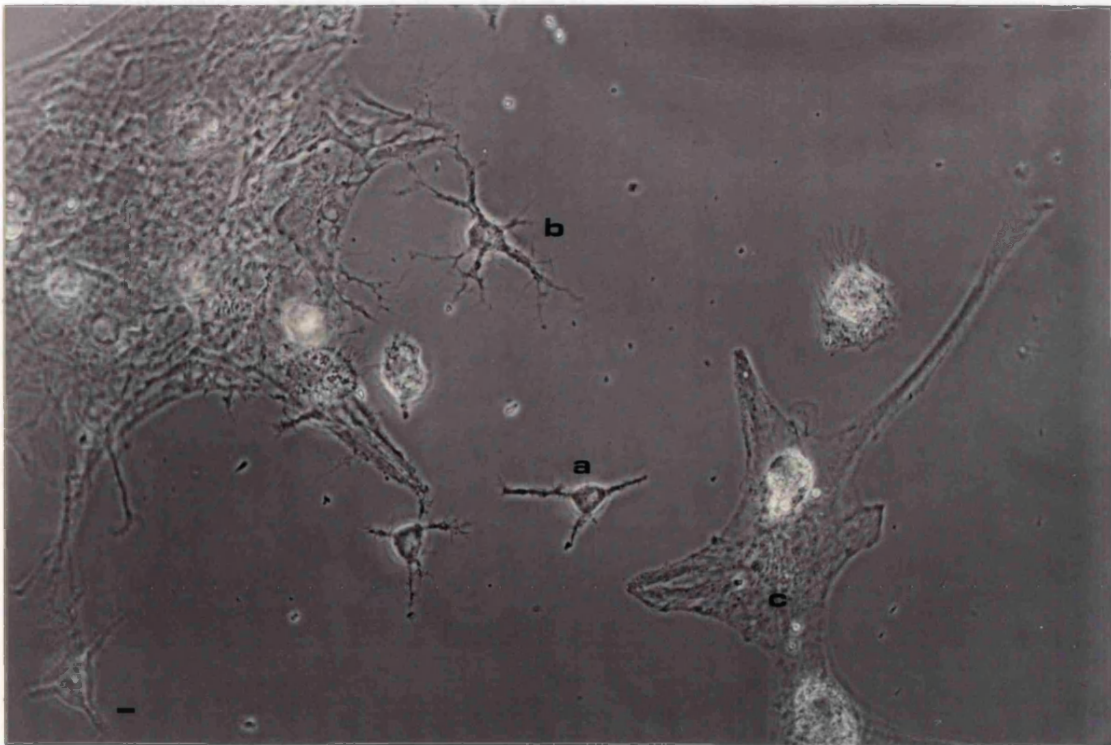
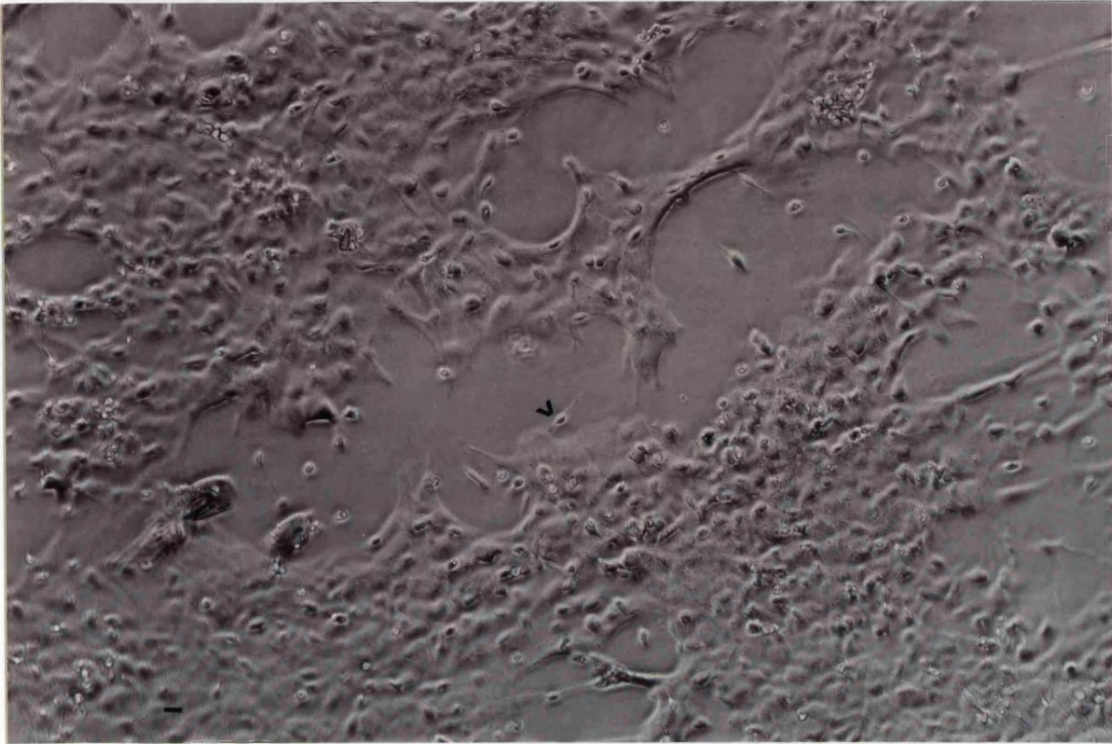


**Figure 5.4.**

**Photomicrographs of neostriatal cultures aged 14 days.** (A) Low power view (x 100). At this stage squamous glia have grown to cover most of the glass slip. The majority of neurones have been overgrown by glia and are unavailable for patching. Some neurones can still be found in lacunae in the mat. Such neurones are most suitable for patching after 2-3 weeks in culture. A patchable neurone whose cell body has not been overgrown is present in the centre of the field of view (indicated by an arrow head). (B) High power view (x 400). The cell shown here (arrow head) is an ovoid neurone suitable for patching. The soma is clean and smooth, and the processes are relatively short. The neurone is at the lower end of the size range for cells used in the study, the long axis of the soma being in the region of 12  $\mu\text{m}$ .

**A**



**B**

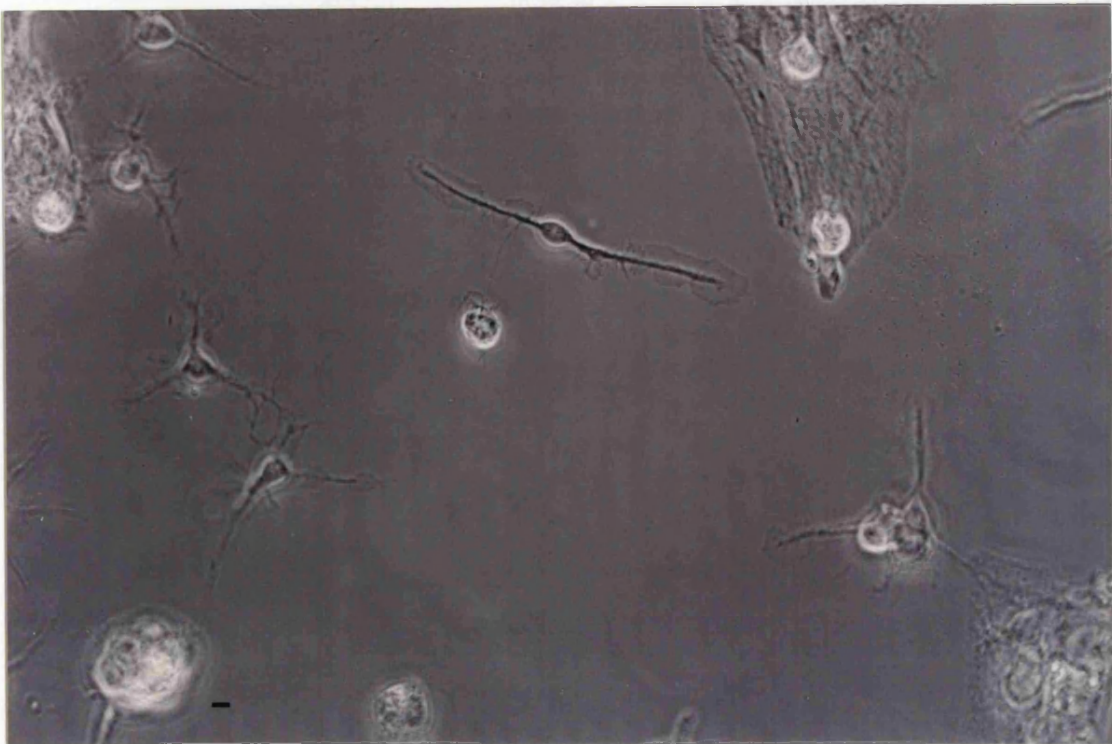
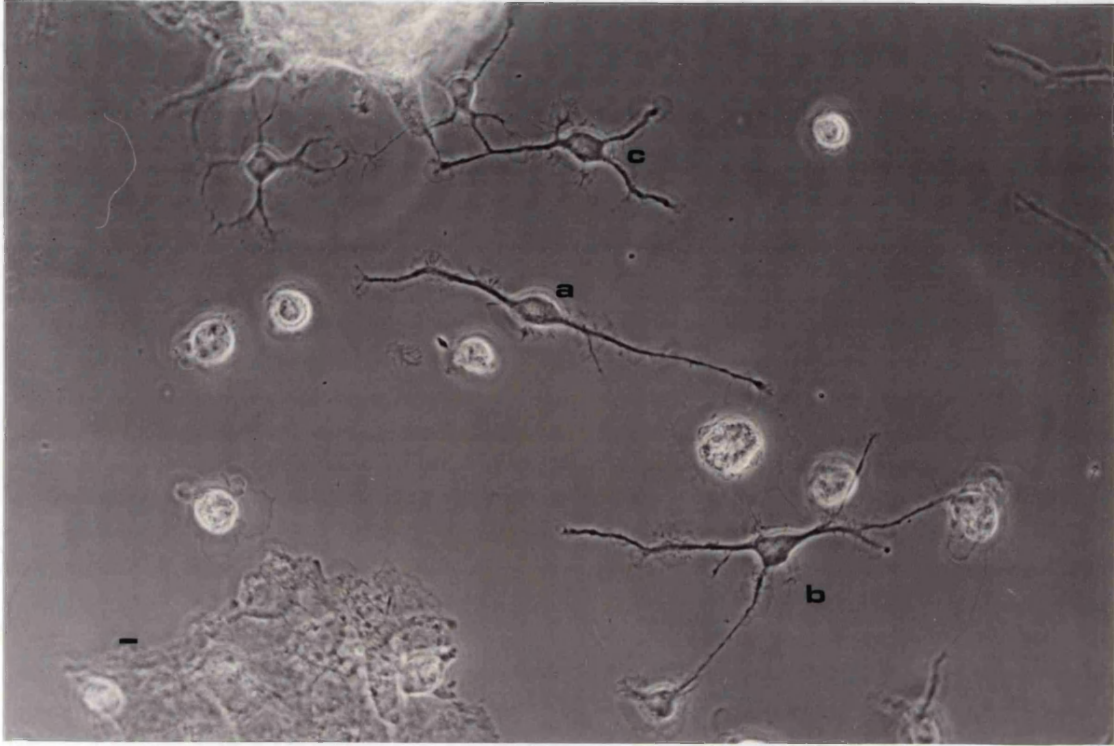


**Figure 5.5.**

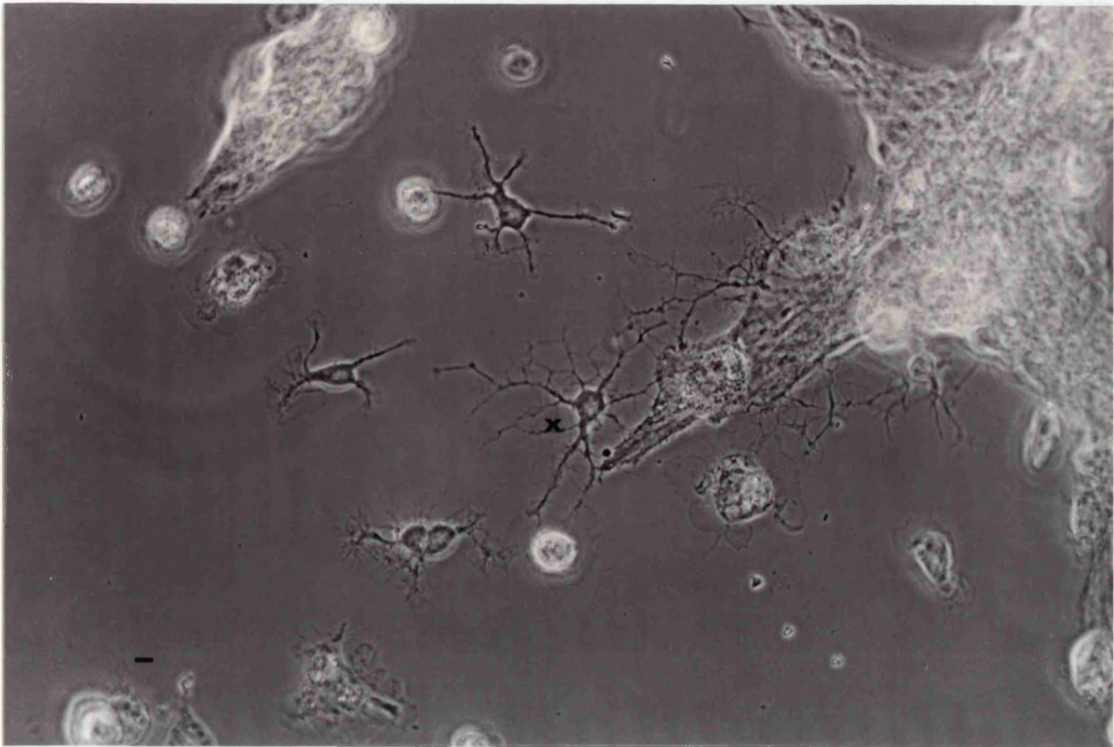
**The appearance of "mature" neurones and glia in culture.**

(A) High power (x 400). This photograph shows the appearance of typical ovoid and triangular neurones which would be used for patching. The middle neurone (a) is a medium-sized ovoid neurone (long axis of soma  $\approx 16 \mu\text{m}$ ) with two major processes. The lower neurone (b) is a triangular neurone, of similar size, with three main processes. The upper neurone (c) has an irregularly-shaped soma, possesses three main processes, and would be classed as a triangular neurone. (B) High power (x 400). The central cell (x) is a glial cell with numerous, branching processes. The remaining cells are unidentifiable and would not be patched.

**A**



**B**



## Section 6. Whole cell patch clamp results.

### 6.1. Whole cell parameters

Cell resting membrane potential (RMP) was measured to the nearest millivolt. Figure 6.1. shows the distribution of resting potentials. Most cells were highly polarized, having resting potentials more negative than -60 mV. The small number of cells with RMP less negative than -51 mV were considered to be unhealthy and results from such cells were discarded.

The open boxes in figure 6.1.A. represent data from 258 cells. Values have been grouped into 5 mV bins. Resting potentials were widely spread with a distribution skewed towards less negative values. Mean and SEM were  $-78 \pm 0.7$  mV. The modal value lay within the -86 to -90 mV bin.

It was noticed that RMP tended to decline throughout the course of an experiment. (See section 6.3.). When care was taken to measure RMP within the first few seconds after seal formation, much less variability was encountered. The closed boxes in figure 6.1.B. show values in 1 mV bins recorded immediately in 21 cells. For this sub-group the modal value was -90 mV, the mean and standard error were  $-88 \pm 0.8$  mV.

Input resistance measured at the resting potential using a +5 mV, 10 ms test pulse (frequency, 50 Hz) was  $360 \pm 25$  M $\Omega$  (mean  $\pm$  SEM, n = 136). Input resistance for the sub-group was  $345 \pm 45$  M $\Omega$  (mean  $\pm$  SEM, n = 21).

**Table 6.1.**

**Values for whole cell parameters.**

<u>Parameter</u>	<u>Mean</u>	<u>SEM</u>	<u>Range</u>	<u>n</u>
Resting potential (mV)	-78	0.7	-53 to -100	258
Initial resting potential (mV)	-88	0.8	-82 to -98	21
Input resistance (M $\Omega$ )	360	25	50 to 1667	136
Iinitial input resistance (M $\Omega$ )	345	45	179 to 1000	21
Electrode resistance (M $\Omega$ )	6	0.1	3 to 10	184
Series resistance (M $\Omega$ )	15.5	0.7	5 to 30	96
Fast component of capacitance (pF)	12.5	0.5	4 to 28	94

## 6.2. Whole cell currents.

Membrane currents were elicited by voltage clamping the cells and stepping to specified potentials. The type of currents produced depended upon the stepping protocol. Total membrane current appeared to be a complicated mixture of voltage-activated and passive components. The currents activated by small voltage steps either side of the resting potential were designated as "leak" currents for the purpose of this study. Such currents could be derived from the passage of ions through voltage-insensitive channels or they could result from the activation and inactivation of a combination of voltage-sensitive channels, selective for different ions.

Cells held at or near their resting potential displayed currents in response to positive and negative voltage steps. Hyperpolarizing steps produced sustained inward currents. Depolarizing steps gave rise to rapidly-activating, transient inward currents and a mixture of transient and sustained outward currents. Figure 6.2.A. shows an example of currents elicited by 1 s negative and positive steps from the resting potential of -90 mV. The transient inward current is not resolved in recordings digitized at this rate (500 Hz).

Figure 6.2.B. shows the current-voltage relationship for the total late current (1 s after the start of the pulse) and total early current (at a time corresponding to the peak of the transient outward current; in this case 10 ms after the start of the pulse).

### 6.2.1. Inward and outward rectification.

In the vast majority of cells (> 95%) the late current rectified inwardly around the RMP. In most cells, as in the example shown in figure 6.2., the I-V relationship was linear between -130 mV and the RMP (conductance  $4.5 \pm 0.8$  nS; mean  $\pm$  SEM, n = 11). It was also usually linear between the RMP and -40 mV (conductance  $3.0 \pm 0.3$  nS; mean  $\pm$  SEM, n = 30), although in some cells the I-V relationship in this region exhibited a marked sag; data from such cells were not included in the calculations. The outward and inward "leak" currents were significantly different ( $p < 0.05$ , two-tailed t-test for unpaired small samples). The ratio of outward to inward leak conductances was  $0.60 \pm 0.03$  (mean  $\pm$  SEM, n = 11).

In addition to these leak conductances, voltage-dependent currents were apparent. An outwardly-rectifying, sustained current was activated at more positive test potentials as can be seen by the inflection of the late current-voltage curve (figure 6.2.B.) at around -40 mV. It can also be seen that an outwardly-rectifying transient current was activated at much more negative potentials than the sustained one (i.e. the early current was larger than the late current). In the example shown in figure 6.2., a rapidly-activating, transient component is clearly visible in the current record elicited by a step to -60 mV.

For cells bathed in normal extracellular medium containing 3 mM  $K^+$ , the inwardly rectifying current reversed at the RMP, which was initially close to the projected potassium equilibrium potential of -97 mV. For cells bathed in 140 mM  $K^+$  the reversal potential was 0 mV. The leak currents were 3-4 times larger ( $p < 0.01$ , unpaired t-test) and the inward rectification more pronounced with the ratio of outward to inward leaks being  $0.43 \pm 0.06$  (mean  $\pm$  SEM, n = 5). These properties are shown in figures 6.3.A. and 6.3.B.

### 6.2.2. Sodium current ( $I_{Na}$ )

A fast inward current was apparent in all healthy cells (in recordings sampled and filtered at an appropriate frequency) and exhibited characteristics typical of a sodium current. It was often partly obscured by a rapidly-activating outward current. Using the normal recording protocol (i.e. KCl in the recording electrode) it was impossible to produce a satisfactory current-voltage relationship for the inward current. This problem was overcome by substituting 140 mM CsCl for the KCl in the recording pipette. Such a concentration of internal  $Cs^+$  would be expected to block most  $K^+$  currents.

Under these conditions outward currents were small or absent. The resting membrane potential was  $-34 \pm 2.1$  mV (mean  $\pm$  SEM,  $n = 7$ ), significantly less negative than with 140 mM KCl in the pipette ( $p < 0.001$ ; unpaired t-test). Outward leak conductance was  $3.2 \pm 1.9$  nS (mean  $\pm$  SEM,  $n = 7$ ), similar to that seen under standard conditions. The inward current was well defined. An example is shown in figure 6.4.A. Its activation was rapid (peak current within 1.5 ms for all test potentials) as was its inactivation (complete within 3 ms). Activation and inactivation became progressively faster as the magnitude of the depolarizing step increased. With 3  $\mu$ M tetrodotoxin (TTX) present in the bathing medium,  $I_{Na}$  was completely absent ( $n = 6$ ).

Figure 6.4.B. shows the current-voltage relationship for  $I_{Na}$  with 140 mM CsCl in the patch pipette. Activation threshold was between -50 mV and -40 mV, the mean and SEM being  $-45 \pm 1.7$  mV ( $n = 7$ ). The current amplitude was maximal between -10 mV and +5 mV ( $0 \pm 2.2$  mV; mean  $\pm$  SEM,  $n = 7$ ) when stepping from -80 mV. Peak amplitude ranged between 96 pA and 800 pA ( $440 \pm 86$  pA; mean  $\pm$  SEM,  $n = 7$ ). The current reversed close to the calculated sodium equilibrium potential of +86 mV (range +75 mV to +100 mV,  $n = 7$ ). Maximal conductance ( $G_{max}$ ) ranged between 4.0 nS and 11.2 nS ( $6.6 \pm 1.1$  nS; mean  $\pm$  SEM,  $n = 7$ ).

### 6.2.3. Voltage-dependent, sustained potassium current ( $K_s$ )

A depolarization-activated, sustained outward current, as shown in figure 6.5.A., was present to a variable degree. The current activated over tens of milliseconds and persisted throughout the duration of a 1 s step. All cells exhibited such a current when tested immediately but  $K_s$  was particularly susceptible to rundown (despite attempts to minimise this phenomenon by including ATP and GTP in the patch pipette) and often disappeared within a few minutes of seal formation. (See section 6.3.).

Figure 6.5.B. shows an activation curve for  $K_s$ . The threshold for activation (i.e. the potential at which outward rectification of the late current was first noticeable) ranged between -50 mV and -25 mV ( $-35 \pm 0.9$  mV; mean  $\pm$  SEM,  $n = 32$ ; mode = -30 mV). Maximal conductance ranged between 3.1 nS and 36.0 nS ( $11.3 \pm 1.1$  nS; mean  $\pm$  SEM,  $n = 39$ ). The example shown was fitted with the Boltzmann equation. The activation threshold is  $\approx -40$  mV. The half activation voltage ( $V_h$ ) is -7.1 mV, and the slope factor ( $z$ ) is 2.5.

Figure 6.6. shows the effects of high concentrations of the tetraethylammonium ion (TEA) on the "leak" and voltage-activated outward currents. Inclusion of 20 mM TEA in the bathing medium reduced mean  $K_s$  to 68% of its magnitude in control bathing medium ( $n = 9$ ). It was reduced to 31% of its control value in 40 mM TEA ( $n = 2$ ). These differences just failed to reach significance (unpaired t-test for small samples). The leak currents and the transient outward currents were not affected by TEA at these concentrations. The RMP ( $-78 \pm 4.0$  mV; mean  $\pm$  SEM,  $n = 8$ ) was also unaffected by bathing in TEA.

#### 6.2.4. Voltage-dependent, transient potassium currents ( $K_t$ )

Almost all cells possessed rapidly-activating transient outward currents. The proportions of transient and sustained currents varied. Sometimes the transient currents were absent or were small and merely increased the rate of attainment of a plateau current (figure 6.7.A.). More often, however, transient currents dominated the recording (figure 6.7.B.). Peak current occurred between 5 ms and 10 ms after the onset of the depolarization. Maximal conductance of the peak transient component was  $17.9 \pm 1.7$  nS (mean  $\pm$  SEM,  $n = 31$ ).

A prominent feature of the transient outward currents was that they exhibited voltage-dependent inactivation. They could only be elicited by stepping from holding potentials more negative than -20 mV. Their magnitude increased progressively with more negative holding potentials as shown in figure 6.8.A. The sustained current elicited by stepping from -20 mV has been subtracted from these traces. Figure 6.8.B. shows an inactivation curve for the peak of the transient component. Mean and SEM values from 9 cells are plotted. The threshold for removal of inactivation was between -20 mV and -30 mV. Conductance was maximal at -70 mV to -80 mV. (Boltzmann fit:  $V_h = -50.2$  mV,  $z = 4.4$ )

There is evidence to suggest that a number of different transient  $K^+$  currents are expressed by these cells. It appears that a variable mixture of transient currents is activated in each cell but it has proven difficult to separate the individual components. A spectrum of different activation and inactivation characteristics have been encountered. The threshold for activation was highly variable, ranging from -80 mV to -40 mV ( $-50 \pm 1.2$  mV; mean  $\pm$  SEM,  $n = 27$ ). Figure 6.9.A. shows extreme examples of activation curves for two transient conductances. The first had its threshold close to -55 mV and was steeply voltage-dependent ( $z = 6.8$ );  $V_h$  was -30.3 mV. The second had its threshold at -40 mV;  $V_h$  was +8.2 mV and  $z$  was 1.9. Extreme

examples of the inactivation parameters are shown in figure 6.9.B. Inactivation of the first conductance was steeply voltage dependent ( $z = 5.1$ ) with threshold for relief of inactivation at  $-40$  mV,  $V_h$  of  $-58.6$  mV, and total relief at  $-70$  mV. Inactivation of the second conductance was much less steeply voltage dependent ( $z = 2.6$ ); threshold for relief was closer to  $-20$  mV,  $V_h$  was  $-50.7$  mV, and relief was complete only at  $-100$  mV.

A rapidly inactivating A-type transient current was observed in all but a handful of the cells tested. Its decay constant ranged between 10 ms and 50 ms. However, the decay phase of the total outward current was often inadequately fitted by a single exponential function. A more slowly inactivating current having some properties in common with the D-current was also evident in some cells. This slower component, which had a decay constant of hundreds to thousands of milliseconds, is discernible in the current records of figures 6.2.A. and 6.8.A. Part of the current remained inactivated over a matter of seconds, a characteristic typical of D-type currents. Figure 6.10. shows the currents elicited by similar pulses separated by 1 s. It can be seen that a slowly-decaying component of the current was refractory to re-activation.

A-type currents were blocked by 4-aminopyridine (4-AP) at concentrations of  $100 \mu\text{M}$ ,  $1$  mM and  $5$  mM. Figure 6.11.A. indicates that the block was voltage dependent and only partially reversible on washing. Figure 6.11.B. shows the currents elicited in the presence of 4-AP by two  $100$  mV steps  $1$  s apart. On the first step the transient  $\text{K}^+$  current was attenuated or absent whilst on subsequent steps the block was substantially relieved. It can be seen that the slowly-decaying transient component, unlike the D-current in hippocampal neurones (Storm, 1988) was insensitive to block by  $1$  mM 4-AP.

### 6.3. Instability of the recordings

It was noticeable that the resting potential declined rapidly during the five minutes after seal formation. It tended to stabilize thereafter. The RMP was significantly lower than its initial value at all times between 5-30 minutes after seal formation ( $p < 0.01$ , sign test for paired samples). This is demonstrated in figure 6.12.A. Mean and SEM are plotted for 7 cells. Currents also declined and were too unstable for reliable assessments of the effects of drugs or transmitters to be made. Figure 6.12.B. shows an example of the degree of deterioration after 30 mins. Late current is displayed. In this cell the RMP fell from -90 mV to -76 mV. Inclusion of 2 mM ATP and 300  $\mu$ M GTP in the patch pipette failed to prevent RMP deterioration and current run down.

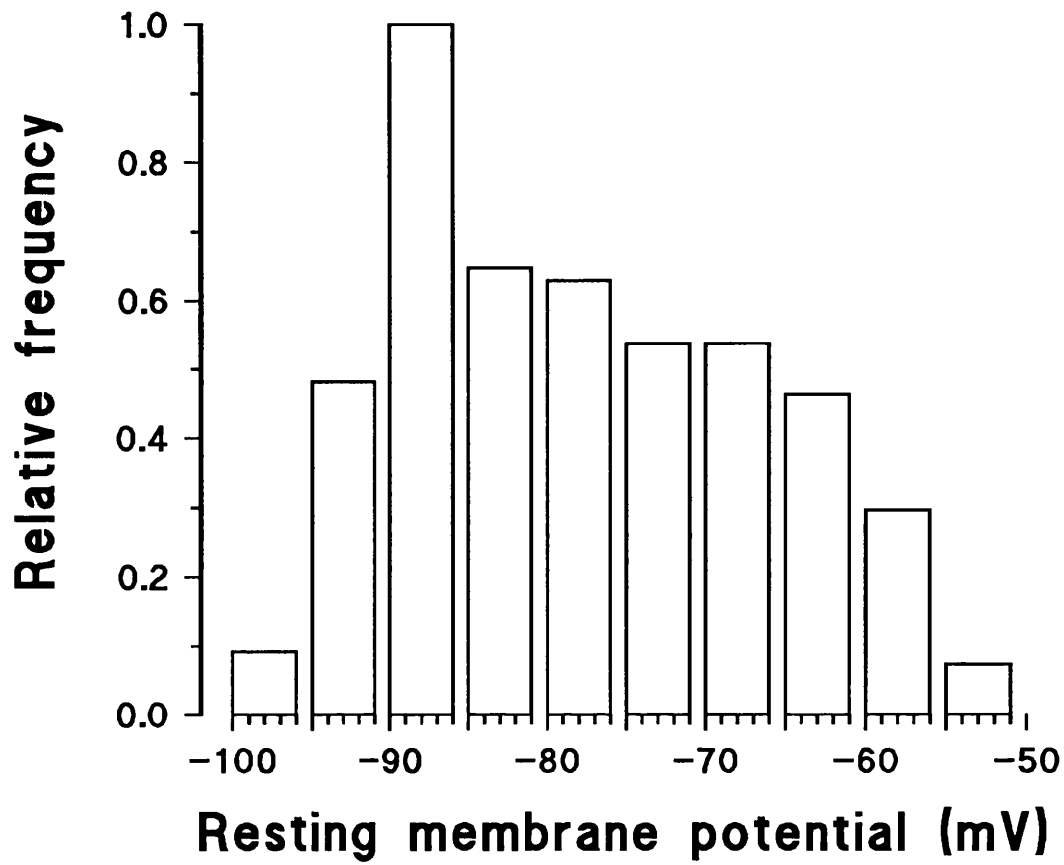
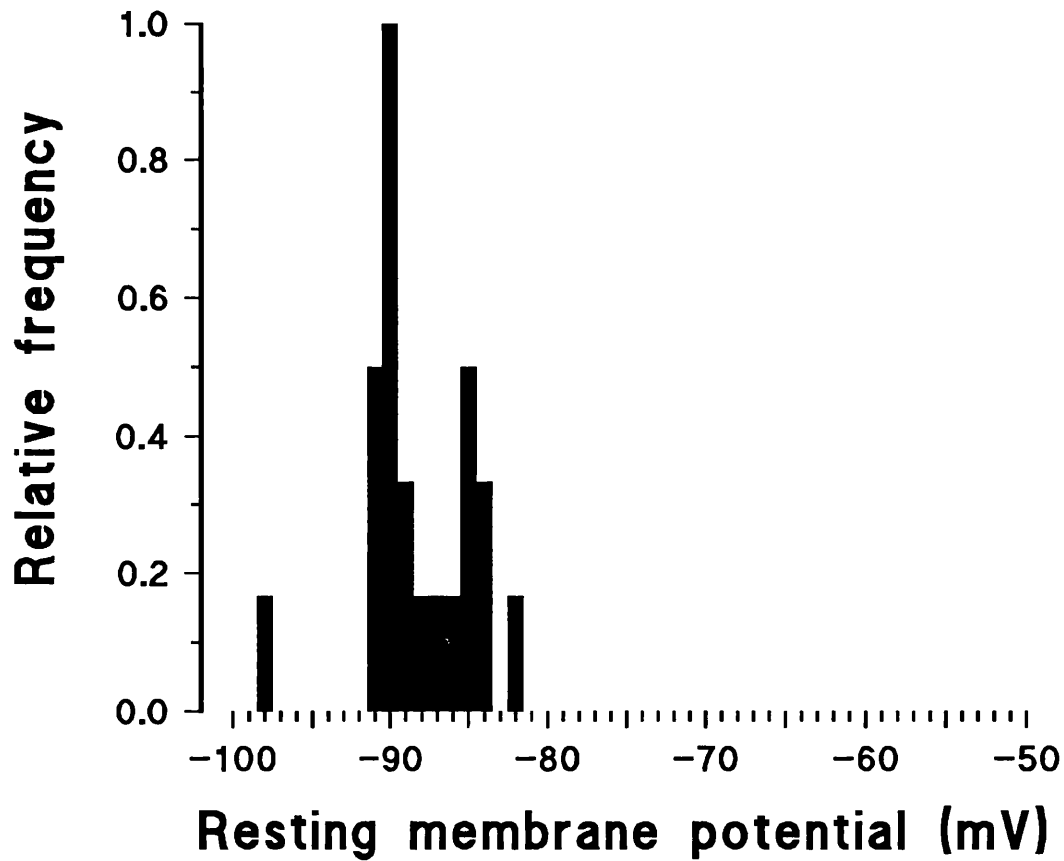
**Table 6.2.**

The magnitude of the various conductances at the beginning and end of the experiment shown in figure 6.12.B.

<u>(nS)</u>	<u>Initially</u>	<u>After 30 mins</u>	
$K_s$	12.8	4.2	(33%)
$K_t$	18.2	9.0	(49%)
$Leak_{out}$	2.2	1.3	(65%)
$Leak_{in}$	3.8	4.1	(108%)

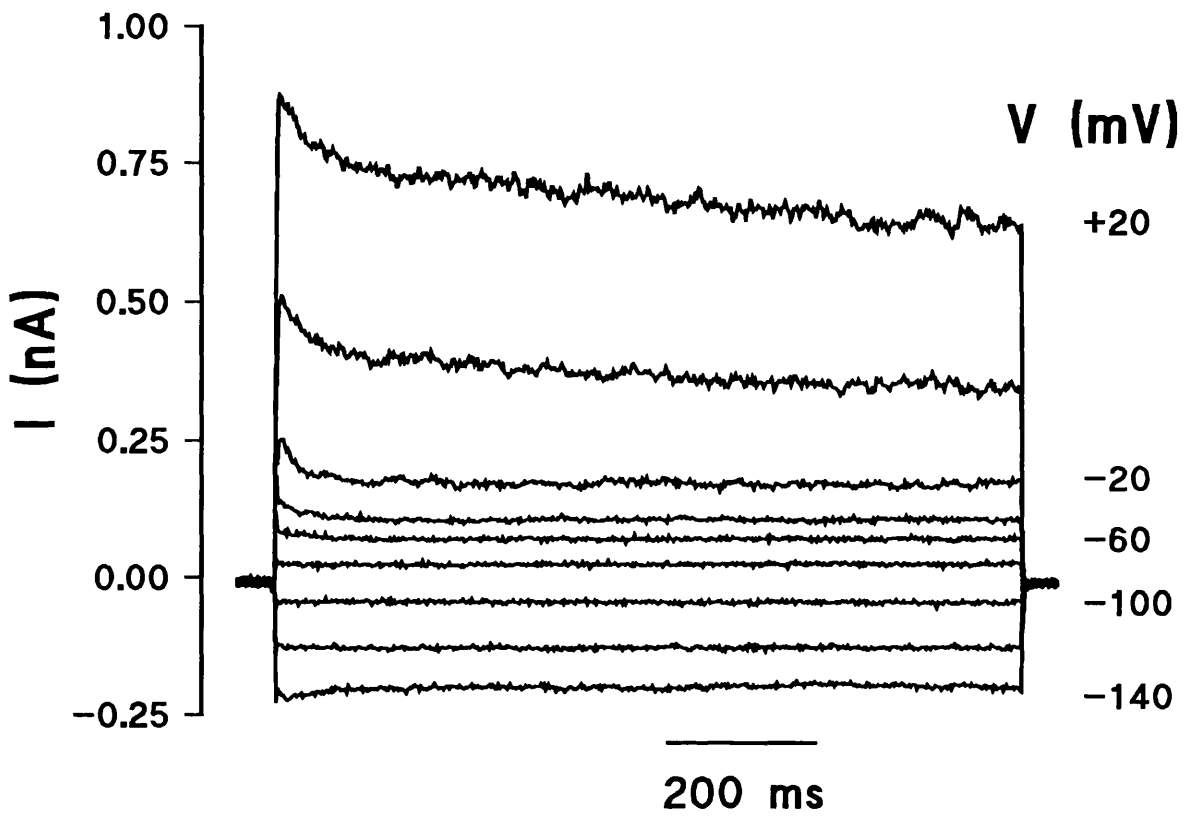
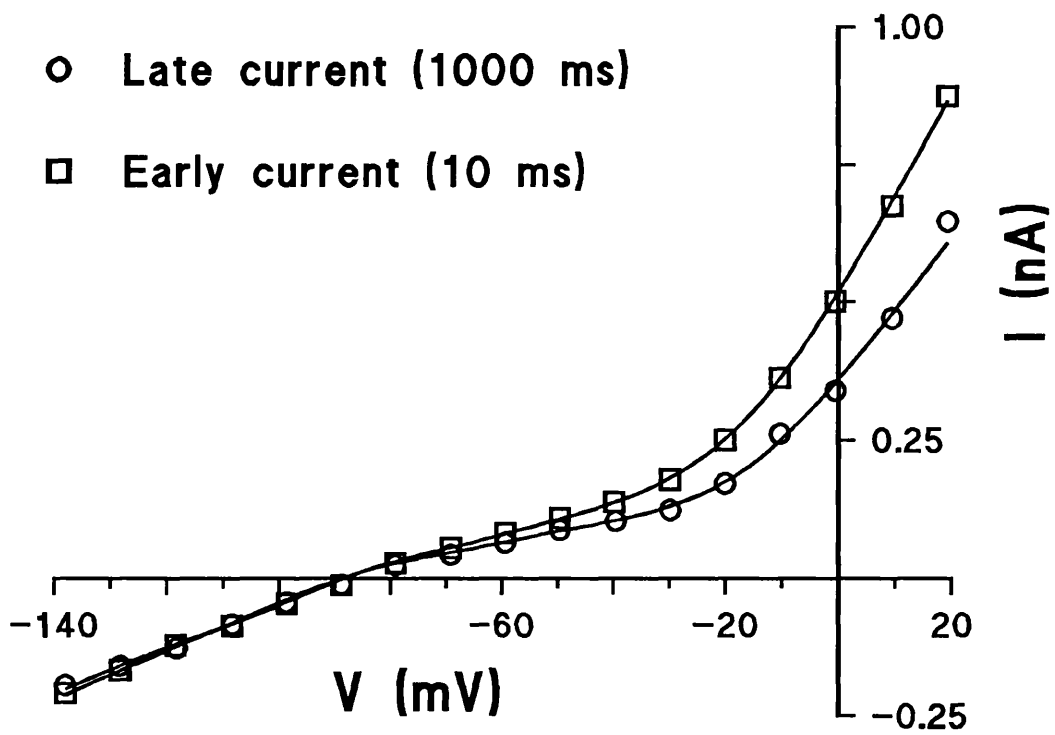
**Figure 6.1.**

**Distribution of resting potentials.** (A) Relative frequency (5 mV bins) of different resting potentials measured at various times after seal formation (n = 258). (B) Relative frequency (1 mV bins) of different resting potentials measured immediately after seal formation (n = 21).

**A****B**

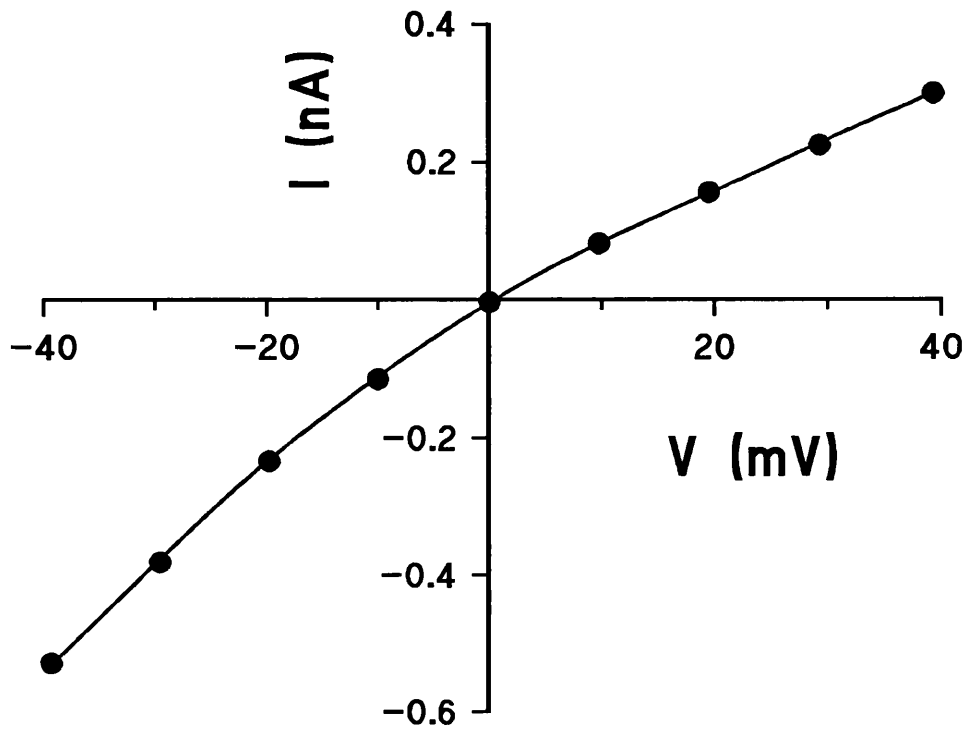
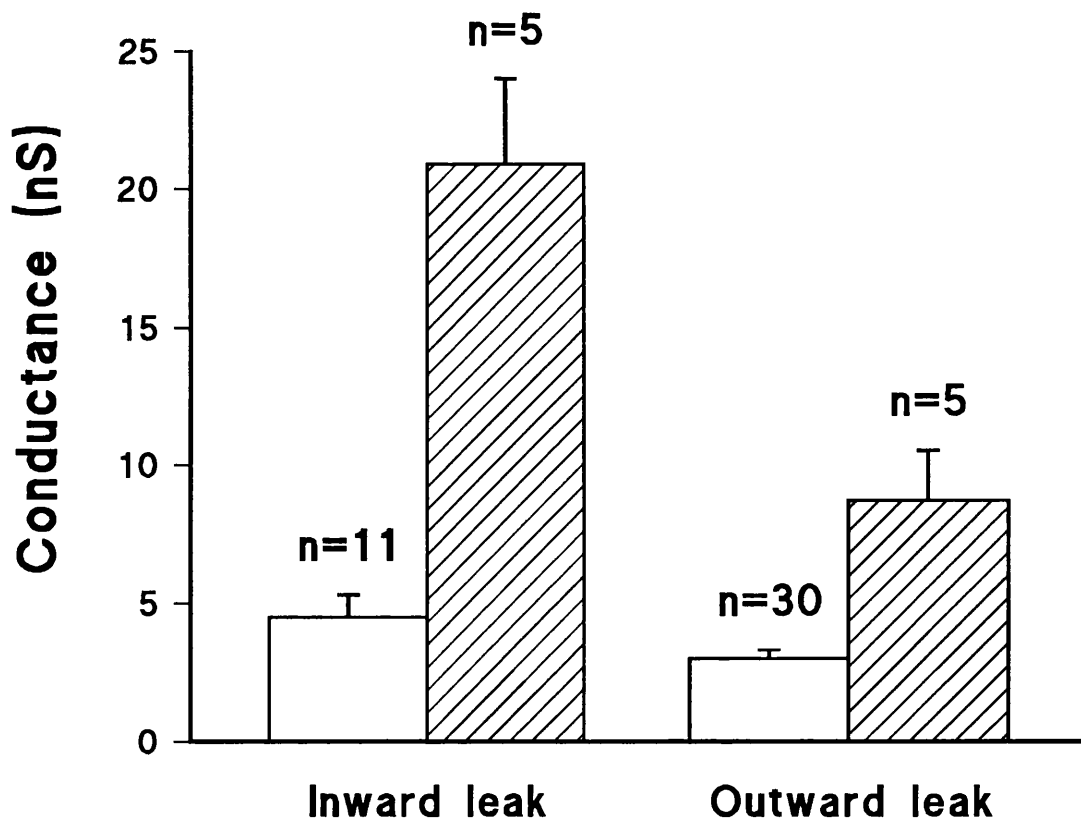
**Figure 6.2.**

Whole cell currents elicited by voltage steps from the resting potential (-90 mV). (A) Record of currents evoked by 1000 ms steps to different potentials. Inward currents are negative and outward ones positive. The cell was bathed in artificial cerebrospinal fluid (aCSF). Sustained and transient outward currents were resolvable at the sampling frequency of 500 Hz but fast inward currents were not. (B) Current-voltage (I-V) relationship for the net early and late currents.

**A****B**

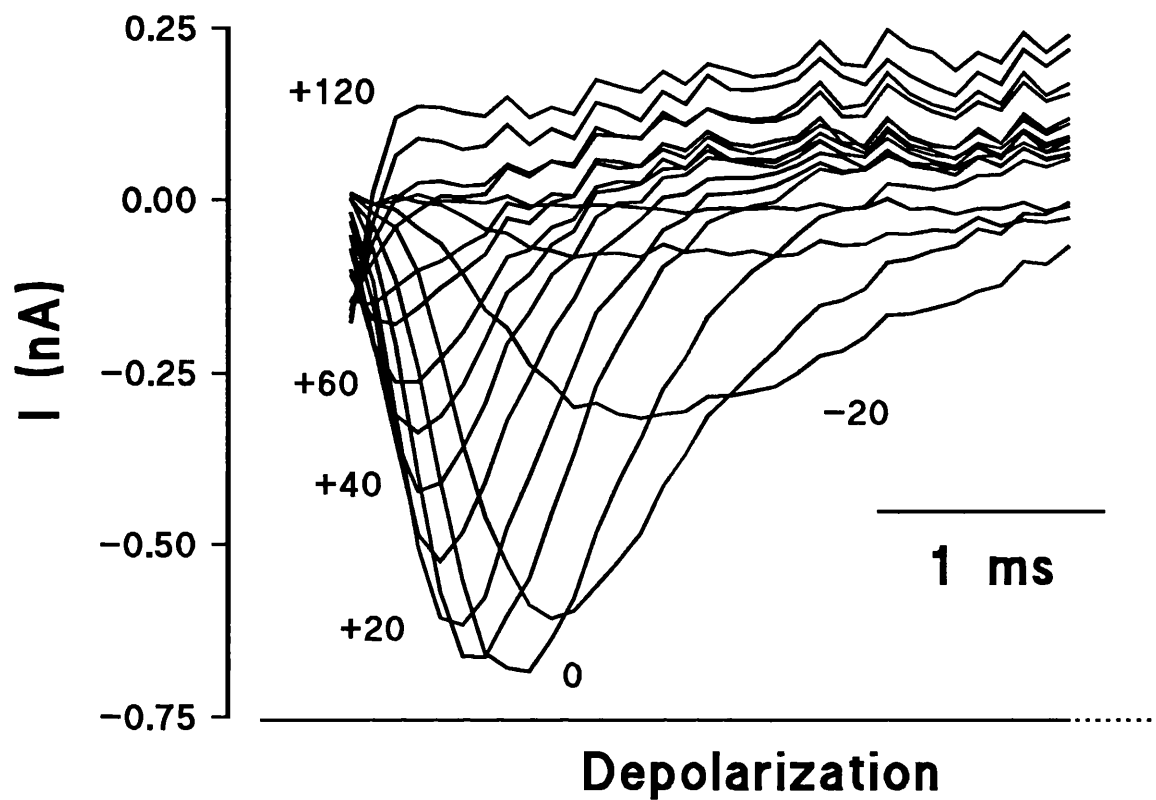
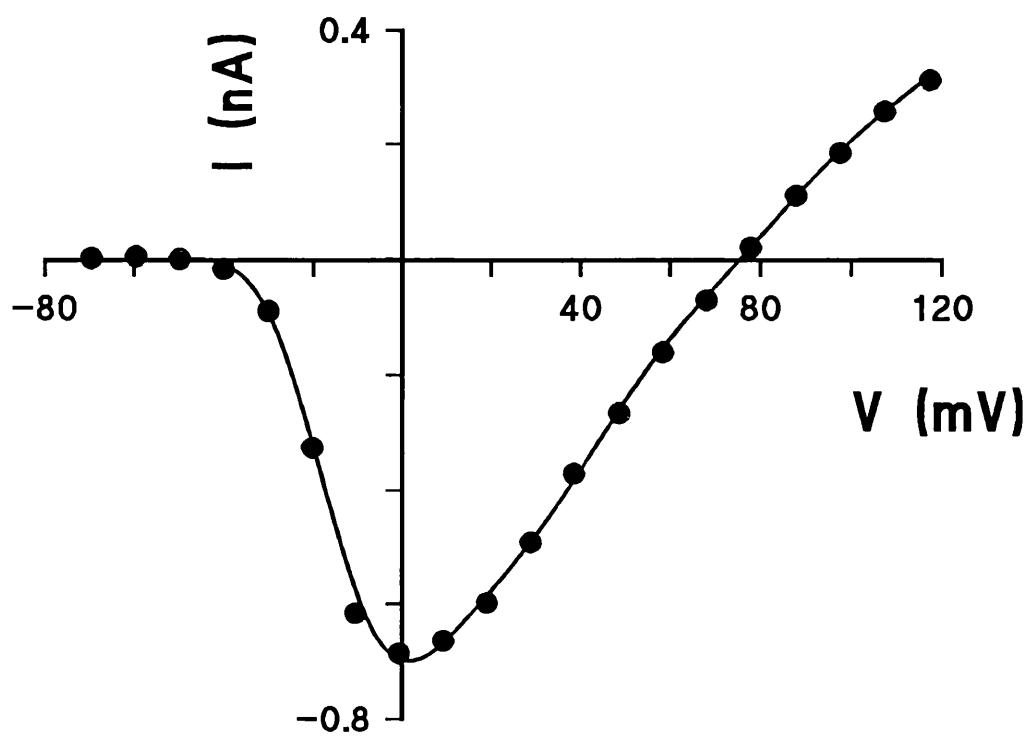
**Figure 6.3.**

**Inwardly-rectifying whole cell currents recorded with cells bathed in a solution containing 140 mM K<sup>+</sup>.** (A) Example of an I-V relationship for a cell bathed in 140 mM K<sup>+</sup>. (B) Bar chart comparing the leak currents either side of the reversal potential for cells bathed in normal aCSF (open boxes) and 140 mM K<sup>+</sup>-containing media (hatched boxes). Mean and SEM values are shown and the sample size for each group is indicated. The inward leak was significantly greater than the outward leak with the cells bathed in aCSF ( $p < 0.05$ ; unpaired t-test) and high K<sup>+</sup> solution ( $p < 0.01$ ). Inward and outward currents were significantly larger in high K<sup>+</sup> solution than in aCSF ( $p < 0.01$ ).

**A****B**

**Figure 6.4.**

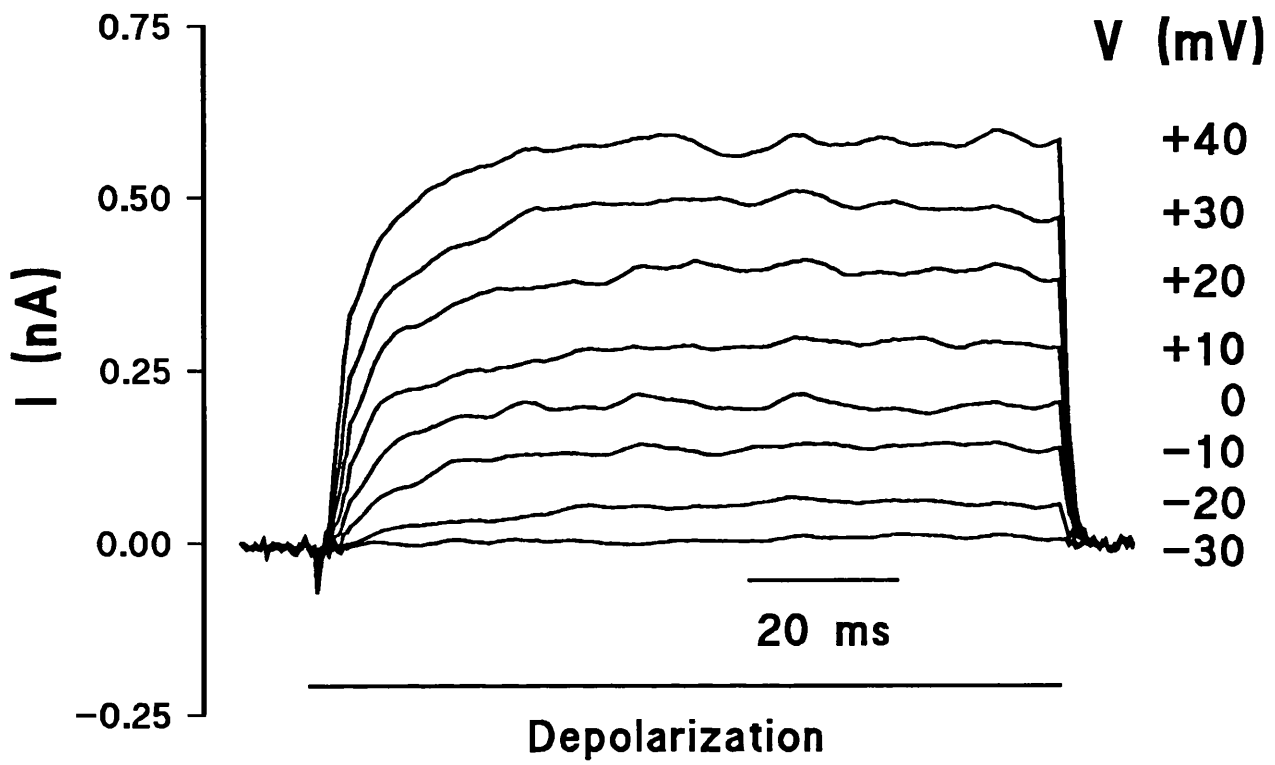
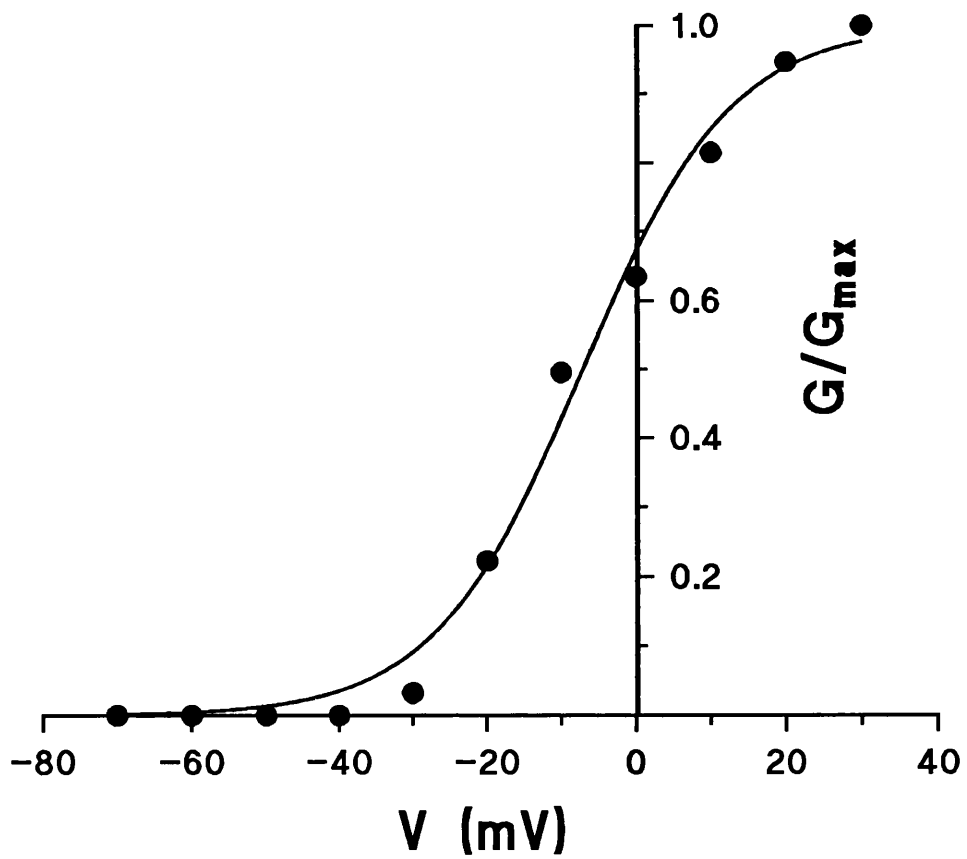
**Sodium currents recorded with 140 mM CsCl in the patch pipette.** (A) Currents elicited by stepping to different potentials from a holding potential of -80 mV. Test potentials (mV) are indicated by the numbers next to the traces. Cells were bathed in aCSF. Sampling frequency was 10 kHz and the records were filtered at 5 kHz. (B) I-V relationship for the peak sodium current shown in part A.

**A****B**

**Figure 6.5.**

**Sustained outward currents elicited by depolarizing steps.**

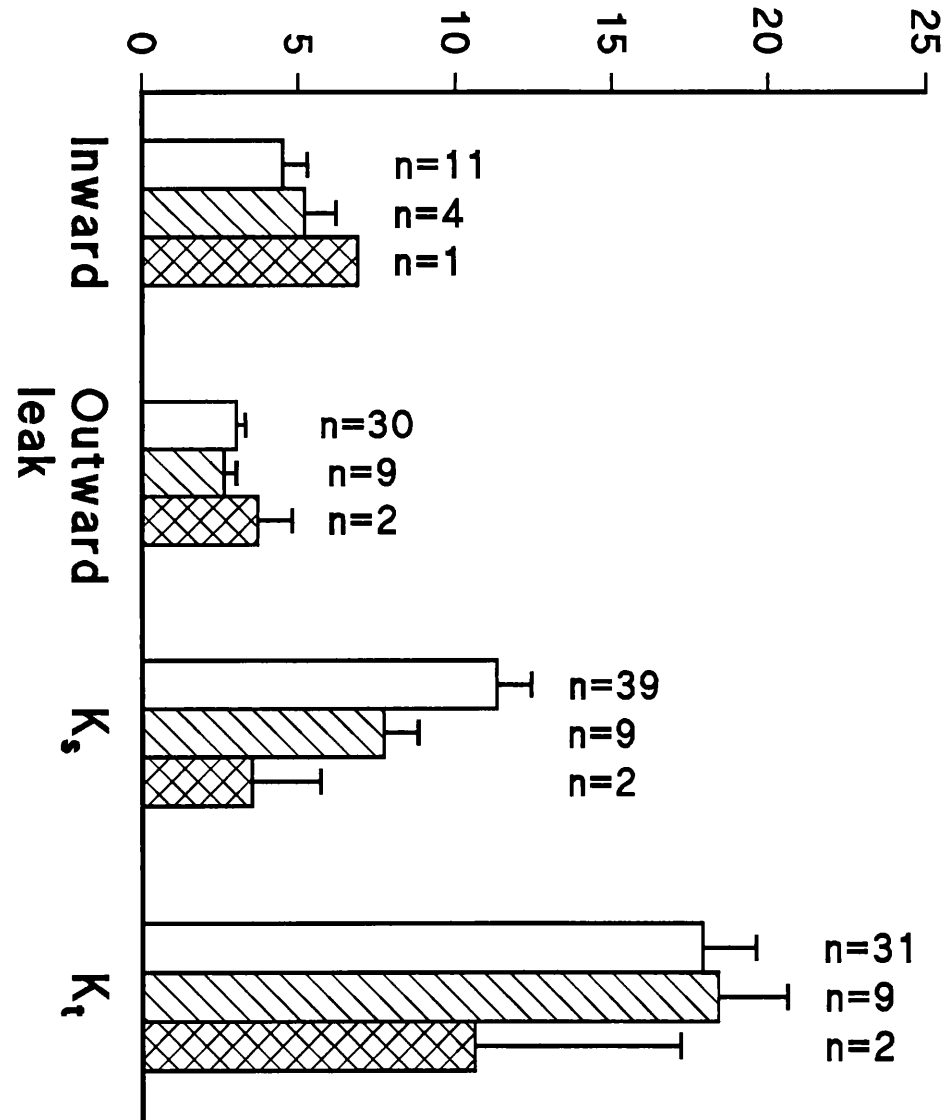
(A) Whole cell potassium currents evoked from a cell bathed in aCSF by stepping from -80 mV. In this particular cell outward currents were predominantly of the sustained type. Records were sampled at 2.5 kHz. The plateau phase was smoothed using Savitzky-Golay cubic averaging, 20 points, 1 pass. (B) An activation curve for the sustained (late) current shown in part A. The proportion of maximal conductance ( $G/G_{\max}$ ) activated at each test potential is plotted. Points were fitted with a Boltzmann function. The half activation potential ( $V_h$ ) is -7.1 mV and the slope factor ( $z$ ) is 2.5.

**A****B**

**Figure 6.6.**

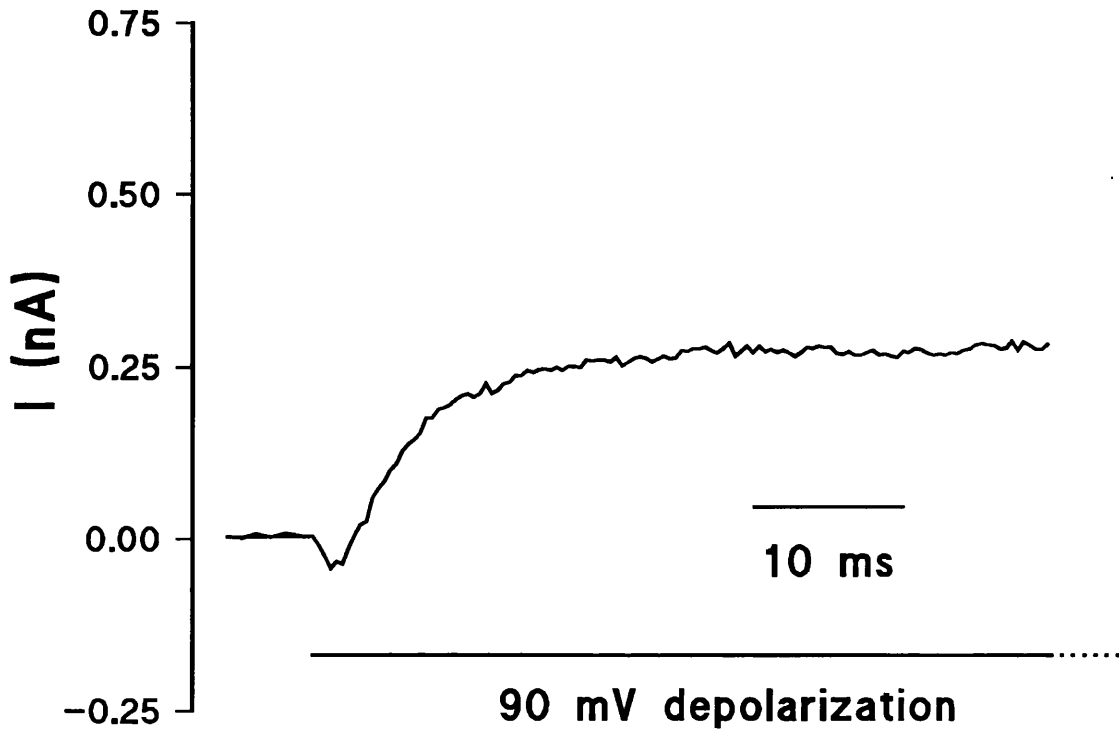
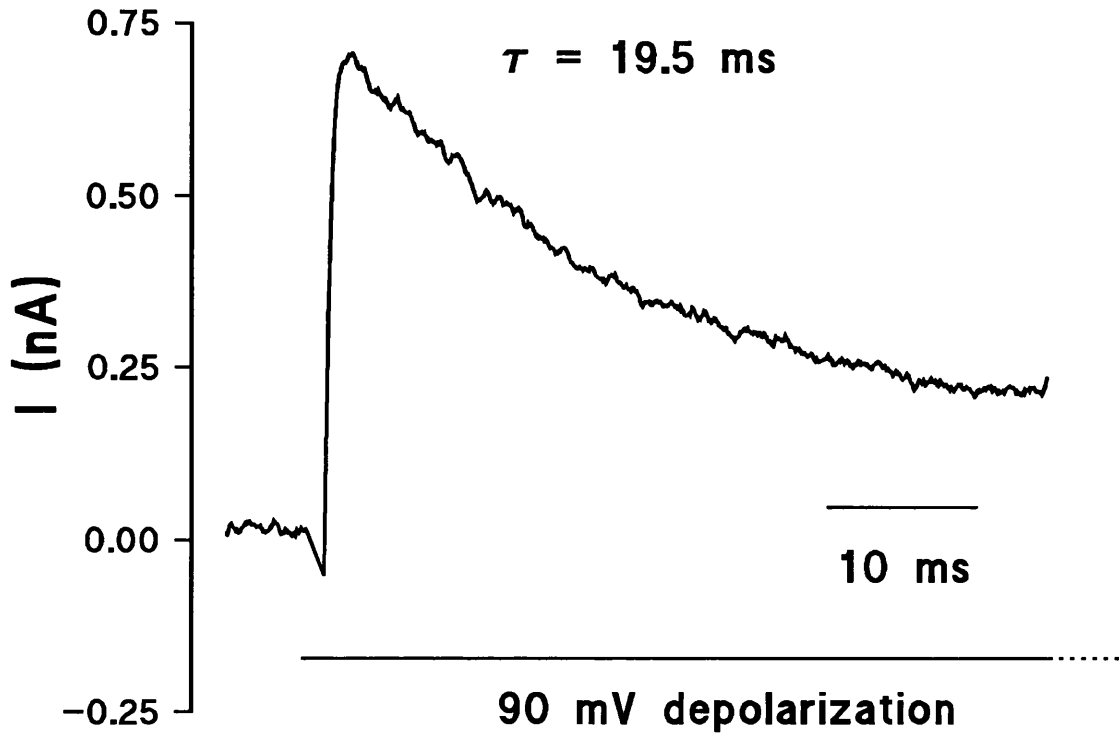
Bar chart showing the effects of tetraethylammonium (TEA) on voltage-activated and leak currents. Mean and SEM values for leak currents, sustained currents ( $K_s$ ) and transient currents ( $K_t$ ) are shown in control aCSF (open bars), 20 mM TEA (hatched bars) and 40 mM TEA (crossed bars). Sample size is indicated for each group. There were no significant differences in the magnitude of any currents between TEA and control groups.  $K_s$  was smaller in 20 mM and 40 mM TEA but the difference just failed to reach significance (unpaired t-test) due to the variability of  $K_s$ .

# Conductance (nS)



**Figure 6.7.**

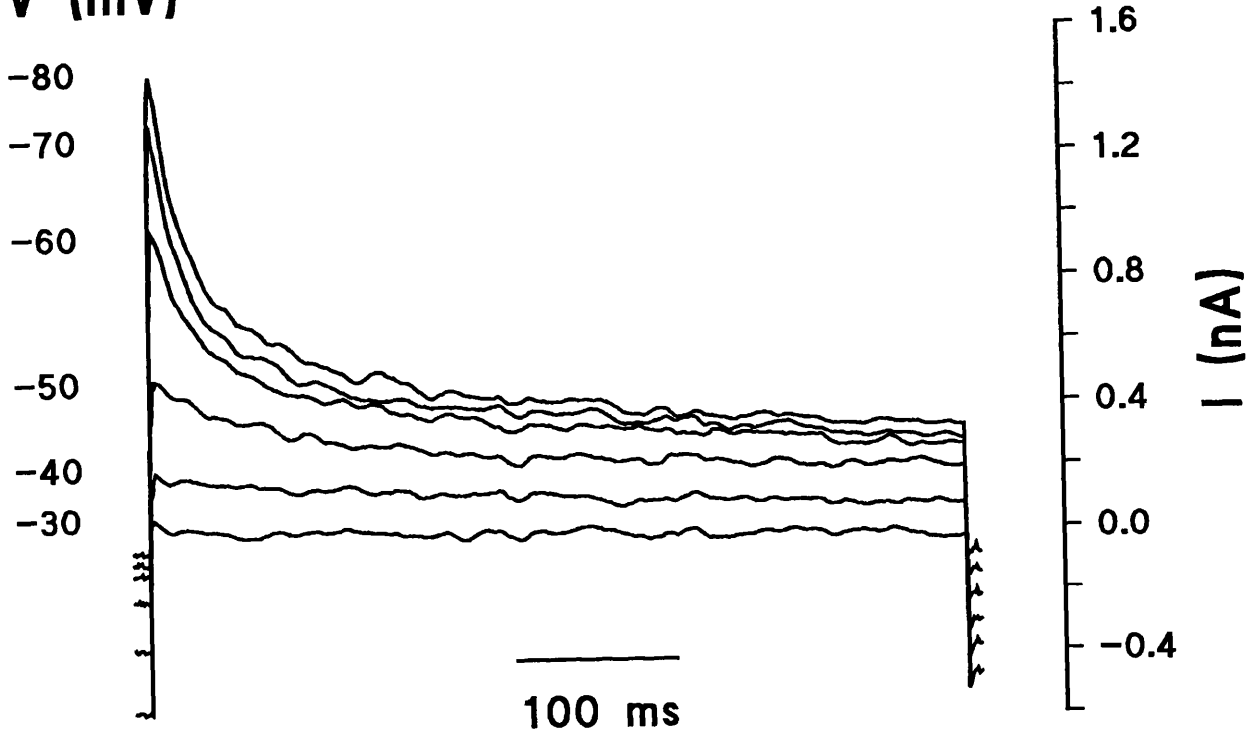
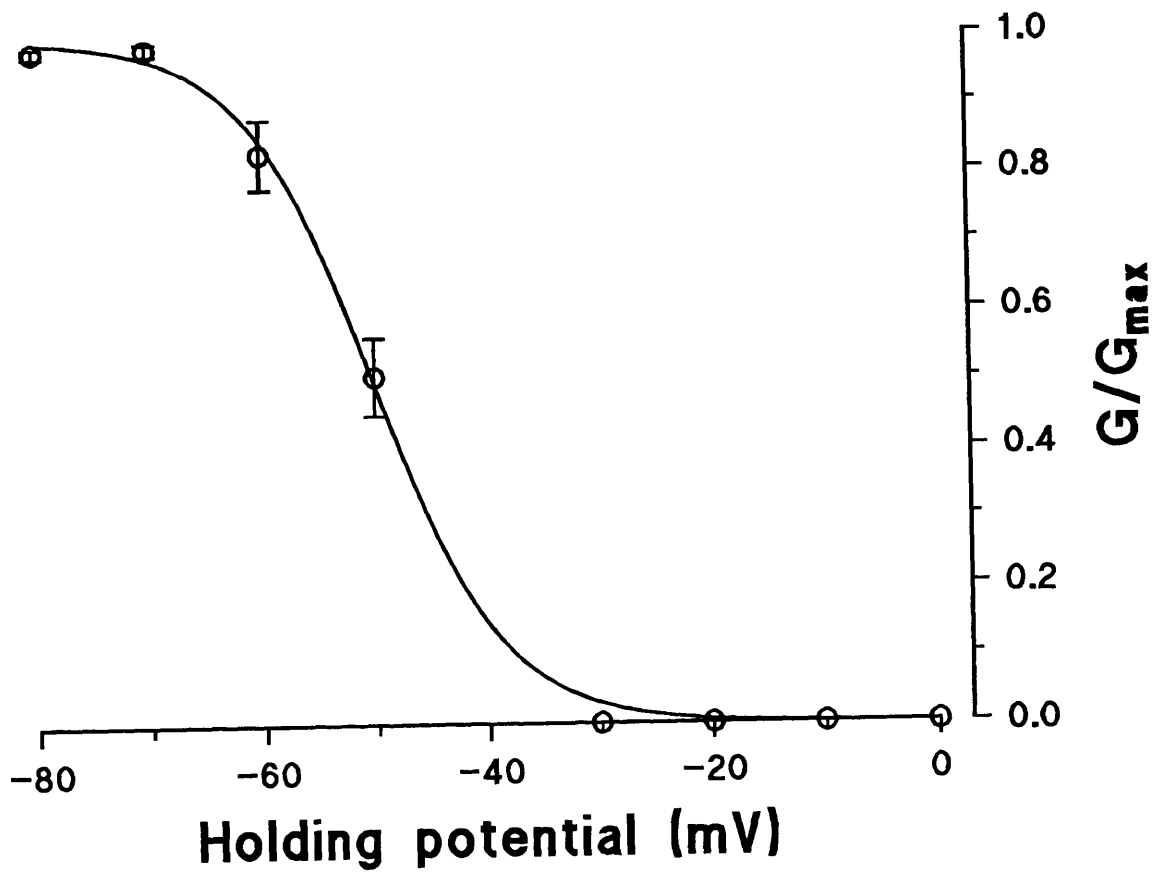
Potassium currents elicited in two different cells by identical 90 mV steps from a holding potential of -80 mV (sampling frequency = 25 kHz, filtering frequency = 5 kHz). (A) In this cell the outward current was predominantly of the sustained type. (B) In this cell transient current dominated the recording. The decay phase was fitted by an exponential function ( $\tau = 19.5$  ms).

**A****B**

**Figure 6.8.**

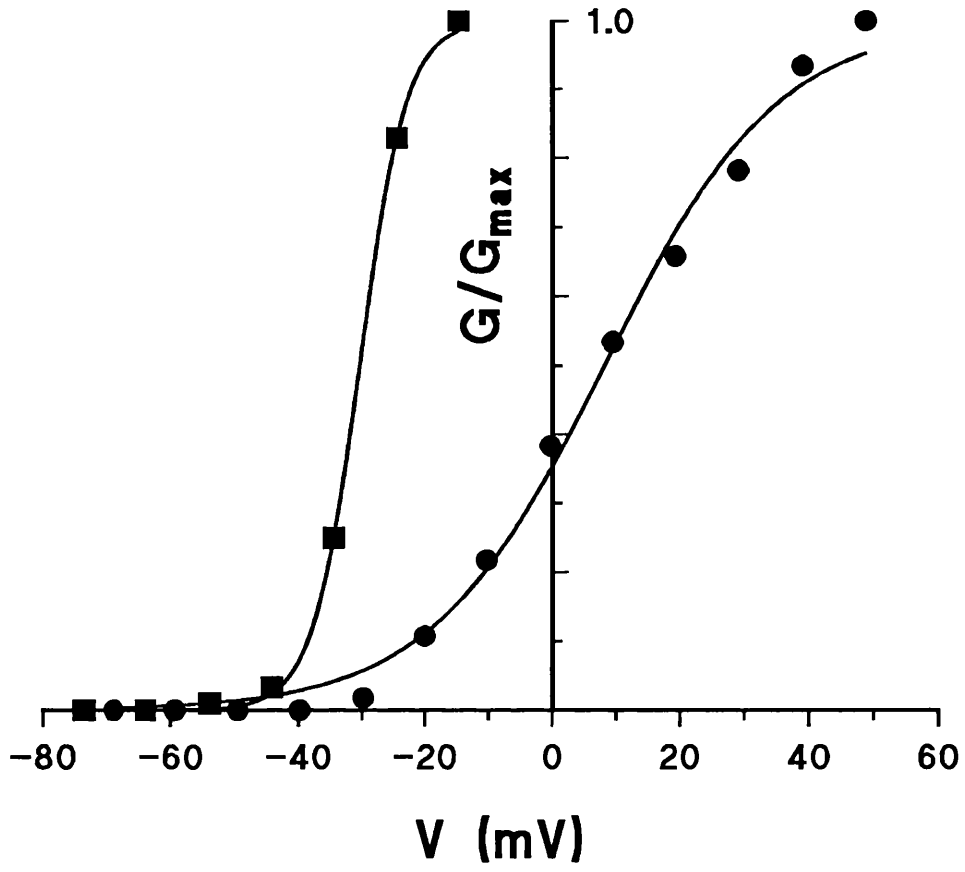
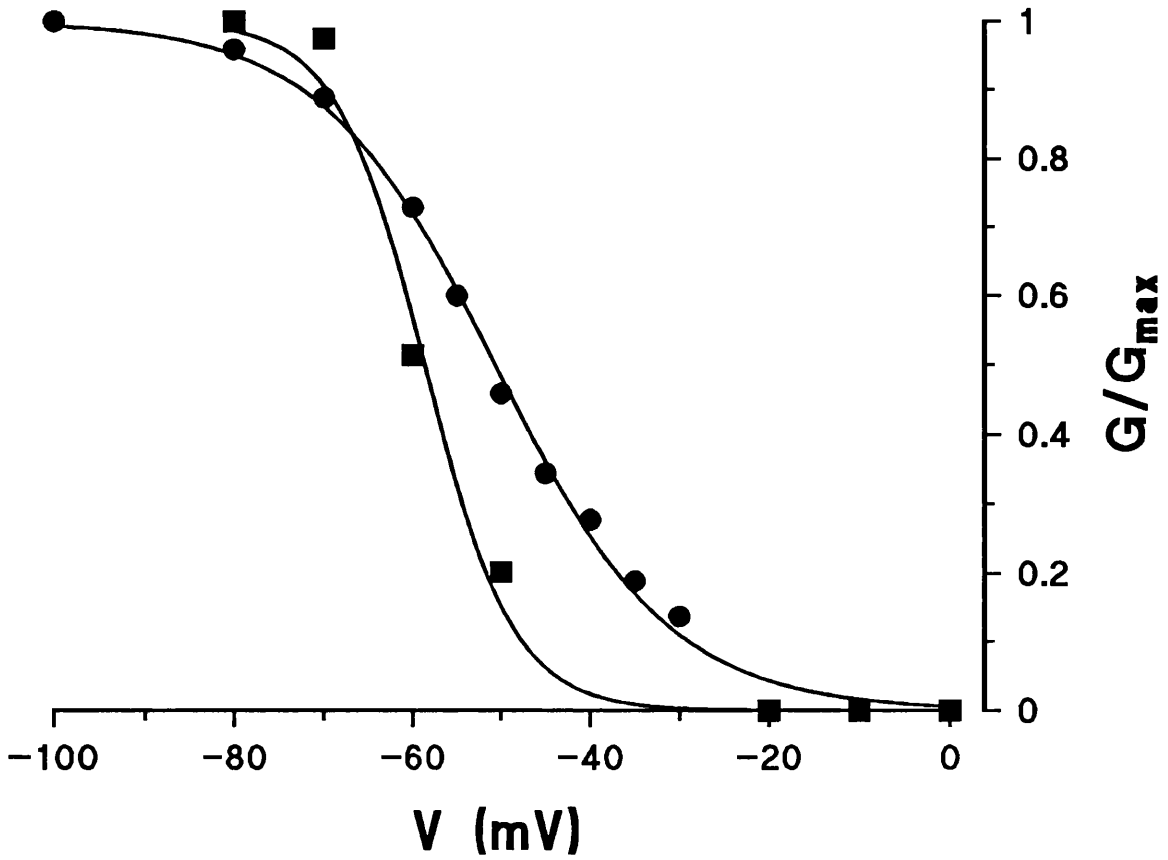
**Inactivation of the transient potassium current.**

(A) Currents elicited by stepping to +20 mV from different holding potentials (indicated to the left of the figure). More and more prominent transient currents could be obtained by stepping from progressively more negative holding potentials. At a holding potential of -20 mV the transient current was completely inactivated; only a sustained current remained. This sustained component was subtracted from the traces before plotting. Records were sampled at 1 kHz and the slow part of the decay phase was smoothed using Savitzky-Golay cubic averaging, 20 points, 1 pass. (B) An inactivation curve for the peak transient current of 9 cells. Mean and SEM values for the proportion of maximal conductance are plotted at each holding potential. A Boltzmann curve was fitted ( $V_h = -50.2$  mV,  $z = 4.4$ ). The threshold for relief of inactivation was around -30 mV and inactivation was completely relieved at -70 mV.

**A****V (mV)****B**

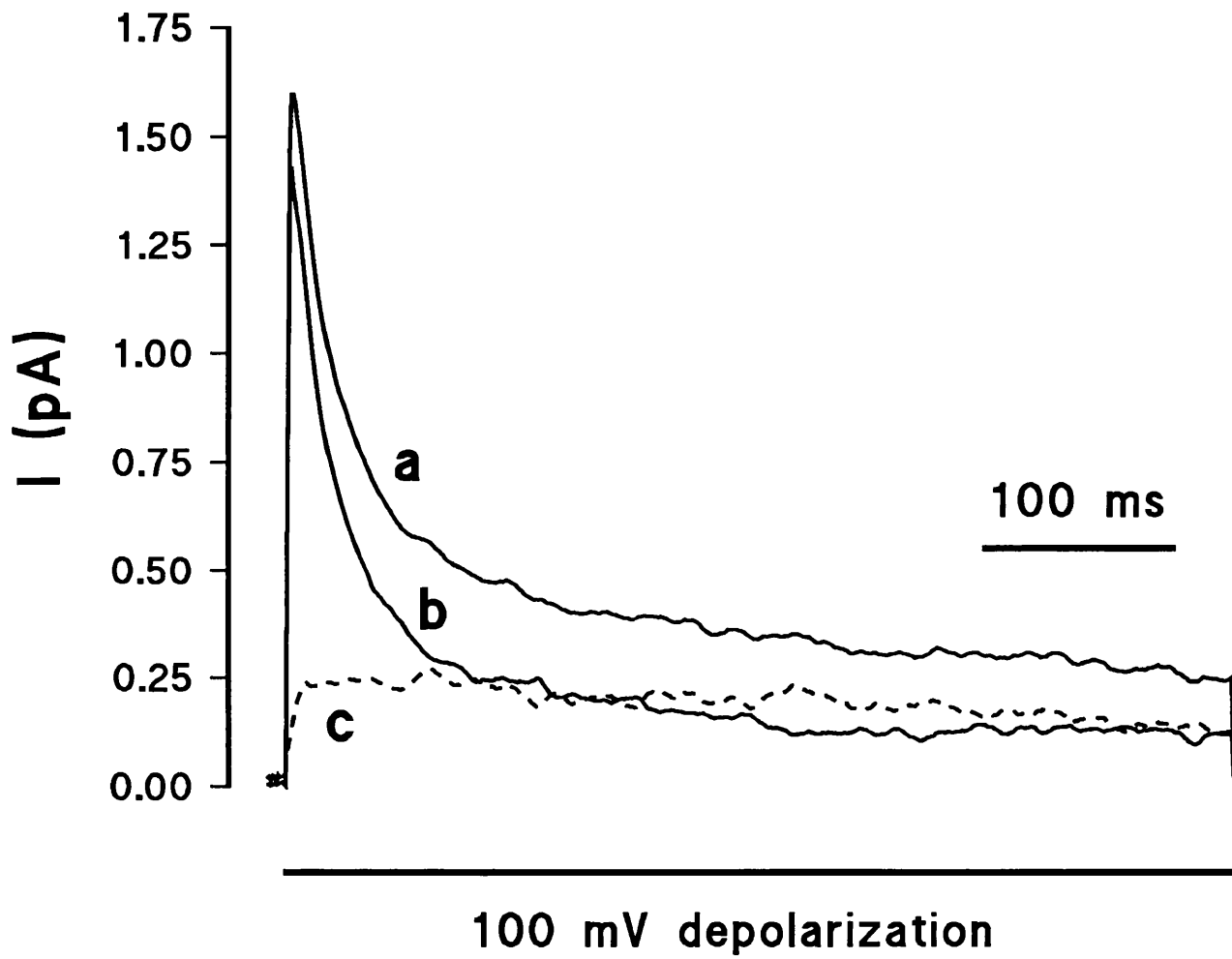
**Figure 6.9.**

The variability of transient currents recorded from different cells. (A) Activation curves for the peak transient current in two cells. One activated at more negative potentials and was fully activated at -20 mV.  $V_h$  was -30.3 mV and  $z$  was -6.8. The other activated less steeply,  $z$  being 1.9 and  $V_h$  being +8.2 mV. (B) Inactivation curves for peak transient current in two cells. For the first current the threshold for relief of inactivation was close to -40 mV, for the second it was around -20 mV. The first inactivated more steeply,  $z$  being 5.1;  $V_h$  was -58.6 mV. The second current had a slope factor of 2.6 and  $V_h$  was -50.7 mV. Inactivation was completely relieved for both currents at -80 mV.

**A****B**

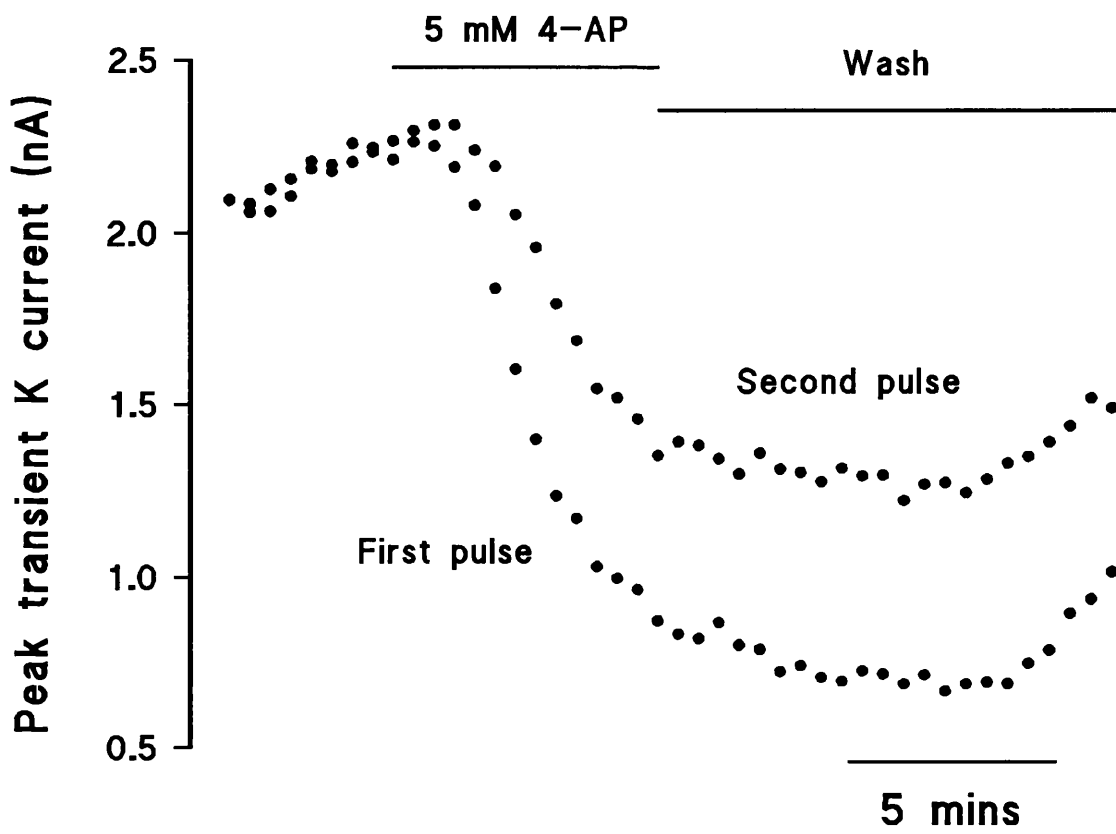
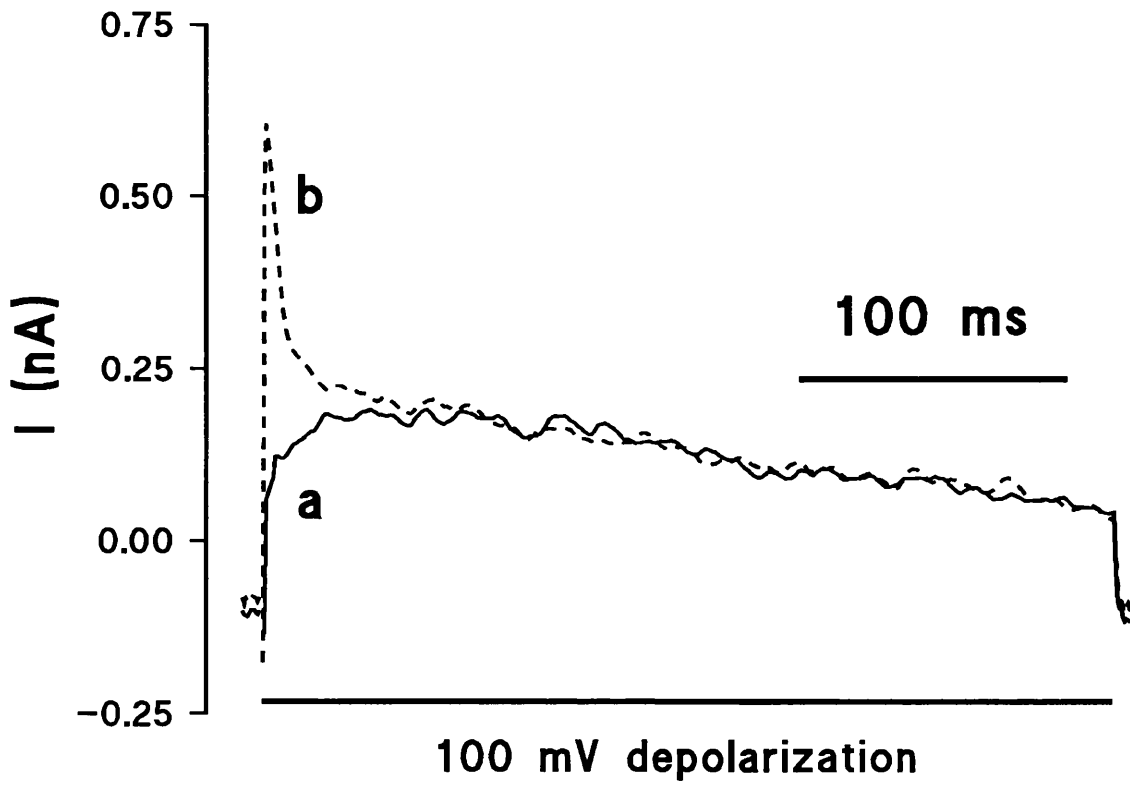
**Figure 6.10.**

A component of current which was refractory to re-activation. Currents elicited by two steps of 100 mV from -80 mV separated by 1000 ms (sampled at 1 kHz, decay phase smoothed by Savitzky-Golay averaging). The first step (a) evoked a larger current than the second (b). The difference current (c) decayed slowly.



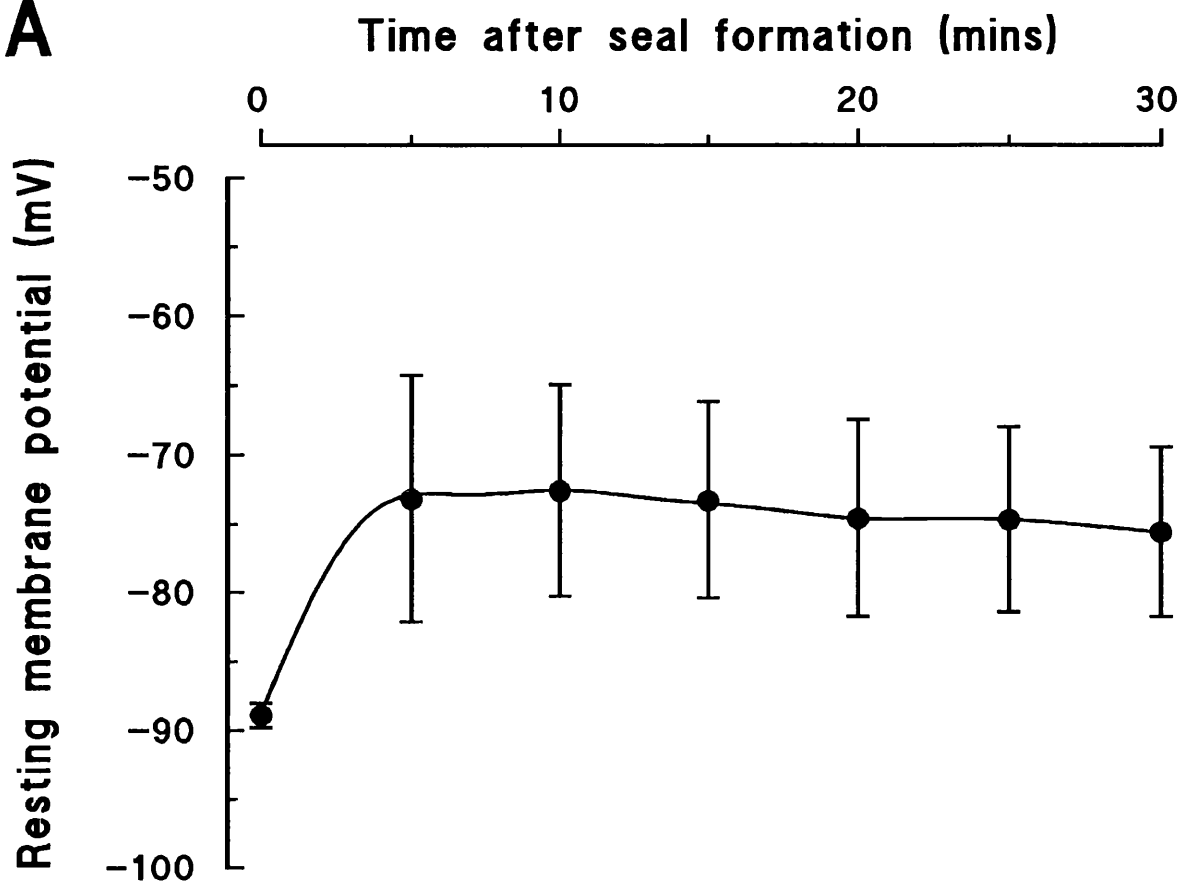
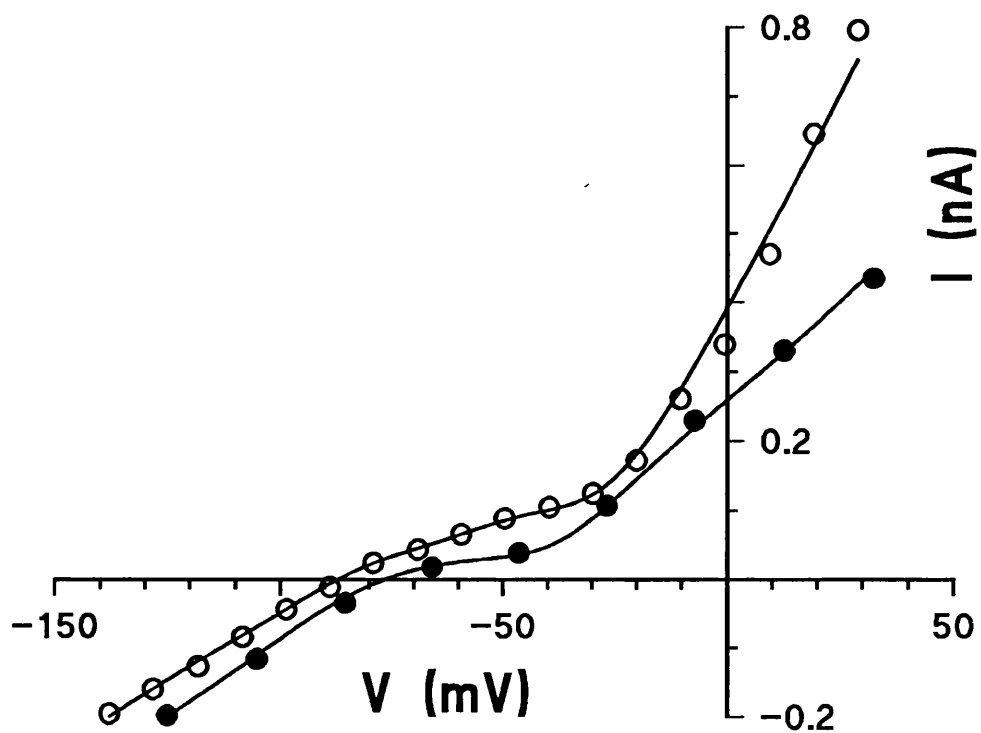
**Figure 6.11.**

**Voltage-dependent blockade of transient currents by 4-aminopyridine (4-AP).** (A) The effects of 5 mM 4-AP on peak transient outward current elicited by 100 mV steps from -80 mV. The magnitude of the peak current was reduced by 4-AP. Two pulses, 1 s apart, were applied every 30 s. The peak current was always larger on the second of the 2 pulses, implying that the first depolarization partially relieved the block. Block was apparent within a few seconds of applying the drug. The block was only partially reversed by washing for 15 minutes. (B) Currents elicited by two 100 mV depolarizations from -80 mV, 1 s apart, in a cell bathed in aCSF containing 1 mM 4-AP. Records were sampled at 1 kHz and the slow part of the decay phases smoothed (Savitzky-Golay). The fast transient outward current was completely absent on the first step (a) but was pronounced on the second (b). In this example there is a relatively large slowly-decaying outward current even in the presence of a concentration of 4-AP which should easily block D-type currents.

**A****B**

**Figure 6.12.**

**Deterioration of resting potential and whole cell currents with time.** (A) The decline of RMP with time after seal formation in 7 cells (mean  $\pm$  SEM). Values were initially clustered tightly around -89 mV but rapidly fell to less negative values within 5 minutes. The magnitude of the fall was highly variable but the decrease was significant at all times between 5-30 minutes after seal formation ( $p < 0.01$ , sign test for paired samples). (B) Late currents (1000 ms after the depolarization) shortly after seal formation (open circles) and 30 minutes later (closed circles). The reversal potential became more positive and the conductance of the late outward current decreased.

**A****B**

## **Section 7. Single channel patch clamp results.**

### **7.1. Formation of seals.**

Cell-attached seals in excess of one gigohm formed relatively easily if care was taken to keep the tip of the recording pipette clean and to choose cells whose membrane appeared smooth. However, meaningful recordings could be made in only a modest percentage of cells for the following reasons. Many seals broke down before enough data could be collected. Recordings from some patches were rendered useless by the appearance of intermittent noise towers. Some patches contained no active channels. Others contained a mass of channels, producing a chaos of multiple current levels. A proportion of patches possessed channels which mysteriously disappeared after only a few minutes of recording. Finally, there were cells which depolarized during the course of an experiment; measurements from such cells were worthless since there was effectively no voltage clamp. Overall, it was possible to make up to six useful cell-attached recordings per day.

Outside-out (O/O) patches were also employed. The outside-out configuration was more difficult to attain. An average of two successful recordings could be achieved per day. Immediately after excision, outside-out patches were usually noisy. The baseline current was undulating and there were episodes of seal breakdown. Channel openings appeared rounded and messy. However, if left to settle down for a period of up to twenty minutes, a marked transformation took place, making clean recordings possible. This phenomenon was presumably due to spontaneous improvement of the seal and disruption of a vesicle formed at the electrode tip.

Arrangin that can't not ↓ raise  
on coal's electrons

Units of Krry

## **7.2. Resolution and noise.**

With a good seal, it was possible to resolve currents of less than 1 pA. The variance of the baseline noise was  $0.150 \pm 0.014 \text{ pA}^2$  when filtering at 2 kHz and  $0.046 \pm 0.005 \text{ pA}^2$  at 1 kHz (mean  $\pm$  SEM, n = 16). Noise levels were not improved by coating the pipette tips with Sigmacote.

## **7.3. Appearance of the channels.**

After seal formation, patches were clamped at a specified holding potential. Channel openings manifested themselves as square wave current deflections. Inward current (with respect to the cell) is designated negative and is represented as a downward deflection. The opposite is true for positive current.

The current passing through an open channel depends on its conductance and on the driving force for permeant ions. The driving force can be varied by applying different holding potentials. Channel conductance is determined by constructing current-voltage plots.

## **7.4. Cell-attached recordings.**

In the cell-attached configuration, the transmembrane potential for the patch (patch potential) is equal to the resting membrane potential minus the potential applied to the recording electrode (pipette potential). The absolute patch potential can be calculated if the resting membrane potential is established by entering the whole cell configuration at the end of an experiment and measuring the potential at which the holding current is zero.

When there is no applied potential (i.e. the pipette potential is clamped at 0 mV), the patch potential is equal to

the resting membrane potential. Positive pipette potentials correspond to hyperpolarization and negative ones depolarization.

In most of the cell-attached experiments described in this study, the potassium concentration of the recording electrode solution approximated that of the intracellular fluid. At potentials either side of the RMP, potassium channel openings result in the movement of potassium ions into the cell (inward current) because there is effectively no potassium gradient across the patch but the inside of the cell is negative. When the pipette potential exactly balances the resting potential there is no chemical or electrical gradient for potassium ions and opening of potassium channels results in no current flow. At more negative pipette potentials there is an outward gradient for potassium; channel opening results in outward current.

Cells normally sit at a resting potential somewhat positive to the potassium equilibrium potential so opening of potassium channels results in outward current. Only when the cell has been hyperpolarized beyond this potential by  $\text{Na}^+/\text{K}^+$  ATPase pump activity would potassium channels pass current in the opposite direction.

Figure 7.1. shows openings and closures, at the resting membrane potential in the cell-attached configuration, of the most commonly encountered channels. Amplitude distribution histograms, which show the proportion of time spent at each current level, are inset. The right-hand Gaussian peaks correspond to the closed state and the left-hand ones to the open state.

Three channel types could easily be distinguished due to their different conductance and patterns of activity. Figure 7.1.A. illustrates the characteristic long openings of a small conductance channel. The unitary current amplitude, as shown by the separation of the peaks of the distribution histogram, was typically 2.0-2.5 pA at the resting potential. Briefer openings

of a much larger conductance "maxi" channel are shown in figure 7.1.B. Its openings were in the region of 20 pA at the resting potential. An intermediate conductance channel with distinctive sub-conductance states is shown in figure 7.1.C. Unitary current amplitude for this channel was 10-12 pA at the resting potential. Similar channels were observed when the  $\text{Cl}^-$  in the pipette was replaced by aspartate.

Figure 7.2. illustrates some properties of small and maxi channels in cell-attached patches. Part A shows current-voltage relationships for a small and large channel present in the same patch. The relationship was approximately Ohmic for both channels. In this example the small channel was recorded over a wide range of potentials and could be resolved at potentials negative to -20 mV. Its projected reversal potential was close to the potassium equilibrium potential of 0 mV. Conductance of the small channel was in the region of 20-35 pS. A maxi channel was active in this patch at potentials positive to -50 mV. The reversal potential for this channel was also close to 0 mV. Its conductance was between 200 and 275 pS.

Patches often contained more than one channel type or multiples of the same channel type. Part B shows a small and maxi channel open simultaneously at a holding potential of -35 mV. Small channels were the most prevalent type, being present in almost all patches. The histogram in part D shows that up to 8 of these channels were present in each patch. In contrast, maxi channels were present in only about half the patches studied. Figure D shows that the maximum number of channels present was 2.

### 7.5. Outside-out (O/O) recordings.

In the outside-out patch configuration, the patch potential is simply equal to the pipette potential. The solutions bathing both faces of the patch are defined by the experimenter so that

the ionic gradients are known precisely. In the present study, O/O recordings were performed with the patch exposed to symmetrical (140/140 mM) or asymmetrical (3/140 mM) potassium solutions. Current flow through potassium channels is outward at pipette potentials positive to the potassium equilibrium potential and inward at potentials negative to it. In the case of symmetrical solutions, the equilibrium potential is, of course, zero. With the outer face bathed in 3 mM KCl, the equilibrium potential is  $\approx -97$  mV.

Small, large and intermediate channels were also recorded in O/O patches. In symmetrical potassium, their conductances were similar to those observed in cell-attached patches. However, channel conductance was found to depend upon external  $[K^+]$ . Channels were two to three times smaller in asymmetrical potassium.

Figure 7.3.A. shows the current-voltage relationship for a small channel in an O/O patch bathed in symmetrical potassium. The channel was active over a wide range of potentials and could be resolved at more positive potentials than was possible in cell-attached. The conductance was 27 pS. Channels of this type were too small to resolve in asymmetrical solutions.

Figure 7.3.B. shows I-V plots for the maxi channel in both symmetrical and asymmetrical potassium solutions. The prevalence of maxi channels in O/O patches was higher than in cell-attached patches, channels being observed in about 95% of patches. In symmetrical potassium the conductance was Ohmic and ranged between 215-275 pS. Current reversal was at the  $K^+$  equilibrium potential of 0 mV. In asymmetrical potassium, the conductance rectified, becoming smaller at more negative potentials. Between +10 mV and -10 mV, the conductance was 90-115 pS. The projected reversal of the current was at very negative potentials. In the example shown, conductance was  $\approx 100$  pS at 0 mV. The points were well fitted by the Goldman-Hodgkin-Katz equation (section 4.3.) with a  $K^+$  permeability coefficient ( $P_K$ ) of  $4.93 \times 10^{-13} \text{ cm}^3 \cdot \text{s}^{-1}$ .

The projected reversal potential was close to the  $K^+$  equilibrium potential of  $-97$  mV.

#### **7.6. A small conductance channel.**

Small channels were present in 85% of cell-attached patches (140 mM  $K^+$  in the patch pipette). The mean number of channels per patch was 2.32. Their conductance was  $27 \pm 0.81$  pS (mean  $\pm$  SEM,  $n = 28$ ) at potentials close to the RMP in symmetrical 140 mM  $[K^+]$ . Mean open probability for this type of channel was  $0.59 \pm 0.088$  ( $n = 9$  patches). Under symmetrical  $[K^+]$  conditions, the current-voltage relationships for small channels were non-linear, and outward currents through these channels were only rarely observed. The conductance of small channels recorded in cell-attached with 40 mM  $K^+$  in the patch pipette was  $18 \pm 1.5$  pS (mean  $\pm$  SEM,  $n = 7$ ), 67% of that seen in 140 mM  $K^+$ .

The conductance was apparently similar in O/O patches bathed in symmetrical 140 mM  $K^+$ , but channels were observed less frequently. A 27 pS channel was seen in one out of five O/O patches bathed in symmetrical  $K^+$ . Small channels were not resolvable in patches bathed with 3/140 mM asymmetrical  $K^+$ .

Figure 7.4.A demonstrates multiple openings of a 26 pS channel active at the resting potential. The amplitude distribution histogram of figure 7.4.B. shows that there were at least 3 small channels active in this patch.

Small channels were active over a wide range of potentials from hyperpolarized to depolarized. Activity in a patch varied from minute to minute but was not dependent upon holding potential. Figure 7.4.C. illustrates the lack of voltage dependence of small channel activity in two cell-attached patches. Patch open probability ( $N.P_o$ ) is plotted against holding potential. Both these patches happened to contain four active channels.

Closures of the small channels were long, lasting for tens of milliseconds. Openings were even longer, lasting for hundreds to thousands of milliseconds. This is illustrated in figure 7.5.A. The open probability (proportion of time spent in the open state) of the 24 pS channel shown here was 0.86, mean open time was 151 ms and mean closed time was 24 ms.

Figure 7.5.B shows an open time frequency histogram for the channel shown in figure 7.5.A. It indicates the frequency of openings of different durations. The distribution is well fitted by a single exponential ( $\tau \approx 150$  ms) indicating that there was probably only one type of opening. The corresponding closed time histogram is shown in figure 7.5.B. It is also well fitted by a single exponential ( $\tau \approx 20$  ms), so there is probably only one type of closure too.

The small channels were insensitive to three well known potassium channel blockers. Channels of small conductance were still observed when the recording electrode contained 5 mM TEA (5/5 patches), 1 mM 4-AP (2/4) or 1  $\mu$ M apamin (5/6).

### **7.7. A large conductance "maxi" channel.**

Maxi channels were seen in 42% of cell-attached patches (140 mM  $K^+$  in the pipette). The mean number of channels per patch was 0.48. Conductance was  $231 \pm 15.7$  pS (mean  $\pm$  SEM,  $n = 12$ ). A sub-conductance state, approximately 40% of the maximal conductance, was rarely observed (see figure 7.6.A, openings at -65 mV). A large channel was observed in one out of eight cell-attached patches when the recording electrode contained 40 mM  $K^+$ . Its conductance was 160 pS, 69% of that seen in 140 mM  $K^+$ .

Maxi channels were more frequently observed in O/O patches. They were present in 100% of O/O patches bathed with symmetrical (140/140)  $K^+$ . The mean number of channels per patch was 1.60 and

the conductance was  $236 \pm 13.5$  pS ( $n = 5$ ). In asymmetrical (3/140)  $K^+$  channel conductance was  $101 \pm 19$  pS ( $n = 11$ ). Channels were present in 92% of patches, the mean number of channels per patch being 1.42.

The activity of maxi channels was strongly voltage-dependent. Figure 7.6.A illustrates channel openings at different holding potentials. The duration of the openings was short at the resting potential of -85 mV but increased progressively with depolarization. Figure 7.6.B. shows the relationship between open probability ( $P_{open}$ ) and holding potential for the channel shown in part A. The shape of the activation curve was sigmoidal for all maxi channels studied but  $V_h$  was highly variable. Some channels exhibited appreciable activity at the resting potential whilst others were active only at considerably more positive potentials. The active maxi channel illustrated in figure 7.6 had a  $V_h$  of -55.6 mV and  $z$  of 1.7. This corresponds to an e-fold change per 23.1 mV.

An interesting feature of some maxi channels was that they exhibited priming behaviour. The activation curve for a relatively inactive maxi channel is presented in figure 7.7.A. The activity curve for the active maxi channel shown in the previous figure is plotted for comparison. Activity increased on depolarization (right-hand solid curve) and decreased on repolarization (left-hand solid curve) but remained higher than before depolarization. Such hysteresis was not restricted to channels whose activity was initially low.

The phenomenon of mode switching, displayed by certain maxi channels, is depicted in figure 7.7.B. Initially, the channel shown here exhibited a low level of activity at the resting potential of -91 mV. After about five minutes it suddenly switched to a much more active mode for no apparent reason. Once in active mode, channels were never seen to return to the inactive mode.

Maxi channels were observed in cell-attached patches when the patch pipette contained 1 mM 4-AP (2/4) or apamin (3/6) but were absent when 5 mM TEA was included (0/5).

### **7.8. An intermediate conductance channel.**

Intermediate channels, which displayed prominent sub-conductance states, were active in 47% of cell-attached patches (140 mM K<sup>+</sup> in the pipette). The mean number of channels per patch was 0.92. The mean open probability for intermediate channels at the RMP was  $0.36 \pm 0.081$  (n = 9 patches). Conductance was  $130 \pm 2.9$  pS (mean  $\pm$  SEM, n = 25) at potentials around the RMP. With 40 mM K<sup>+</sup> in the patch pipette an intermediate channel of conductance 75 pS was seen in 1 out of 8 cell-attached patches (58% of the conductance in 140 mM K<sup>+</sup>).

An intermediate channel of conductance 120 pS was present in one out of five 0/0 patches bathed in symmetrical K<sup>+</sup>. In asymmetrical K<sup>+</sup> an intermediate channel of conductance  $50 \pm 4.0$  pS (n = 7) was seen in 58% of patches and the mean number of channels per patch was 0.75.

Figure 7.8.A. shows the current-voltage relationship for an intermediate channel with sub-states. Conductance for the fully open channel was 120 pS at negative potentials. A pronounced curvature of the I-V relationship indicates that the channel rectified anomalously. Current reversal was observed only in the example shown. No other channels of this type were seen to pass outward currents. The distribution of channel numbers for cell-attached patches is shown in figure 7.8.B. Up to 5 channels were active.

Figure 7.8.C. illustrates the sub-states in detail. Recordings at progressively hyperpolarized potentials revealed more and more sub-states. Three sub-states can be plainly identified in this recording at the resting potential of -90 mV.

In the amplitude distribution histogram of figure 7.8.D. minor peaks corresponding to two of the sub-states can be resolved. The time spent at sub-state levels was small compared with that spent at either the fully open or fully closed level. In the overwhelming majority of cases, sub-states were reached from the fully open state or from a higher sub-state rather than from the closed state or a lower sub-state.

Like the small channel, activity of the intermediate channel was highly variable from minute to minute. Figure 7.9.A. shows bursts of long openings separated by remarkably long closures. Such closures often lasted for minutes. Activity of intermediate channel also varied from patch to patch but was not dependent upon voltage. Figure 7.9.B shows plots of  $N.P_o$  against holding potential for two patches in which activity happened not to vary much with time. Channel openings for the relatively inactive channel are shown in figure 7.10.A. Occasional openings occurred in bursts. Figure 7.10.B. shows openings for the active channel. This channel was predominantly in the open state, there being intermittent closures.

The intermediate channel with sub-states was observed in patches where the recording electrode contained 5 mM TEA (1/5) or 1 mM 4-AP (1/4) but not 1  $\mu$ M apamin (0/6)

### **7.9. Channels active at RMP.**

The vast majority of patches contained channels which were active at the resting potential. Small and intermediate conductance channels were often active. Maxi channels usually exhibited little activity ( $P_{open} < 0.1$ ) at RMP but were occasionally active to a considerable degree even without priming.

### **7.10. Other channels.**

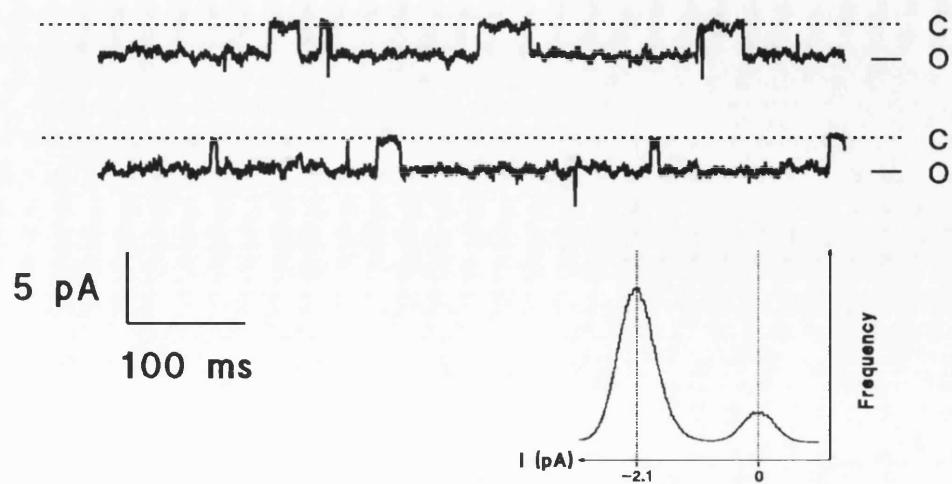
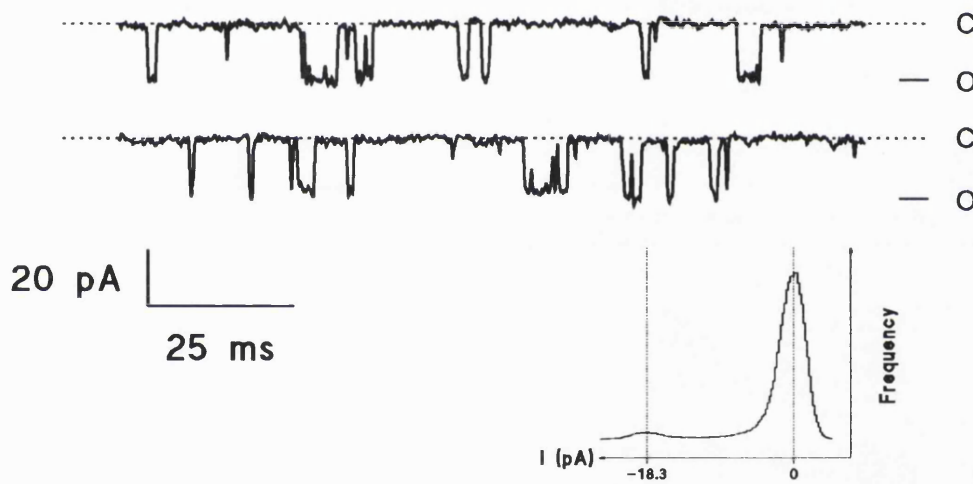
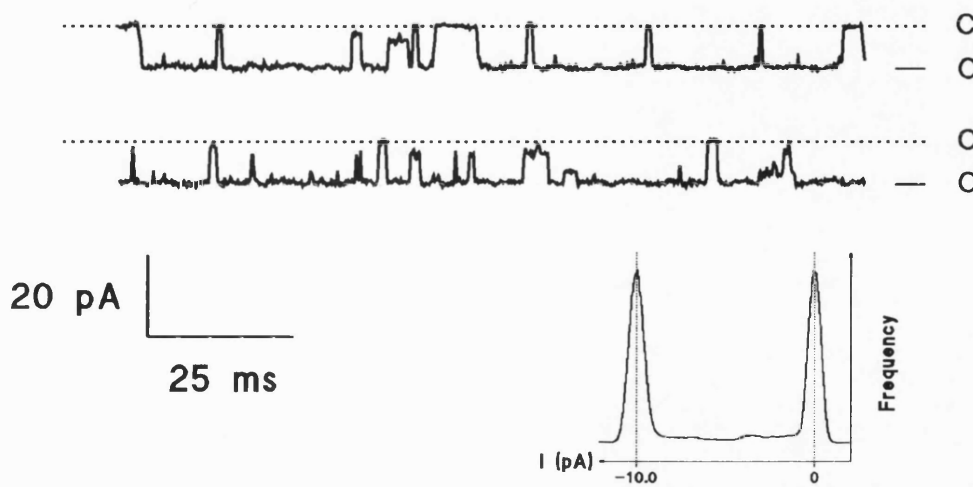
The commonest and most easily distinguishable channel types have been described in the previous sections. Other channels, which were difficult to differentiate in terms of conductance, were also observed. A voltage-dependent channel, much smaller than the maxi channel, was activated at potentials positive to -40 mV. An extremely flickery channel, whose conductance was almost impossible to assess, was sometimes seen at the RMP, as was a channel in the region of 100 pS (see below). A strongly-rectifying channel of about 50 pS at the RMP was highly active at hyperpolarized potentials but was infrequently observed.

### **7.11. Dopamine and quinpirole.**

Channels of a similar conductance to the dopamine- and quinpirole-activated channels described by Freedman and Weight (1988 & 1989) in acutely dissociated striatal neurones were observed infrequently. Channels in the range 80-110 pS were seen in cell-attached patches where the recording electrode contained control solution (3/30), 10  $\mu$ M quinpirole (1/14) or 100  $\mu$ M dopamine (5/22).

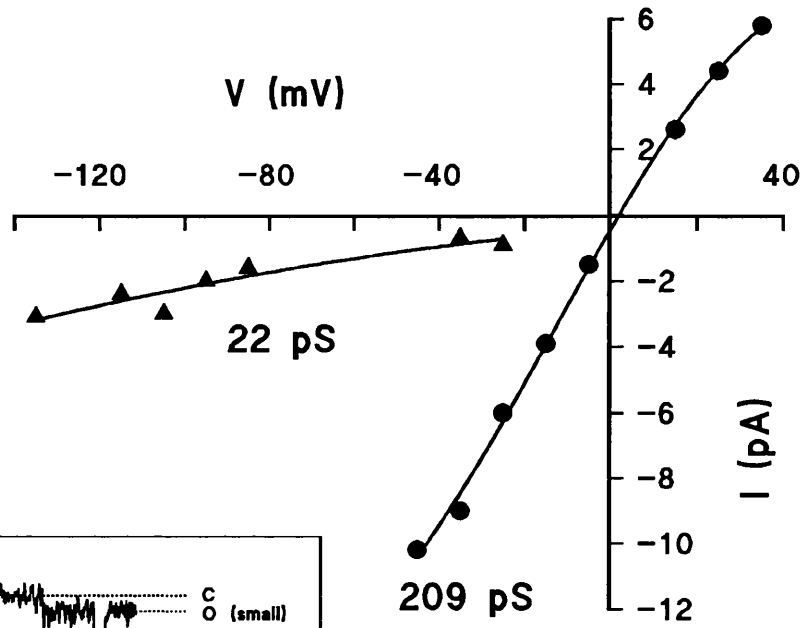
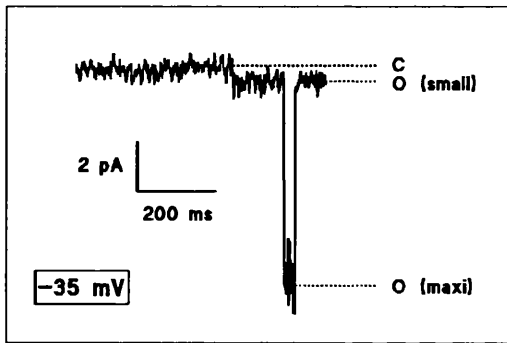
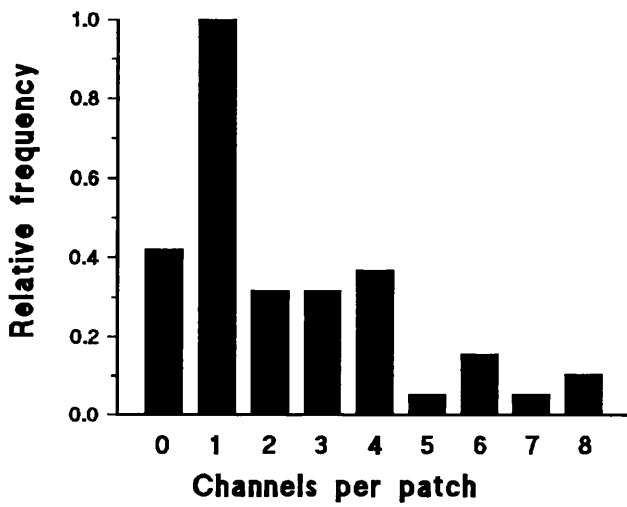
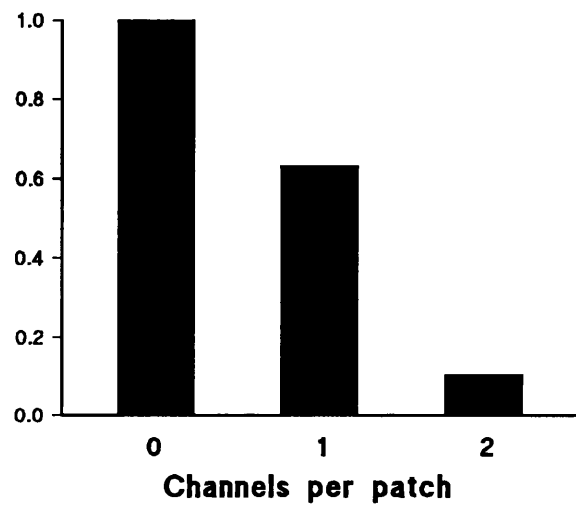
**Figure 7.1.**

Single channel recordings of the three most common channel types active at the resting membrane potential (RMP) in the cell-attached configuration. Patch pipettes contained high  $K^+$  (140 mM) solution. Inward current is represented as a downward deflection. Closed (c) and open (o) levels are indicated. Inset amplitude distribution histograms show the unitary current amplitude at the resting potential for each channel. Filtering frequency (f) was 1 kHz. (A) Long openings and closures of a 24 pS channel, RMP = -82 mV. (B) Brief openings of a large conductance ("maxi") channel, RMP = -85 mV. (C) Long openings of a 120 pS channel with obvious sub-conductance states, RMP = -90 mV.

**A****B****C**

**Figure 7.2.**

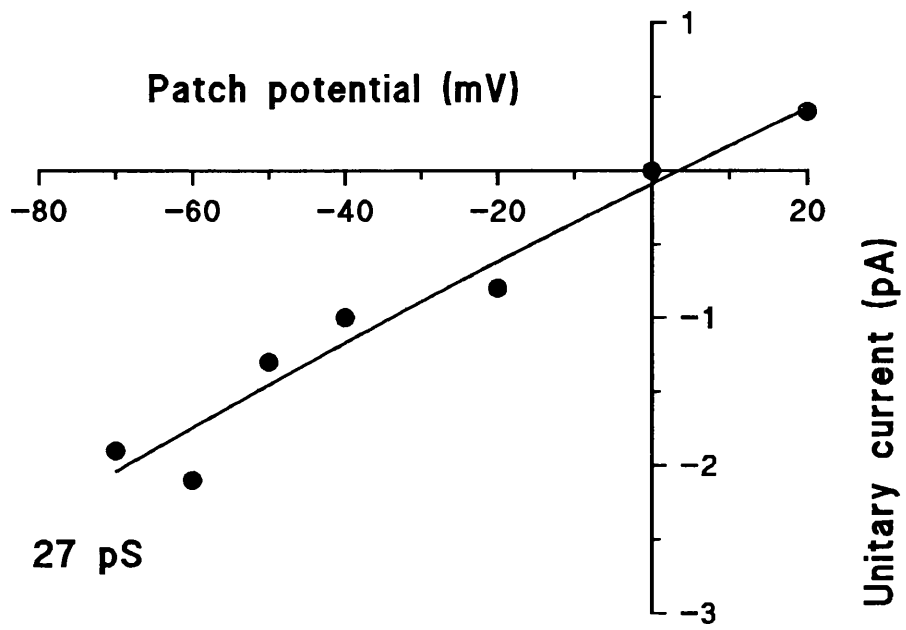
**Small channel and maxi channel in cell-attached patches (140 mM K<sup>+</sup> in the patch pipette).** (A) Current-voltage (I-V) relationship for a 22 pS and 209 pS channel present in the same patch. Unitary current amplitude was plotted against absolute holding potential. (B) A small channel and maxi channel open together at -35 mV (f = 5 kHz). C = closed, O = open. (C) Frequency distribution for the number of small channels per patch. (D) Frequency distribution for the number of maxi channels per patch.

**A****B****C****D**

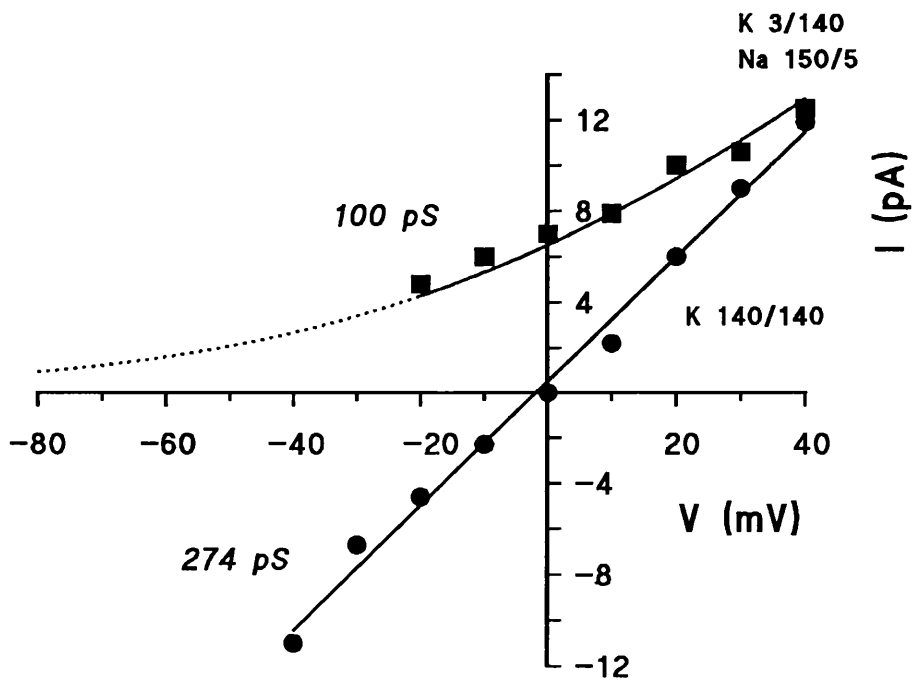
**Figure 7.3.**

**Current-voltage relationships for small and maxi channels in outside out (O/O) patches.** (A) I-V plot for a 27 pS channel in a patch bathed with symmetrical (140/140 mM) K<sup>+</sup> solution. (B) I-V plot for maxi channels in symmetrical (140/140) and asymmetrical (3 mM outside/140 mM inside) K<sup>+</sup> solutions. **Symmetrical** conditions are represented by circles. The points are well fitted by a linear regression with slope 274 pS and the reversal is close to 0 mV. **Asymmetrical** conditions are represented by squares. The I-V relationship is non-linear, constant-field rectification being apparent. The points are well fitted by the Goldman-Hodgkin-Katz current equation (see the text). The K<sup>+</sup> permeability coefficient is  $4.93 \times 10^{-13} \text{ cm}^3 \cdot \text{s}^{-1}$ . Conductance over the range -10 mV to +10 mV is 100 pS and the projected reversal potential is approaching the potassium equilibrium potential of -97 mV indicating that the channel is highly selective for K<sup>+</sup>.

**A**

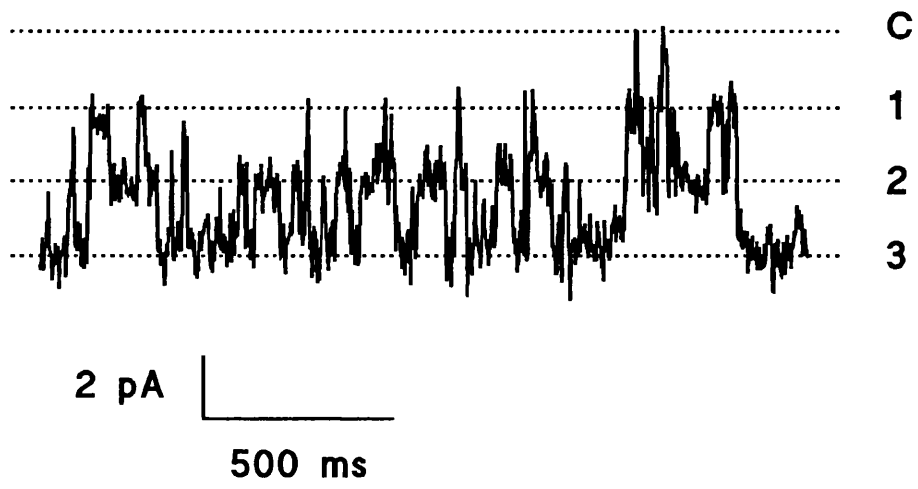
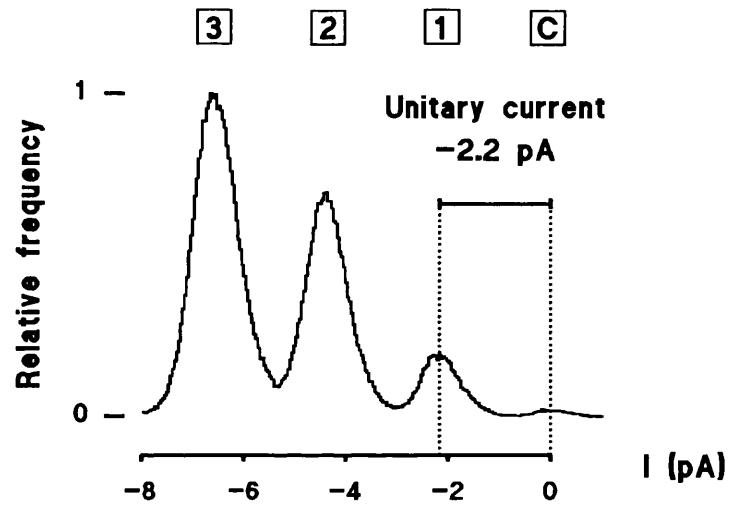
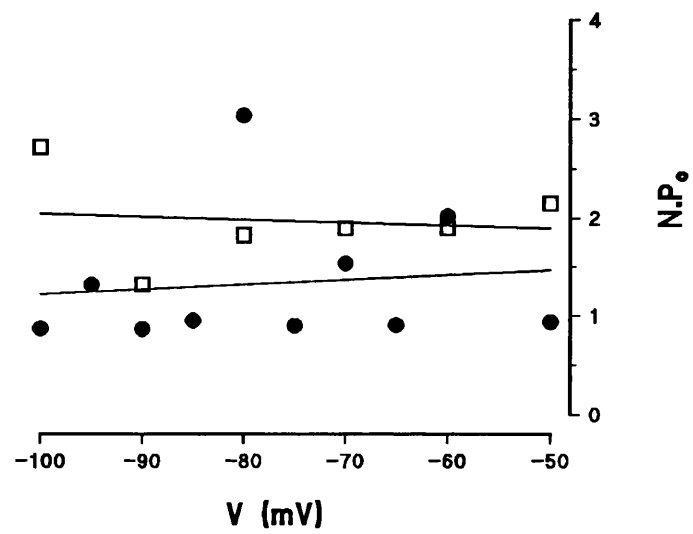


**B**



**Figure 7.4.**

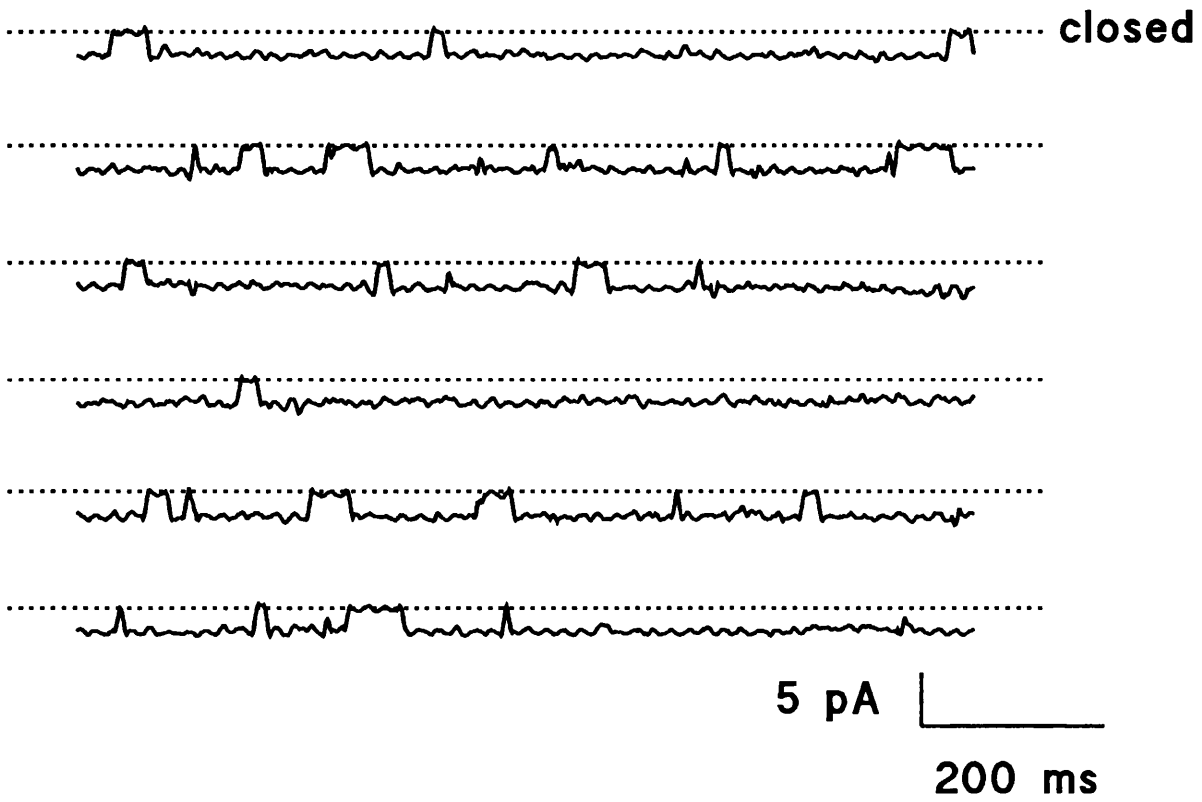
**Some properties of the small channel in cell-attached patches.** (A) Current records for multiple small channels highly active at the resting potential ( $f = 2$  kHz). Lines represent the closed level and 1-3 channels open simultaneously. (B) Amplitude distribution histogram for the same patch showing multiples of the unitary current. (C) Activity-voltage plot for two patches illustrating the lack of voltage dependence of these channels at negative potentials. Both patches contained at least four channels. Open probability for the patch ( $N \cdot P_o$ ) is plotted against holding potential.  $N$  = number of channels in the patch,  $P_o$  = open probability of the individual channels.

**A****B****C**

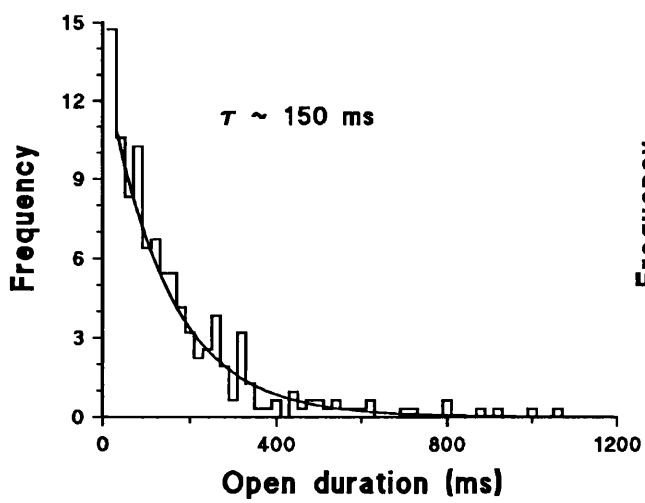
**Figure 7.5.**

**Openings and closures of the small channel.** (A) Cell-attached current records demonstrating the long openings and closures of a single channel at the resting potential of -82 mV. ( $f = 1$  kHz, and smoothed with Savitzky-Golay cubic averaging, 20 points, 1 pass).  $P_{\text{open}}$  for this channel was 0.86. (B) Open time histogram showing the number of openings of different durations. The plot is well fitted by one exponential ( $\tau \approx 150$  ms). (C) Closed time histogram; fitted with one exponential ( $\tau \approx 20$  ms).

# A



# B



# C

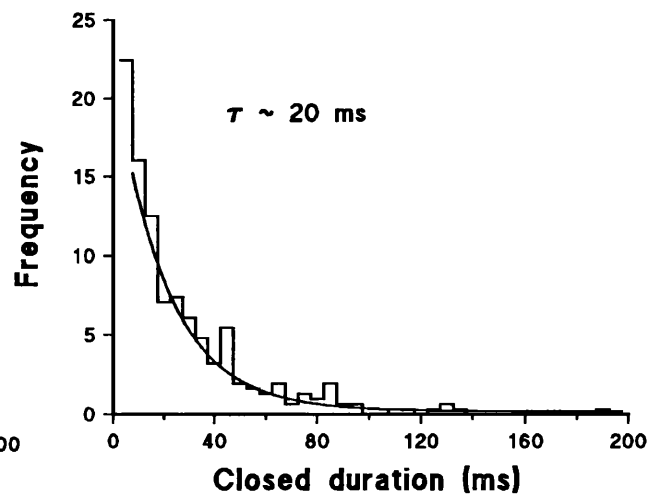
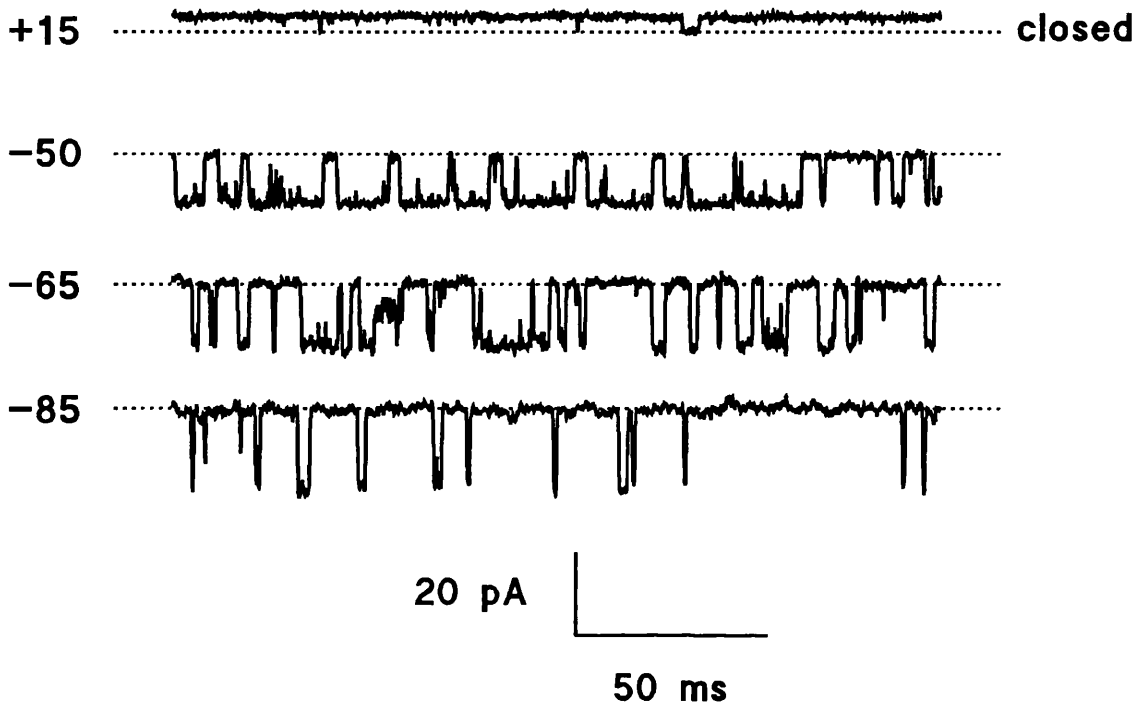


**Figure 7.6.**

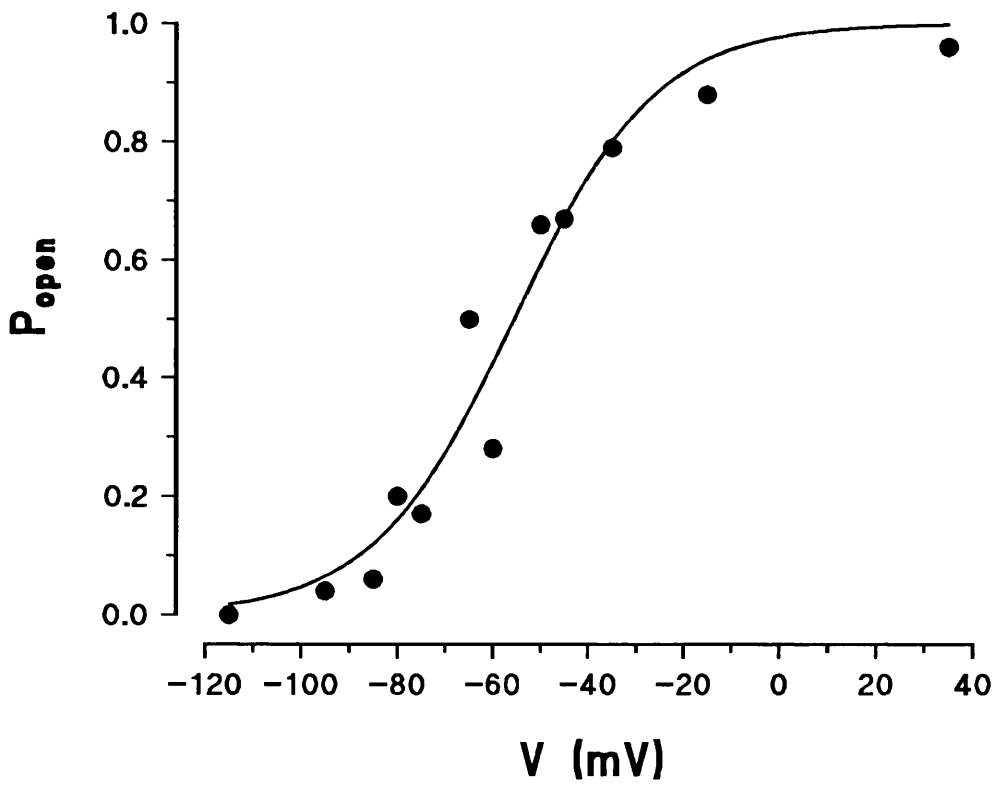
**Voltage-dependent activity of the maxi channel.** (A) Cell-attached records showing openings of the maxi channel at different holding potentials ( $f = 2$  kHz). Openings become progressively longer with depolarization. (B) Activity-voltage plot.  $P_{\text{open}}$  vs. holding potential for the channel shown in (A). The points were fitted by a Boltzmann function with gating valency ( $z$ ) of 1.7 and  $V_h$  of  $-55.6$  mV. This corresponds to an e-fold change per 23.1 mV.

# A

V (mV)

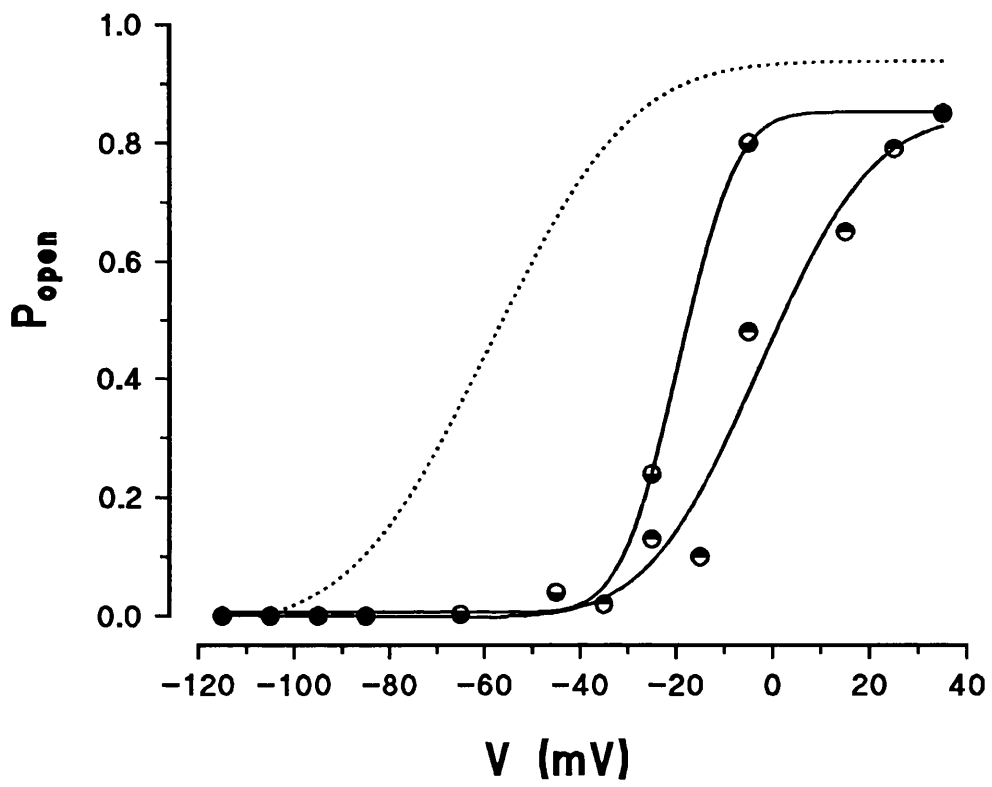
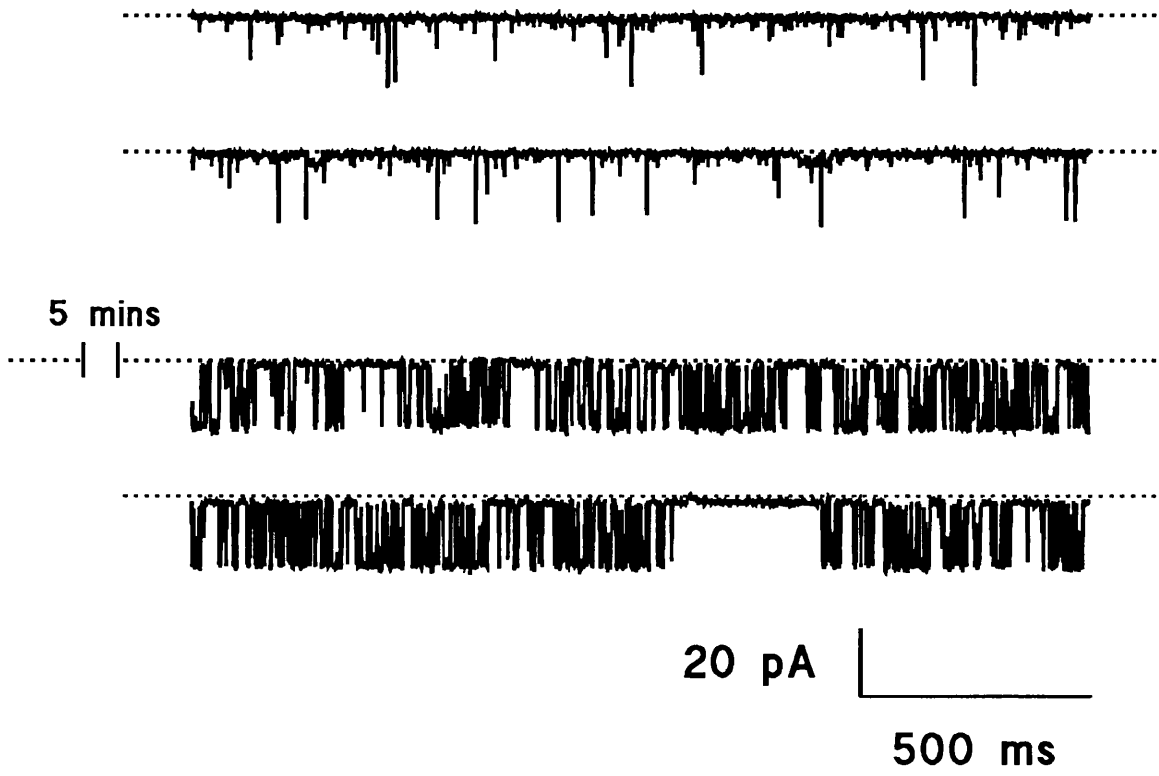


# B



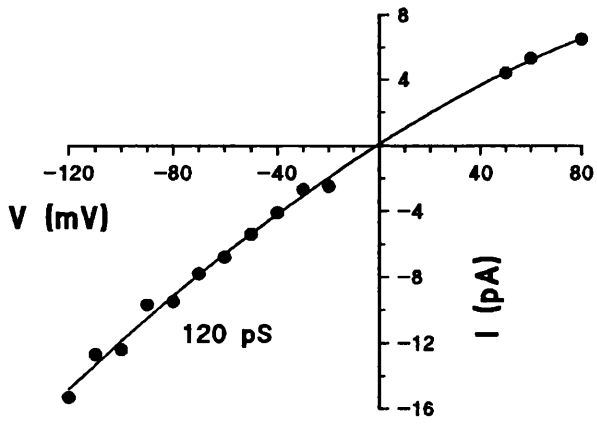
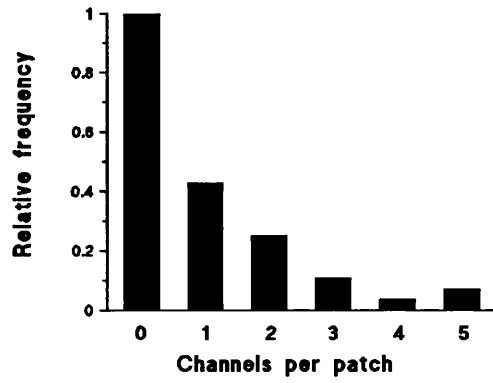
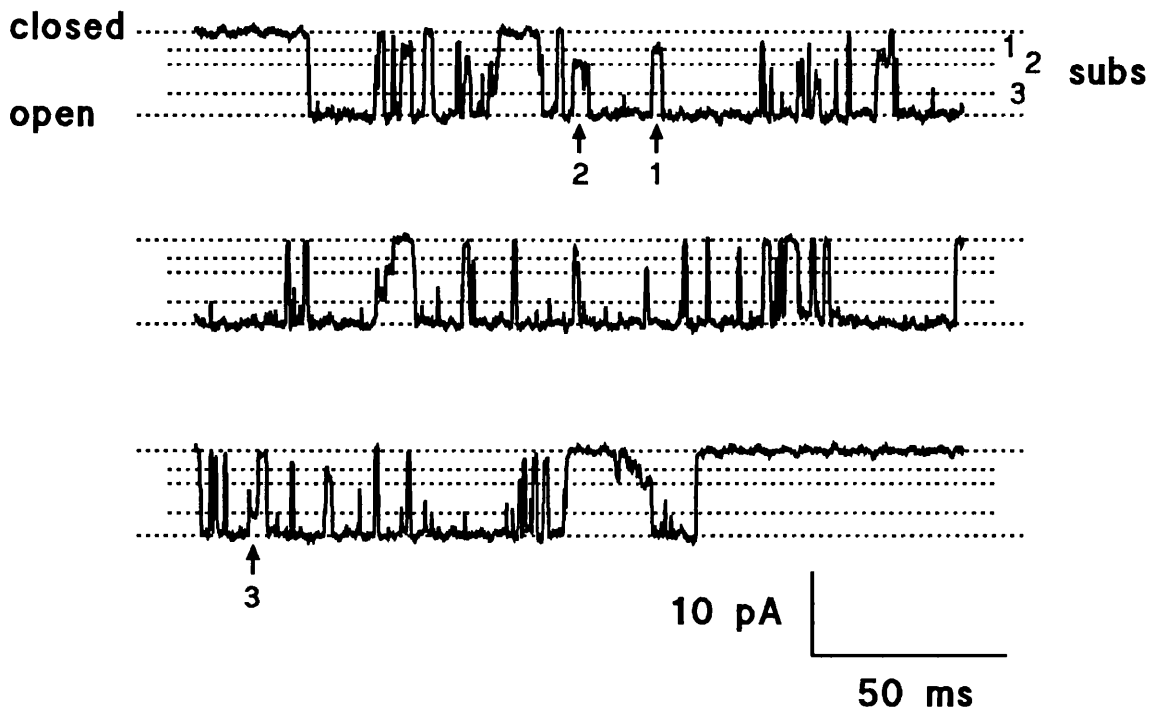
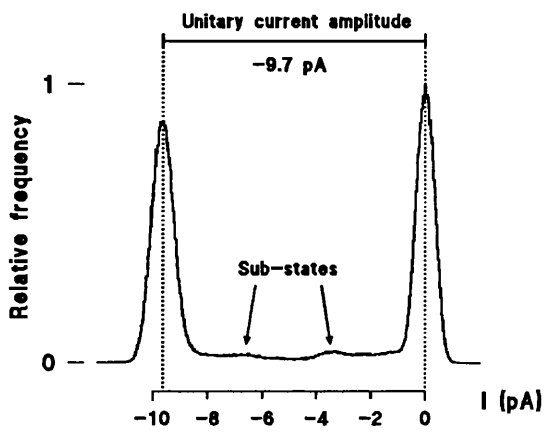
**Figure 7.7.**

**(A) Priming of the maxi channel.** The activity-voltage plot is shown for a relatively inactive maxi channel (solid lines). The active maxi channel from the previous figure is also shown for comparison (dotted). The  $P_{\text{open}}$  during depolarization is represented by circles with closed upper halves. The Boltzmann function had a  $V_h$  of +4.5 mV;  $z$  was 1.7 (an e-fold change per 23.4 mV).  $P_{\text{open}}$  during repolarization is represented by circles with closed lower halves;  $V_h = -15.9$  mV;  $z = 3.1$  (an e-fold change per 12.8 mV). **(B) Mode switching of the maxi channel.** The first two records show an inactive maxi channel in a cell-attached patch recorded at the resting potential of -92 mV ( $f = 2$  kHz). The second set of records shows the same patch five minutes later after the channel suddenly switched to a much more active mode. The dotted line indicates the closed state. A small channel is also present in this patch.

**A****B**

**Figure 7.8.**

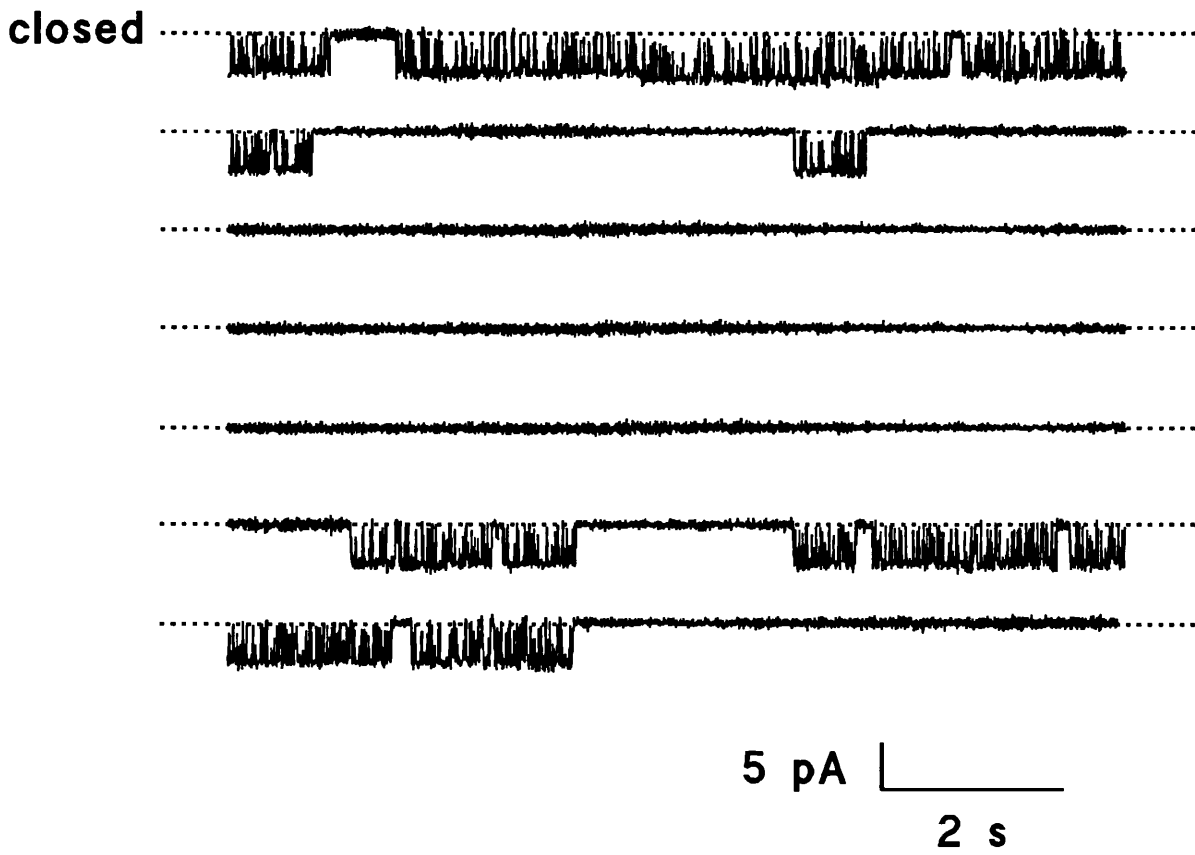
Some properties of the intermediate channel with sub-conductance states (cell-attached). (A) I-V relationship. The conductance for the fully open state of this particular channel is 120 pS over the negative potential range. There is some inward rectification. (B) Frequency distribution for the number of intermediate channels per patch. (C) Current records at the resting potential (-90 mV) showing three conspicuous sub-states indicated by the numbered arrows ( $f = 2$  kHz). (D) Two of the sub-states are apparent from the amplitude distribution histogram. The histogram also shows that the channel spends most of its time in the fully open or fully closed state.

**A****B****C****D**

**Figure 7.9.**

**(A) Long closures of the intermediate channel.** Current records of the channel shown in the previous figure (holding potential  $-50$  mV,  $f = 2$  kHz). The intermediate channel often exhibited bursts of openings separated by closures which lasted for tens of seconds. **(B) Activity-voltage plots for the intermediate channel (cell-attached).** The activity of the intermediate channel varied from patch to patch but did not display voltage-dependence at negative potentials. The relationship between patch open probability ( $N.P_o$ ) and holding potential is shown for an inactive and an active channel.

# A



# B

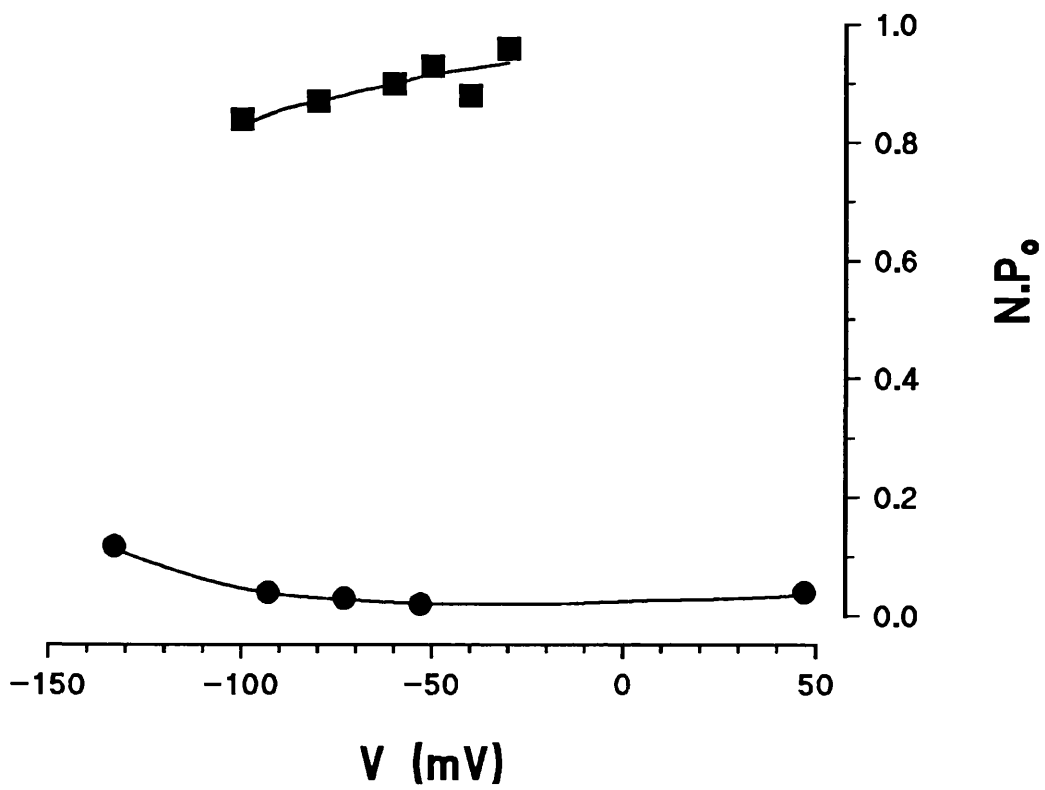
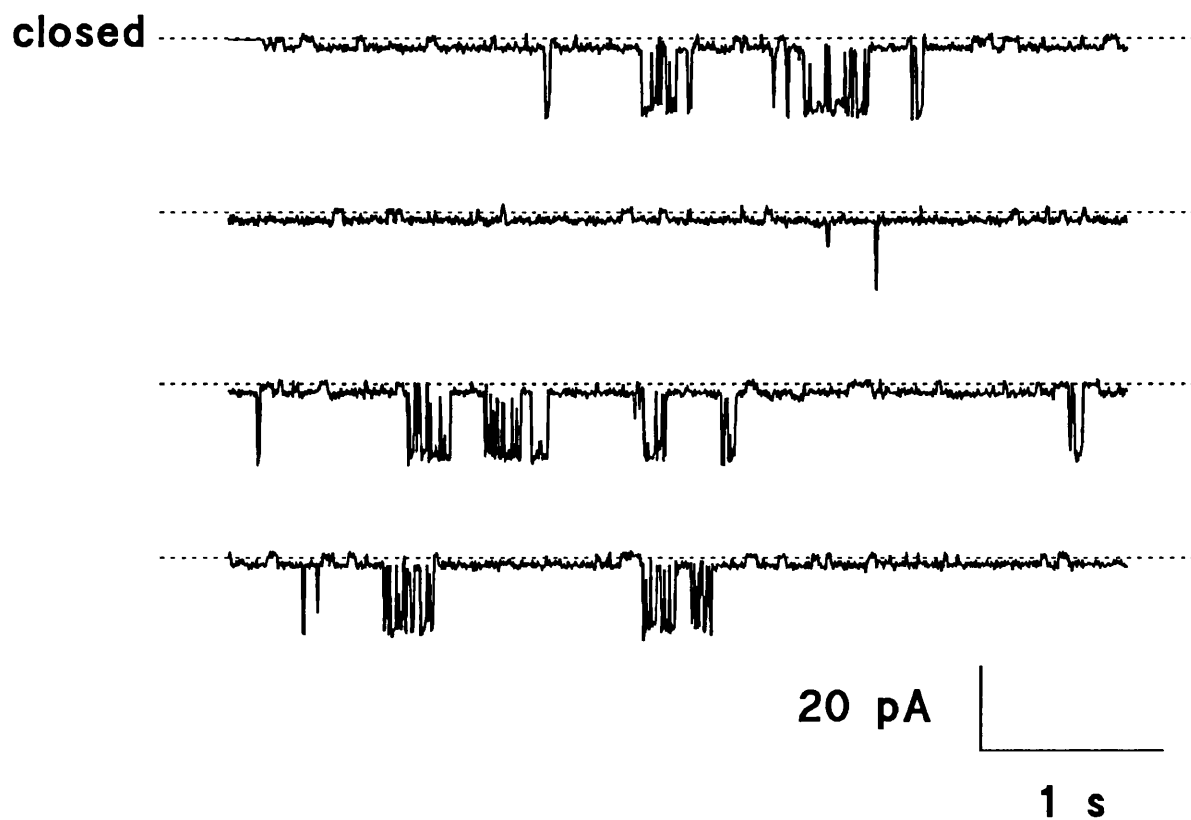


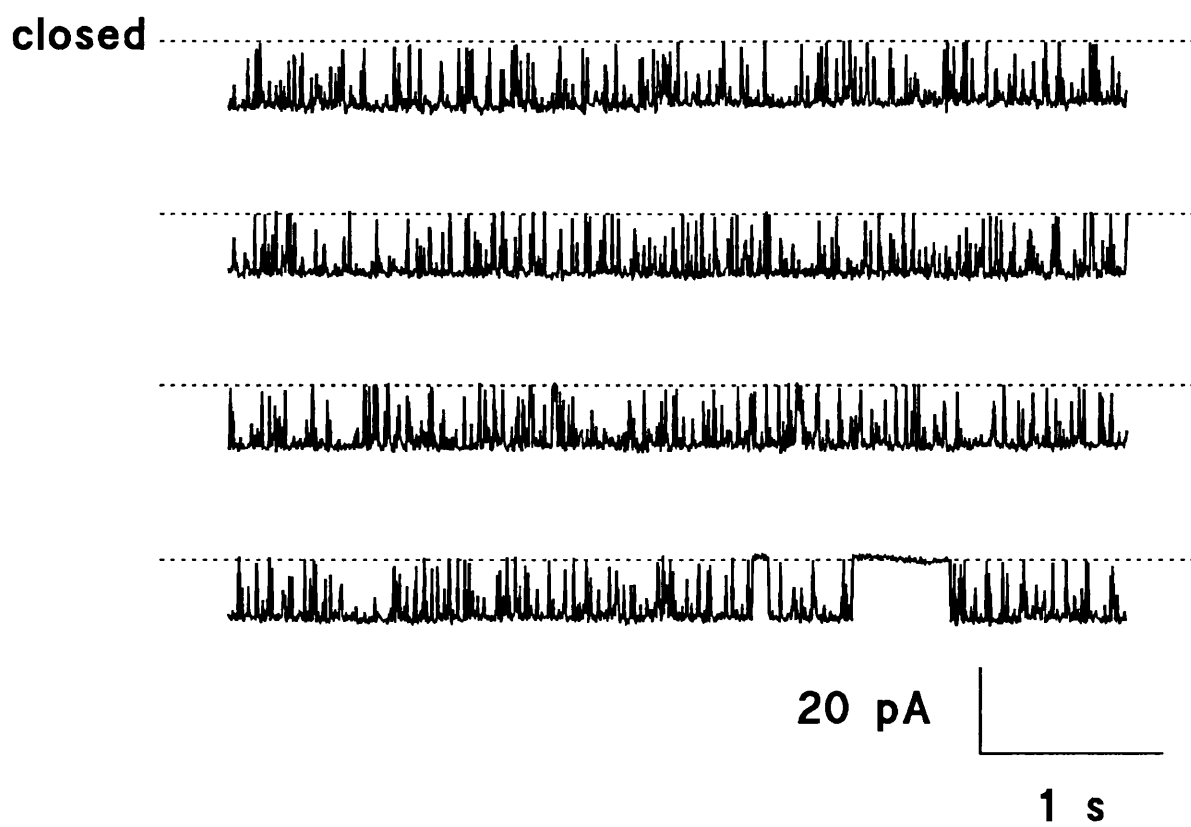
**Figure 7.10.**

**Examples of intermediate channels exhibiting low and high activity.** (A) Current records of the relatively inactive intermediate channel shown in figure 7.9.B. ( $f = 2$  kHz). A small channel is also present in this patch. (B) Current records of the active channel shown in figure 7.9.B. ( $f = 2$  kHz).

# A



# B



## Part V. DISCUSSION AND CONCLUSIONS.

### 8. Discussion.

#### 8.1. Suitability of the protocol.

##### 8.1.1. Culture

Previous investigations have employed complex procedures in order to culture neurones. Embryonic tissue has usually been used due to the belief that post-natal neurones will not thrive in culture. Surmeier *et al* (1988b) reported "compromised viability of striatal neurons taken from postnatal animals, especially when plated on synthetic substrates, such as poly-D-lysine". Some experimenters have grown glial mats on glass slips before plating with locus coeruleus neurones (Masuko *et al*, 1986) or hippocampal neurones (Forsythe and Westbrook, 1988).

It is certainly possible that the use of embryonic tissue or plating on to glial mats would enhance neuronal survival. However, such protocols were not necessary for culturing neostriatal neurones. Neostriatal tissue from post-natal rat pups aged up to 6 days was found to be appropriate for culturing purposes. Tissue of this age yielded sufficient neurones of patchable quality.

Plating directly onto poly-lysine-coated slips produced cultures which looked very similar to those described by Surmeier *et al* (1988b). Different types of neurones could be distinguished from each other and from glia using morphological criteria. Similar proportions of type I (ovoid) and type II (triangular) neurones were observed.

After 2-3 weeks in culture, neurones possessed all the attributes necessary for successful patching. They were identifiable, robust, electrically compact, well attached to the underlying substrate and had smooth, clean membranes.

### 8.1.2. Electrophysiology.

The patch clamp technique was applied effectively to the recording of single channel  $K^+$  currents. Cell-attached patches were generally stable and recordings could often be carried out for a considerable period of time (maximum  $\approx$  1 hour). Outside-out patches were also successfully pulled, but were more difficult to attain. Inside-out patches proved almost impossible to achieve. Pulling the pipette tip away from the cell in cell-attached mode resulted in the formation of a vesicle which did not spontaneously resolve and could not be persuaded to do so by exposing it to an air/water interface.

Whole cell recordings were less successful than cell-attached or outside-out recordings because of rapid deterioration of the preparation. Inclusion of ATP and GTP in the patch electrode did not prevent current run-down and decline of the resting potential. Nevertheless, useful information could be obtained from whole cell recordings carried out within 5 minutes of seal formation.

The success rates for patching were very similar to those reported by Freedman & Weight (1988 & 1989) who used acutely dissociated adult striatal neurones. They were able to procure "4 or 5 good cell-attached recordings per day with somewhat fewer recordings in the whole cell configuration". They also reported that "whole cell currents and potentials showed a marked run-down after  $\approx$  5 min; the...data were all obtained within 5 min of beginning the recording".

The phenomenon of run-down could be accounted for by dialysis of diffusible intracellular regulators during recording. There is plenty of evidence to suggest that important regulators are lost from the cytoplasm in this manner. For example, Yakel *et al* (1988) recorded whole cell responses to 5-HT in cultured striatal neurones. The responses were lost rapidly (i.e. within 5 minutes) when cells were patched with low resistance electrodes

but were more persistent when high resistance electrodes were employed. Therefore, possible strategies to overcome the problem of dialysis include the use of higher resistance electrodes. However, a disadvantage of high resistance electrodes is that they give rise to greater voltage clamp errors. Another approach would be to use nystatin in the recording pipettes to permeabilize patches to ions but to restrict the efflux of large molecules. Unfortunately, this also increases series resistance. It would be interesting to see whether the inclusion of appropriate concentrations of cyclic nucleotides (or other known intracellular modulators) is effective in preventing run-down.

The smallest resolvable current was  $\approx 0.5$  pA in a good patch. Other authors have resolved currents five times smaller than this (e.g. Sakmann & Trube, 1984). The noise level was not improved by coating the pipettes so the the major noise source was probably the patch itself. A possible explanation for the noise could be that the baseline level did not, in fact, represent the state where all channels were closed. It could be that at least one channel was always open. "Baseline" noise would then be determined by open channel noise. Open channels could, for example, be subjected to unresolvable (flickery) ion block. In fact, the "baseline" noise was always of comparable level to the noise observed during openings of the small channels.

## **8.2. Resting potential and whole cell capacitance.**

The resting membrane potential was around -90 mV (mean:  $-88 \pm 0.7$  mV; mode: -90 mV) when measured immediately after entering whole cell mode. This is close to the  $K^+$  equilibrium potential ( $\approx -97$  mV at room temperature), signifying that the resting membrane was 100-150 times more permeable to  $K^+$  than to  $Na^+$  (assuming an intracellular  $[Na^+]$  of 10 mM).

The  $[K^+]_{out}$  gradients employed in this study were selected to mimic the conditions *in vivo* as closely as possible. However, the exact  $[K^+]_{out}$  in the local environment of neurones is not known. It has been shown that the resting potential in neostriatal neurones is extremely sensitive to  $[K^+]_{out}$ . Bargas *et al* (1988) reported that acutely dissociated neostriatal neurones had resting potentials near to -66 mV in 6.25 mM  $[K^+]_{out}$  and -81 mV in 3 mM  $[K^+]_{out}$ .

Measurements of RMP using sharp intracellular microelectrodes (Bargas *et al*, 1988; Jiang & North, 1991) have given more negative values than previous measurements using patch electrodes (Trussell & Jackson, 1985; Freedman & Weight, 1988; Yakel *et al*, 1988; Surmeier *et al*, 1989; Jiang & North, 1991). Dialysis is unlikely to have been a problem with intracellular electrodes since their tip dimensions are extremely small, so stable RMPs would be expected. The authors of patch experiments have reported rapid current run-down; deterioration of the RMP also occurs. In the patch clamp studies it was not specified how soon after entering the whole cell configuration RMP was recorded. The difference in RMP could be accounted for if RMP was measured after it had already declined.

Jiang & North (1991) found that medium spiny (principal) neurones could be distinguished from other (secondary) neurones on the basis of RMP and input resistance. The RMP of principal neurones was -89 mV, the same as in the present study, compared with -60 mV for secondary neurones.

The fast component of cell capacitance ranged between 4-28 pF (mean 12.5 pF). Assuming a specific membrane capacitance of  $1 \mu F \cdot cm^{-2}$  (see e.g. Hille, 1984), these values correspond to spheres with diameters in the range 11-30  $\mu m$  (mean  $n = 20 \mu m$ ). This is almost identical to the range of neuronal diameters encountered in the study. Therefore, it is reasonable to assume that the fast component of capacitance cancelled by the Axopatch controls approximated to the capacitance of the neuronal soma.

### 8.3 Inward rectification and input resistance.

There have been indications from current clamp experiments that neostriatal neurones exhibit inward rectification. The present study showed that the "leak" current either side of the resting potential was, indeed, non-linear and in a direction counter to Constant Field predictions. In fact, inward rectification persisted in symmetrical high  $[K^+]$ . The outward currents, then, cannot strictly be labeled leak currents. Rather, the inward current, and probably the outward current too, result from gated processes.

In their recent paper, Jiang & North (1991) described the inwardly-rectifying currents of rat neostriatal (principal) neurones in a slice preparation in some detail. The inwardly-rectifying currents observed in the present study showed qualitative similarities, but were much smaller. In both studies, the inward current developed rapidly and its magnitude was increased when external  $[K^+]$  was raised. The rectification occurred around  $E_K$  in symmetrical and asymmetrical  $[K^+]$  gradients i.e. the gating as well as the conductance appeared to depend on  $[K]_{out}$ . Jiang & North found the inward current component to be sensitive to  $3 \mu M$  external  $Ba^{2+}$  and identified it as  $K_{IR}$ . It was clearly distinguishable from  $I_H$ , the slowly-developing mixed  $Na^+/K^+$  current, which was a prominent feature of secondary neurones with much less negative resting potentials.

The range of input resistances reported for acutely dissociated or cultured striatal neurones has been remarkably similar in different patch clamp experiments. The values recorded in the present study are in close agreement with those recorded by other experimenters (Trussel & Jackson, 1985; Freedman & Weight, 1988; Yakel et al, 1988). Resistances were typically between 50-1600  $M\Omega$ . Mean resistances were of the order of hundreds of  $M\Omega$ s (e.g. 360  $M\Omega$  in the present study, 700  $M\Omega$  in the Freedman & Weight study). In contrast, the mean input resistance measured for neostriatal principal neurones in intact

slices, using sharp electrodes or patch electrodes, was lower than the lowest value recorded in any culture or dissociated neurone experiment. Jiang & North (1991) reported a value of 39 M $\Omega$  at the resting potential. This compared with a value of 117 M $\Omega$  for secondary cells.

The difference between the medium sized neurones in the present study and those in the Jiang & North study is that the latter retained the extensive arborization normally found *in vivo*. Neurones in their study and the present study displayed identical resting potentials, so the resting  $G_K:G_{Na}$  must be the same. However, the absolute resistance was much smaller for neurones in slices. This implies that a large proportion of the neuronal conductance normally resides in the dendrites and could explain why the currents were smaller in neurones lacking a full complement of processes.

#### **8.4. Whole cell currents.**

##### **8.4.1. Types of current.**

Whole cell currents were recorded at different sampling frequencies. At the highest frequency a rapidly-activating and inactivating inward current could be recorded. This was attributed to sodium influx since it was absent with TTX (a selective blocker of voltage-gated Na<sup>+</sup> channels; Narahashi *et al*, 1964) in the bathing medium. With Cs<sup>+</sup>-containing patch electrodes the reversal potential for this current was almost identical the calculated  $E_{Na}$ . This implies that the channels through which the inward current passed were highly impermeable to Cs<sup>+</sup>.

Transient and sustained outward currents were presumed to have arisen mainly from outward potassium movement. A component of the outward current could have been due to the inactivation of a steady state-inward current. Also, the [Cl<sup>-</sup>] was roughly

symmetrical across the cell membrane, so outward currents could conceivably have resulted from inward  $\text{Cl}^-$  movement through depolarization-activated channels. Patch pipettes contained EGTA to buffer calcium at nanomolar levels. Equilibration of ions occurs rapidly after seal formation (Marty & Neher, 1983) and is essentially complete within tens of seconds. Intracellular  $[\text{Ca}^{2+}]$  was likely, therefore, to have been swiftly clamped at levels lower than those required for activation of the  $\text{Ca}^{2+}$ -sensitive  $\text{K}^+$  conductances described by other authors (Galarraga *et al*, 1989; Pineda *et al*, 1992). M-current activation could have contributed to the outward current but this possibility was not specifically investigated.

#### **8.4.2. Comparison with the currents recorded by others.**

Fast sodium currents have been measured in striatal neurones in two previous patch clamp studies. Freedman & Weight (1988) used unidentified, acutely dissociated adult striatal neurones from the rat. Ogata & Tatebayashi (1990) recorded from acutely dissociated adult medium-sized neurones of the guinea-pig neostriatum. Table 8.1. compares the properties of the sodium currents in these two preparations with those recorded in the present study. The most noticeable difference between the currents of acutely dissociated adult cells and cultured cells is the size of the maximum current. The much smaller current recorded in cultured cells may be attributable to a smaller density of  $\text{Na}^+$  channels in immature neurones.

**Table 8.1.**

Comparison of  $I_{Na}$  recorded in cultured and acutely dissociated striatal neurones. Ogata & Tatebayashi (O & T) recorded currents from a holding potential of -80 mV and their intracellular solution contained high  $[Cs^+]$ ; conditions similar to the present study. Freedman & Weight (F & W) held at -90 mV and used standard intracellular solution containing high  $[K^+]$ . Mean values are presented.

	<u>This study</u>	<u>F &amp; W</u>	<u>O &amp; T</u>
Activation Threshold (mV)	-45	-49	-60
Peak $I_{Na}$ (nA)	0.44	6.0	2.0
Voltage at which peak $I_{Na}$ occurs (mV)	0	-25	-20
Voltage at which reversal occurs (mV)	+75	+35	+60

Slowly-developing, sustained inward currents which persisted in TTX (3  $\mu$ M), Cd<sup>2+</sup> (1 mM) and Ca<sup>2+</sup>-free bathing solutions were occasionally encountered in the present study but were not investigated in detail. These currents bear comparison with the persistent sodium currents reported in hippocampus and neostriatum (French & Gage, 1985; Hoehn *et al*, 1993).

During the course of the present study new papers have appeared describing whole cell potassium currents in cultured and acutely dissociated neostriatal neurones (Surmeier *et al*, 1991 a & b, 1992 a & b; Kitai & Surmeier, 1993). It appears that Surmeier's group was able to perform more stable whole cell recordings on these neurones than was possible in the present study.

A sustained outward current which was activated by depolarization after a delay was only briefly mentioned by these experimenters (Surmeier *et al*, 1988a). It was found to be blocked by 20 mM TEA. This contrasts with the present study in which a considerable proportion of the sustained current remained in 40 mM TEA.

As in the present study, prominent transient outward currents, whose magnitudes increased with more negative holding potentials, could be elicited by depolarization. Surmeier's group were successful in separating the currents into different components. In addition to HVA- and LVA-type A-currents (Surmeier *et al*, 1989), they identified a D-current which emerged during the second to fourth post-natal weeks (Surmeier *et al*, 1991a).

The two different activation curves for transient currents recorded in the present study corresponded closely to those of the HVA and LVA currents of Surmeier *et al* (1991a). There was also a hint of D-type current in this study, showing slow inactivation and slow recovery from inactivation (thousands of milliseconds), but it was small compared with the rapidly-

decaying current and proved impossible to isolate. Like the A-currents recorded by Surmeier's group, HVA and LVA currents were blocked by 4-AP at millimolar concentrations. The voltage-dependence of the block was particularly noticeable and was similar to that described for the A-current of molluscan neurones (Thompson, 1982). Surmeier *et al* (1991a) found the slowly-inactivating currents to be blocked by smaller concentrations of 4-AP than were necessary to block A-currents. In contrast, slowly-decaying currents which persisted in 1 mM 4-AP (figure 6.11.B) were observed in this study.

#### **8.4.3. Summary of whole cell properties.**

Whole cell experiments allowed important properties of cultured neostriatal neurones to be established. Firstly, the RMP is highly negative. Secondly the neurones exhibit inward rectification.

The investigations have also shown that rapidly-activating, transient outward currents are a prominent feature of these neurones and that a large component of the outward current is dependent on the voltage-history of the cell. At the resting potentials encountered in this study, inactivation would be completely removed so all the channels underlying this current would be available for activation. The activation threshold for rapidly-activating outward currents was below that of  $I_{Na}$ . So, they will be important in determining sub-threshold phenomena.

A current having some properties in common with a D-type current (slow decay and prolonged inactivation) may have a role as integrator, allowing successive depolarizations to summate. However, at least a component of the slowly-decaying current was insensitive to concentrations of 4-AP which block the D-current in other tissues.

### **8.5. Single channel currents.**

Protocols were designed to record steady-state channels rather than transient, voltage-activated ones. In the first instance, recordings were carried out at the RMP to see what type of channels were active under "resting" conditions. Channels active at depolarized or hyperpolarized holding potentials were then examined. The smallest channels that could be resolved in this study were in the region of 15 pS.

Using cell-attached and outside-out configurations, it was possible to characterize channels in terms of their conductance, activity patterns (duration of openings and closures), voltage-dependence, presence of sub-states, and sensitivity to blockers included in the patch pipette.

The three most commonly encountered and most easily identifiable channels were of small, large and intermediate conductance. Small and intermediate channels were active over a wide range of potentials including those corresponding to the RMP. Their activity was not voltage-dependent at negative potentials. The largest channel was strongly activated by depolarization.

#### **8.5.1. Selectivity.**

Two pieces of evidence showed that the small, large and intermediate channels with sub-states were not  $\text{Cl}^-$  channels. Firstly, in cell-attached experiments current flow reversed (or was projected to reverse) close to the  $\text{K}^+$  equilibrium potential of 0 mV rather than at the negative  $\text{Cl}^-$  equilibrium potential (-74 mV, assuming an intracellular  $[\text{Cl}^-]$  of 8 mM; Guyton, 1986). Secondly, channel conductance and reversal potential were not obviously different when the  $\text{Cl}^-$  in the recording electrode was replaced by aspartate.

There is little doubt that the channels conducted  $K^+$ , the major cation present in the recording electrode, but could they also conduct  $Na^+$ ? In other words, were they non-selective cation channels? Recordings were made with high  $[K^+]$  in the patch pipette to increase conductance and improve resolution and detection of the channels. In cell-attached patches, the precise ionic gradients are unknown, so it is impossible to make accurate determinations of  $K^+ : Na^+$  selectivity using this configuration. For O/O patches bathed in symmetrical solutions, the reversal potential for all ions was obviously 0 mV, so no information concerning selectivity could be obtained.

Defined, asymmetrical solutions are required to effectively assess selectivity. In the case of the maxi channel, conductance was so large that measurement was possible in O/O patches under asymmetrical  $[K^+]$  conditions. Projected reversal was at negative potentials approaching the  $K^+$  equilibrium potential and far from the positive  $Na^+$  equilibrium potential. An example current-voltage relationship for a maxi channel in asymmetrical conditions was shown in figure 7.3.B. The points were well fitted by the G-H-K equation and the projected reversal potential was close to -97 mV, indicating very high selectivity for  $K^+$  over  $Na^+$ .

The small and intermediate channels were by far the most prevalent channels. It has been difficult to prove that they were selectively permeable to  $K^+$ . These channels did not often pass outward current, and their I-V relationships were curved, so reversal potentials could only be estimated. The errors associated with measuring unitary current (i.e. scatter of points on the I-V plot) meant that it was difficult to estimate reversal potentials with any degree of precision. For these reasons, it was not possible to assess the reversal potential shift in 40 mM external  $K^+$  compared with 140 mM  $K^+$ .

As has been noted in section 8.2., the resting membrane as a whole was highly selective for  $K^+$  over  $Na^+$  so it is more than

likely that the channels active at the RMP were very  $K^+$  selective. Some indication that the channels were, in fact, selective  $K^+$  channels comes from the observation that their conductance was greater in higher external  $[K^+]$ . The conductance of  $K^+$  channels has been found to be dependent upon the  $[K^+]$  bathing their outer face in many other studies.  $K^+$  channels are generally quoted as being 2-3 times smaller in physiological  $[K^+]$  gradients compared with symmetrical high  $[K^+]$ . The  $[K^+]_o$ -dependence of conductance in the present study is very similar to that reported by other authors for a wide variety of  $K^+$  channels (e.g. Freedman & Weight, 1988; Gruol *et al*, 1991). When recorded in 3 mM external  $K^+$ , large and intermediate channel conductances were reduced to approximately 40% of their values in 140 mM  $K^+$ . In 40 mM external  $K^+$ , all three channel conductances were reduced to  $\approx$  65% of their values in 140 mM  $K^+$ .

### 8.5.2. Maxi channel properties.

$\text{Ca}^{2+}$ - and voltage-sensitive maxi  $\text{K}^+$  channels have been thoroughly characterized in many different cell types. They have been described in sympathetic neurones (Smart, 1987), hippocampal neurones (Franciolini, 1988; Lancaster *et al*, 1991; Yoshida *et al*, 1991; Wann & Richards, 1993a), neocortical neurones (Zona & Avoli, 1989) and cerebellar granule cells (Fagni *et al*, 1991) but have not previously been reported in neostriatal neurones. The calcium-sensitivity of the large conductance channel was not assessed in the present study. However, the size of the conductance ( $\approx 250$  pS in symmetrical high  $[\text{K}^+]$  and  $\approx 100$  pS in physiological  $[\text{K}^+]$ ), its  $\text{K}^+$  selectivity and its sigmoidal activation by voltage are sufficient to identify it as the maxi  $\text{K}^+$  channel (Marty, 1983; Latorre & Miller, 1983). Although  $\text{Ca}^{2+}$ -sensitivity of maxi channels in neostriatal neurones has not been assessed, similar channels in cultured hippocampal neurones were found to be activated by  $\text{Ca}^{2+}$  (Wann & Richards, 1992). The lack of channels in patches recorded with 20 mM TEA in the pipette is consistent with the channels being blocked by this drug as is the case in other tissues.

#### 8.5.2.1 Conductance and selectivity.

As has been found in other cells, the I-V relationship was linear in symmetrical  $\text{K}^+$  and channel conductance varied quite widely from patch to patch (range  $\approx 200$ -275 pS). In physiological  $[\text{K}^+]$  gradients the channel conductance was in the region of 100 pS and currents rectified according to the G-H-K equation. The  $P_K$  in neostriatal neurones ( $4.9 \times 10^{-13} \text{ cm}^3 \cdot \text{s}^{-1}$ ) was very similar to that found for maxi channels in neocortical neurones ( $5.2 \times 10^{-13} \text{ cm}^3 \cdot \text{s}^{-1}$ ; Zona & Avoli, 1989) and was slightly greater than in hippocampal neurones ( $3.7 \times 10^{-13} \text{ cm}^3 \cdot \text{s}^{-1}$ ; Wann & Richards, 1993a). The projected reversal potential was close to the  $\text{K}^+$  equilibrium potential, as for maxi channels in other tissues, indicating high  $\text{K}^+$  selectivity.

#### 8.5.2.2. Activity.

Maxi channels were more active in sympathetic neurones (Smart, 1987) than in non-neuronal cells such as muscle (Barrett *et al*, 1982). In the present study maxi channels were always sigmoidally activated by depolarization but they could exist in active or inactive modes (i.e.  $V_h$  varied greatly). Maxi channels reported in the majority of cell types (e.g. Franciolini, 1988; hippocampal neurones) have been similar to the inactive maxi channels in the present study ( $V_h = +4.5$  mV, e-fold change per 23.4 mV for the channel shown in figure 7.7.). However, there have also been reports of much more active channels. For example, Smart (1987) described the maxi channel as being the most active channel type at the RMP and Fagni *et al* (1991) reported an unusually active maxi channel in cerebellar granule cells ( $V_h = -75$  mV, e-fold change per 11 mV c.f. active channels reported in the present study:  $V_h = -55.6$  mV, e-fold change per 23.1 mV).

The channels were sometimes observed to spontaneously switch between modes. Mode-switching behaviour has been reported for maxi channels in cultured rat skeletal muscle (McManus & Magleby, 1988) but the mode transitions were different from the ones observed in this study. McManus & Magleby described brief, temporary departures from normal bursting activity. This behaviour is very different from the permanent "awakening" of initially inactive channels seen in neostriatal neurones.

#### 8.5.2.3. What could account for different activity levels?

The activity mode could be influenced by intracellular messengers. For example, the maxi channel in ventromedial hypothalamic neurones is sensitive to changes in intracellular ATP (Treherne & Ashford, 1991). Recent cloning studies of the *Drosophila* maxi channel (Adelman *et al*, 1992) have revealed a putative ATP-binding site. This raises the possibility that ATP

sensitivity may not be restricted to hypothalamic neurones, but is perhaps a common feature of maxi channels.

Mode switching could be accounted for by sudden changes in the level of intracellular  $\text{Ca}^{2+}$  or other modulators. Maxi channels have been shown to be subject to regulation by arachidonic acid, ANGII, G-proteins and phosphorylation (See Butler *et al*, 1993).

There is also a possibility that maxi channels exist as structurally distinct sub-types having intrinsically different voltage sensitivities. Butler *et al* (1993) showed that several maxi channel variants could result from alternative splicing of a common gene.

#### **8.5.2.4. Priming.**

Maxi channel priming, whereby depolarization permanently shifts the activation curve to more negative potentials, has not been previously described. It is not known by what mechanism such priming or hysteresis takes place. It is difficult to envisage a physiological role for this phenomenon. This finding is not peculiar to neostriatal neurones, however; it also occurs in hippocampal pyramidal neurones (K.T. Wann, personal communication).

#### **8.5.2.5. Functions.**

Yoshida *et al* (1991) demonstrated that maxi channels in cell-attached patches of hippocampal neurones are activated during the "upstroke" of the action potential. They concluded that the kinetic properties of the channels are such that they contribute to action potential repolarization and the generation of fast AHPs. Similar roles for maxi channels in neostriatal neurones is indicated by the fact that TEA, charybdotoxin or  $\text{Ca}^{2+}$

channel blockers retarded action potential repolarization and decreased the amplitude of the fast AHP (Pineda *et al*, 1992).

Smart (1987) found the maxi channel to be the most prevalent channel type at RMP in cultured rat sympathetic neurones. Maxi channels were sometimes active at the RMP in neostriatal neurones in the present study. They obviously play some part in determining the properties of the resting membrane.

### 8.5.3. Properties of the small and intermediate channels.

#### 8.5.3.1. Description.

**Table 8.2.**

**Characteristics of the small and intermediate channels.**

<u>Property</u>	<u>Small</u>	<u>Intermediate</u>
Conductance	27 ± 0.8 pS	130 ± 2.9 pS
Prevalence	85% of patches	47% of patches
Multiples	Up to 8	Up to 6
Voltage-dependence	None	None
Activity	High Long openings Active at RMP	Variable Bursts Active at RMP
Block:		
4-AP	No	No
TEA	No	No
apamin	No	?
Sub-states	?	Yes

The small and intermediate channels could underly inward rectification at the macroscopic level because their single channel I-V relationships were non-linear, conductance being greater at negative potentials. In addition, outward currents were rarely seen, so gating at potentials positive to  $E_K$  could also contribute to rectification. The small channels were of comparable conductance to classical inward rectifiers found in heart cells (Sakmann & Trube, 1984; Matsuda, 1988). It is interesting to note that the intermediate channels exhibited sub-states, a common feature of inwardly-rectifying channels.

#### **8.5.3.2. Comparison with other channels.**

The small and intermediate channels observed in the present study showed some similarities to "resting"  $K^+$  channels in other neurones.

Simonneau *et al* (1987) reported inwardly-rectifying and non-rectifying intermediate conductance channels (symmetrical 140 mM  $K^+$ ) which were active at potentials corresponding to the RMP in cultured mouse DRG cells. 90 pS channels possessing obvious sub-states had a linear I-V relationship at negative potentials but did not pass outward current. A second type of inward rectifier had a conductance in the region of 120 pS, passed outward current, but exhibited strong anomalous rectification at the single channel level. These authors also identified a 120 pS channel which did not rectify and displayed a small degree of activity at the RMP.

A 25 pS channel recorded in cultured rat cerebellar Purkinje neurones (Gruol *et al*, 1991) was voltage-dependent, its activity being greatest at  $\approx +30$  mV, but it was appreciably active at the RMP. Openings occurred in clusters and the channel showed marked inactivation. Resting channels of 14-15 pS were also observed; their openings were of short duration and activity was increased by depolarization.

A 19 pS channel in inside-out patches from cultured rat hippocampal neurones (Lancaster *et al*, 1991) was  $\text{Ca}^{2+}$ -dependent. The channel was insensitive to voltage, was not blocked by TEA or apamin, and its I-V relationship was non-linear. Its conductance and activity (i.e. long openings) were similar to those of the small channel found in neostriatal neurones. The channel was strongly activated by  $\text{Ca}^{2+}$  at negative potentials. If the resting intracellular  $[\text{Ca}^{2+}]$  was sufficiently high to activate such channels, they could contribute to resting  $\text{K}^+$  conductance. Resting channels, which resembled those seen in the present study, were observed in cultured hippocampal neurones (Richards & Wann, 1993; Wann & Richards, 1993b). These authors reported "pedestal" currents in cell-attached patches which were due to long openings of 26 pS  $\text{K}^+$  channels. They also reported two types of intermediate channel (mean conductance  $\approx$  113 pS); one was voltage-independent and the other was activated by depolarization.

Koyano *et al* (1992) reported voltage-independent channels of conductance 115 pS & 26 pS in cultured bullfrog sympathetic ganglion cells. The smaller channel, which they did not describe in detail, was present in multiples and exhibited long openings at the RMP. Activity of the 115 pS channel varied from patch to patch. The channel did not rectify in symmetrical  $\text{K}^+$  solutions but rectified outwardly in accordance with Constant Field predictions. It was activated by muscarinic agonists via an intracellular messenger cascade. The authors likened this channel to ATP-sensitive  $\text{K}^+$  channels (Ashford *et al*, 1988) and 5-HT-sensitive channels in *Aplysia* neurones (Siegelbaum *et al*, 1982).

#### **8.5.4. Resting channels.**

The channels responsible for the resting conductance in neostriatal neurones were probably insensitive to TEA because RMP was unaffected by inclusion of this blocker in the bathing

medium. On the other hand, dialysis of the cells with 140 mM CsCl significantly reduced the RMP suggesting that resting  $K^+$  channels are partially blocked by internal  $Cs^+$ .  $Cs^+$  also reduced the RMP of neostriatal neurones patched in slices (Jiang & North, 1991).

The small and intermediate channels were the most frequently observed channels active at potentials corresponding to the RMP under the present experimental conditions. Maxi channels occasionally exhibited appreciable activity at RMP. The average contribution of each channel type to the resting conductance can be estimated if certain assumptions are made.

Sakmann and Neher (1983b) performed a detailed study to assess the area of the membrane patches that were recorded from in the cell-attached configuration. They calculated that the patch area, when using electrodes with similar dimensions to those employed in the present study, was in the region of  $5 \mu m^2$ .

The mean diameter of the long axis of neurones patched in the present study was  $\approx 16 \mu m$ . A reasonable estimate of the total membrane area can be made by approximating the cells to spheres of equivalent diameter (section 8.2.). In this case, the surface area would be  $\approx 800 \mu m^2$ . The total membrane area would, therefore, be approximately 160 times larger than the patch area. The mean number of small channels per patch was 2.32, so a typical neurone would be expected to possess  $\approx 375$  such channels. By similar reasoning, an average-sized neurone should possess  $\approx 150$  intermediate channels and  $\approx 75$  maxi channels.

The conductance of  $K^+$  channels in physiological  $[K^+]$  gradients is roughly 40% of that in symmetrical 140 mM  $K^+$ . Maxi channels have a conductance of  $\approx 100$  pS. The conductances of intermediate and small channels are estimated to be  $\approx 55$  pS and  $\approx 11$  pS respectively.

The mean contribution of each channel type to the resting conductance (G) would be:

$$G = N_{TOT} \cdot G_{SC} \cdot P_o$$

$N_{TOT}$  = total number of channels per cell

$G_{SC}$  = single channel conductance

$P_o$  = mean open probability.

For the small channels:

$$G = 375 \times 11 \text{ pS} \times 0.59 \\ \approx 2.4 \text{ nS}$$

For the intermediate channels:

$$G = 150 \times 55 \text{ pS} \times 0.36 \\ \approx 3.0 \text{ nS}$$

For an active maxi channel with a  $P_o$  of 0.1 at RMP:

$$G = 75 \times 100 \text{ pS} \times 0.1 \\ \approx 0.75 \text{ nS}$$

The mean input conductance measured in the whole cell configuration was 2.8 nS. This figure is remarkably close to the conductances calculated above. It would seem, therefore, that the small and intermediate channels could account for the major portion of the cell resting conductance. If active at RMP, maxi channels could also make a sizable contribution by virtue of their large conductance.

Judging by the fact that RMP declines during whole cell patch experiments, the resting  $G_K:G_{Na}$  ratio is normally maintained by some diffusible intracellular constituent. Agonists acting to alter the levels of such a constituent could influence cell excitability by altering the resting conductance.

#### **8.6. What phenotype do cultured neurones express?**

It could be argued that cultured neurones are unlikely to develop normally since they are grown for long periods in an unnatural environment without appropriate inputs or target cells. These conditions could lead to arrested development, so that the immature neuronal phenotype persisted, or they could lead to the expression of an abnormal phenotype. Another possibility is the selective survival of a particular sub-set of neurones. (Surmeier *et al*, 1988b). Many electrophysiological properties of cultured cells are very similar to those seen in intact neurones in slices or acutely dissociated adult neurones. Mature and immature neurones exhibit inward currents, A-currents and sustained outward currents. The major differences between cultured neurones and acutely dissociated adult neurones are likely to be simply due to their dissimilar ages. Surmeier *et al* (1991a) showed that neostriatal neurones in culture do not de-differentiate during the first few weeks in culture. The currents recorded from acutely dissociated immature neurones were the same as those recorded from cultured neurones of the same age. This suggests that development in culture may proceed fairly normally. There is much evidence to suggest that normal development in other tissues is dependent upon the presence of appropriate inputs and targets (e.g. Patterson, 1978; Landis, 1985; Purves and Lichtman, 1985). However, extensive intrastriatal connections exist *in vivo* which means that neostriatal neurones are both targets and inputs for other neostriatal neurones. This may render the neurones less dependent on extrastriatal inputs and targets for survival and maturation. (Ramon y Cajal, 1928; Fry and Cowan, 1972; Surmeier *et al*, 1988b).

Neurones require 4 weeks after birth to attain the mature phenotype. During the first 4 post-natal weeks they possess a smaller channel density and are therefore able to generate smaller currents. They are more excitable than adult neurones because the D-current is not yet fully developed (Surmeier *et al*, 1991). In addition their complement of receptors, such as those for dopamine, is incomplete (Pardo *et al*, 1977).

#### **8.7. Actions of ACh and DA on neuronal currents.**

Data from Surmeier's group suggest that the effects of dopamine on medium spiny neurones are excitatory rather than inhibitory. The principal actions of dopamine and ACh may not be to open or close particular  $K^+$  channels but to shift the gating characteristics of voltage-activated conductances. Their experiments on cultured and acutely dissociated neurones showed that ACh shifted both activation and inactivation of transient  $K^+$  conductances to more negative values (Akins *et al*, 1990). DA inhibited a D-type  $K^+$  current (Stefani *et al*, 1990b) and shifted the activation curve for  $I_{Na}$  to more negative values (Surmeier *et al*, 1991b). They concluded (Kitai & Surmeier, 1993) that ACh would act to stabilize neurones whilst dopamine would render them more excitable. These findings are in contrast to those of Freedman & Weight (1988 & 1989). Their observations that DA opens  $K^+$  channels (and therefore has an inhibitory effect on the neurones) is not in agreement with these studies or the present one.

### **8.8. Differences between the results of the present study and those of Freedman & Weight.**

There were notable differences between the patch clamp recordings reported here and those described by Freedman & Weight (1988 & 1989). They used acutely-dissociated, unidentified adult striatal neurones rather than the cultured neostriatal neurones employed in the present study. They reported "no channel openings" at the resting potential in the absence of DA agonists. In this study there were usually many openings of small and intermediate conductance channels when no such agonists were present; depolarization-activated maxi channels were also prominent.

In the present study, the resting potentials recorded under similar ionic conditions were 35 mV more negative than those of Freedman & Weight. The macroscopic currents were smaller in the present study, except for a large A-current which was absent from their recordings. Dopamine or quinpirole, even at high concentrations, did not activate distinct K<sup>+</sup> channels. This does not preclude the possibility that DA-like agonists modified the activity of channels which are already active.

Some of the discrepancies, such as the presence of A-current and the small magnitude of the sodium current, could be explained by the fact that the neurones utilized in the present study were immature. Lack of dopamine sensitivity could have been due to paucity of DA receptors, but it is expected that neurones aged 2-3 weeks would have attained around 40% of their adult complement (Pardo *et al*, 1977), sufficient to generate a response to DA agonists.

Another possible explanation for the disparate results is that Freedman & Weight recorded from a different sub-set of neurones from the ones examined in the present study. Support for this comes from the fact that their neurones also differed from mature neurones investigated by Surmeier's group in that

they did not exhibit D-current, a characteristic feature of the inexcitable principal cells.

The lack of detectable resting channels in Freedman & Weight's neurones cannot be explained by age differences, after all they still exhibit negative RMPs. The very negative RMPs are not a property of immature neurones since adult neurones in slices (Jiang & North, 1991) exhibited equally negative RMPs.

It remains a mystery why Freedman & Weight's neurones, in common with other neurones exhibiting agonist activated  $K^+$  channels (Miyake *et al*, 1989; Einhorn *et al*, 1991), did not display resting channels under similar recording conditions to those employed in the present study. A major difference between this study and the one by Freedman & Weight, which could account for their failure to detect resting channels, is that their dissociation procedure involved the use of tryptic enzymes which may have altered the properties of channel proteins.

### **8.9. Questions.**

The present study raises a number of questions. It would be particularly interesting to see whether the macroscopic inward rectification, the RMP and the single channels are affected by the same blockers (e.g.  $Ba^{2+}$ ). Perhaps the most interesting questions are, what regulates the activity of resting channels, what causes maxi channels to alter their activity state, and could there be a physiological role for priming?

## 9. Conclusions.

The principal neostriatal neurones in culture exhibit electrophysiological properties similar to those in acutely dissociated and slice preparations, although, at the time of patching, cultured neurones express a phenotype which is closer to that of immature neurones than mature ones.

Their resting membrane potential is highly negative, being close to the potassium equilibrium potential. This indicates that the resting membrane is more than 100 times more permeable to  $K^+$  than to  $Na^+$ .

Examination of gross membrane properties indicated prominent inward rectification and the presence of rapidly-activating outward currents which were available for activation at negative potentials but inactivated at more positive potentials.

The channels thought to be largely responsible for the resting potassium conductance and the inwardly-rectifying properties of the membrane have been identified. Small channels with conductance  $\approx 27$  pS and intermediate channels of  $\approx 130$  pS in symmetrical 140 mM  $K^+$  were highly prevalent and were active over a wide range of potentials; their activity showed no voltage-dependence at negative potentials. The intermediate channel exhibited conspicuous sub-conductance states. The I-V relationships of both channels were curved in symmetrical  $K^+$ . Neither channel type was sensitive to 4-AP or TEA, and the small channels were not apamin-sensitive.

A large conductance, maxi channel has also been demonstrated. Its activity was highly voltage-dependent. Open probability increased sigmoidally with depolarization. For this reason it is expected to have a role in action potential repolarization and the generation of afterhyperpolarizations. A previously unreported property, that of maxi channel priming (or hysteresis of voltage-dependent activity), was observed. The

mechanism by which such hysteresis occurs and its physiological significance remain to be determined. Although depolarization always increased maxi channel activity, the level of activity at a particular holding potential varied from patch to patch. In some patches, maxi channels showed a substantial amount of activity at the resting potential and, therefore, contributed to resting  $K^+$  conductance.

The negative RMP and the availability of rapidly-activating, sub-threshold K-currents contributes to the characteristic electrical responses of these neurones. They are well known to fire infrequently and be relatively inexcitable. These properties are pivotal to their function of regulating motor activity. Only when they receive strong, co-ordinated excitatory inputs from associated pre-motor areas are they stimulated sufficiently to fire and cause disinhibition of motor output pathways. Weak or uncorrelated excitatory inputs fail to stimulate firing because the resting potential is far from the sodium current threshold and small depolarizations are opposed by the rapidly-activating, sub-threshold  $K^+$  conductances.

## REFERENCES.

Adams D.J., Nonner W. (1990) Voltage-dependent potassium channels: gating, ion permeation and block. In "Potassium channels: structure, classification, function and therapeutic potential" (ed. Cook N.S.) pp. 40-69. Ellis Horwood Ltd., Chichester, UK.

Adelman J.P., Shen K.-Z., Kavanaugh M.P., Warren R.A., Wu Y.-N., Lagrutta A., Bond C.T., North R.A. (1992) Calcium-activated potassium channels expressed from cloned complementary DNAs. *Neuron* 9, 209-216.

Akaike A., Sasa M., Takaori S. (1988) Muscarinic inhibition as a dominant role in cholinergic regulation of transmission in the caudate nucleus. *J. Pharmacol. Exp. Ther.* 246, 1129-1136.

Akins P.T., Surmeier D.J., Kitai S.T. (1990) Muscarinic modulation of a transient  $K^+$  conductance in rat neostriatal neurons. *Nature* 344, 240-242.

Aquilonius S.-M., Sjostrom R. (1971) Cholinergic and dopaminergic mechanisms in Huntington's chorea. *Life Sci.* 10, 405-414.

Ashcroft F.M., Harrison D.E., Ashcroft S.J.H. (1984) Glucose induces closure of single potassium channels in isolated rat pancreatic  $\beta$ -cells. *Nature* 312, 446-448.

Ashford M.L.J., Boden P.R., Treherne J.M. (1990a) Glucose-induced excitation of rat hypothalamic neurones is mediated by ATP-sensitive potassium channels. *Pflügers Arch.* 415, 479-483.

Ashford M.L.J., Boden P.R., Treherne J.M. (1990b) Tolbutamide excites rat glucoreceptive ventromedial hypothalamic neurones by direct inhibition of ATP- $K^+$  channels. *Br. J. Pharmacol.* 101, 531-540.

Ashford M.L.J., Sturgess N.C., Trout N.J., Gardner N.J., Hales C.N. (1988) Adenosine 5' triphosphate-sensitive ion channels in neonatal rat cultured central neurones. *Pflügers Arch* 412, 297-304.

Barbeau A. (1962) The pathogenesis of Parkinson's disease: a new hypothesis. *Can. Med. Ass. J.* 87, 802-807.

Bargas J., Galarraga E., Aceves J. (1988) Electrotonic properties of neostriatal neurons are modulated by extracellular potassium. *Exp. Brain Res.* 72, 390-398.

Bargas J., Galarraga E., Aceves J. (1989) An early outward conductance modulates the firing frequency of neostriatal neurons of the rat brain. *Exp. Brain Res.* 75, 146-156.

Barrett J.N., Magleby K.L., Pallotta B.S. (1982) Properties of single calcium-activated potassium channels in cultured rat muscle. *J. Physiol. (London)* 331, 211-230.

Benham C.D., Bolton T.B. (1983) Patch-clamp studies of slow potential-sensitive potassium channels in longitudinal smooth muscle cells of rabbit jejunum. *J. Physiol (London)* 340, 469-486.

Benham C.D., Bolton T.B., Lang K.J., Takewaki T. (1985) The mechanisms of action of  $Ba^{2+}$  and TEA on single  $Ca^{2+}$ -activated  $K^+$  channels in arterial and intestinal smooth muscle cell membrane. *Pflügers Arch.* 403, 120-127.

Bernardi G., Floris V., Marciani M.G., Morocutti C., Stanzione P. (1976) The action of acetylcholine and L-glutamic acid on rat caudate neurons. *Brain Res.* 114, 134-138.

Bernstein J. (1902) Untersuchungen zur Thermodynamik der bioelektrischen Ströme. Erster Theil. *Pflügers Arch.* 82, 521-562.

Bernstein J. (1912) *Elektrobiologie*. Viewag, Braunschweig. pp215.

Bishop G.A., Chang H.T., Kitai S.T. (1982) Morphological and physiological properties of neostriatal neurons: an intracellular horseradish peroxidase study in the rat. *Neurosci.* 7, 179-191.

Blatz A.L., Magleby K.L. (1986) Single apamin-blocked Ca-activated K<sup>+</sup> channels of small conductance in rat skeletal muscle. *Nature* 323, 718-720.

Bloom F.E., Costa E., Salmoiraghi G.C. (1965) Anesthesia and the responsiveness of individual neurons of the caudate nucleus of the cat to acetylcholine, norepinephrine and dopamine administered by microelectrophoresis. *J. Pharmacol. Exp. Ther.* 150, 244-252.

Bolam J.P., Wainer B.H., Smith A.D. (1984) Characterization of cholinergic neurons in the rat neostriatum. A combination of choline acetyltransferase immunocytochemistry, Golgi impregnation and electron microscopy. *Neurosci* 12, 711-718.

Bolam J.P., Powell J.F., Wu J.-Y., Smith A.D. (1985) Glutamate decarboxylase-immunoreactive structures in the rat neostriatum: a correlated light and electron microscopic study including a combination of Golgi impregnation with immunocytochemistry. *J. Comp. Neurol.* 237, 1-20.

Brown D.A. (1988) M-currents: an update. *TINS* 11, 294-299.

Brown D.A., Adams P.R. (1980) Muscarinic suppression of a novel voltage-sensitive K<sup>+</sup>-current in a vertebrate neurone. *Nature (London)* 283, 673-676.

Brown J.R., Arbuthnott G.W. (1983) The electrophysiology of dopamine (D<sub>2</sub>) receptors: a study of the actions of dopamine on corticostriatal transmission. *Neurosci.* 2, 349-355.

Buchwald N.A., Price D.D., Vernon L., Hull C.D. (1973) Caudate intracellular response to thalamic and cortical inputs. *Exp. Neurol.* 38, 311-323.

Bülbring E., Tomita T. (1987) Catecholamine action on smooth muscle. *Pharmacol. Rev.* 39, 49-96.

Butcher S.G., Butcher L.L. (1974) Origin and modulation of acetylcholine activity in the neostriatum. *Brain Res.* 71, 161-171.

Butler A., Tsunoda S., McCobb D.P., Wei A., Salkoff L. (1993) mSlo, a complex mouse gene encoding "maxi" calcium-activated potassium channels. *Science* 261, 221-224.

Calabresi P., Mercuri N., Stanzione P., Stefani A., Bernardi G. (1987a) Intracellular studies on the dopamine-induced firing inhibition of neostriatal neurones *in vitro*: evidence for D<sub>1</sub> receptor involvement. *Neurosci.* 20, 757-771.

Calabresi P., Misgeld U., Dodt H.U. (1987b) Intrinsic membrane properties of neostriatal neurons can account for their low level of spontaneous activity. *Neurosci.* 20, 293-303.

Calabresi P., Mercuri N., Stefani A., Bernardi G. (1990a) Synaptic and intrinsic control of membrane excitability of neostriatal neurons. I. An *in vivo* analysis. *J. Neurophysiol.* 63, 651-662.

Calabresi P., Mercuri N., Bernardi G. (1990b) Synaptic and intrinsic control of membrane excitability of neostriatal neurons. II. An *in vitro* analysis. *J. Neurophysiol.* 63, 663-675.

Calne D.B., Langston J.W. (1984) Aetiology of Parkinson's disease. *Lancet* ii, 1457-1459.

Capiod T., Ogden D.C. (1987) The properties of single apamin-sensitive potassium ion channels in guinea-pig hepatocytes. *J. Physiol. (London)* 394, 46P.

Chang H.T. (1988) Dopamine-acetylcholine interaction in the rat striatum: a dual-labeling immunocytochemical study. *Brain Res. Bull.* 21, 295-304.

Chang H.T., Wilson C.J., Kitai S.J. (1982) A Golgi study of rat neostriatal neurons: light microscopic analysis. *J. Comp. Neurol.* 208, 107-126.

Cherubini E., Herrling P.L., Lanfumey L. (1988) Excitatory amino acids in synaptic excitation of rat striatal neurones *in vitro*. *J. Physiol. (London)* 400, 677-690.

Clapham D.E., De Felice L.J. (1984) Voltage-activated K channels in embryonic chick heart. *Biophys. J.* 45, 40-42.

Connor J.A., Stevens C.F. (1971) Voltage clamp studies of a transient outward membrane current in gastropod neural somata. *J. Physiol (London)* 213, 21-30.

Constanti A., Galvan M. (1983) Fast inward-rectifying current accounts for anomalous rectification in olfactory cortex neurones. *J. Physiol. (London)* 335, 153-178.

Conti F., Neher E. (1980) Single channel recordings of K<sup>+</sup> currents in squid axons. *Nature (London)* 285, 140-143.

Cook D.L., Hales C.N. (1984) Intracellular ATP directly blocks K<sup>+</sup> channels in pancreatic B-cells. *Nature* 311, 271-273.

Cooper & Shrier (1985) Single-channel analysis of fast transient potassium currents from rat nodose neurones. *J. Physiol. (London)* 369, 199-208.

De Long M.R. (1972) Activity of basal ganglia neurons during movement. *Brain Res.* 40, 127-135.

De Long M.R. (1973) Putamen: activity of single units during slow and rapid arm movements. *Science Wash. DC.* 179, 1240-1242.

DiFiglia M., Aronin N. (1982) Ultrastructural features of immunoreactive somatostatin neurons in the rat caudate-nucleus. *J. Neurosci.* 2, 1267-1274.

Dotz H.U., Misgeld U. (1986) Muscarinic slow excitation and muscarinic inhibition of synaptic transmission in the rat neostriatum. *J. Physiol.* 380, 593-608.

Dolly J.O., Halliwell J.V., Black J.D., Williams R.S., Pelchen-Matthews A., Breeze A.L., Mehraban F., Othman I.B., Black A.R. (1984) Botulinum neurotoxin and dendrotoxin as probes for studies on neurotransmitter release. *J. Physiol (Paris)* 79, 280-303.

Duvoisin C. (1967) Cholinergic-anticholinergic antagonism in Parkinsonism. *Arch. Neurol.* 17, 124-136.

Einhorn L.C., Gregerson K.A., Oxford G.S. (1991) D<sub>2</sub> dopamine receptor activation of potassium channels in identified rat lactotrophs: whole-cell and single-channel recording. *J. Neurosci.* 11, 3727-3737.

Ewald D.A., Williams A., Levitan I.B. (1985) Modulation of single Ca<sup>2+</sup>-dependent K<sup>+</sup> channel activity by protein phosphorylation. *Nature* 315, 503-506.

Fagni L., Bossu J.L., Bockaert J. (1991) Activation of a large-conductance Ca<sup>2+</sup>-dependent K<sup>+</sup> channel by stimulation of glutamate phosphoinositide-coupled receptors in cultured cerebellar granule cells. *Eu. J. Neurosci.* 8, 778-789.

Feldberg W., Vogt M. (1948) Acetylcholine synthesis in different regions of the central nervous system. *J. Physiol. (London)* 107, 372-381

Findlay I. (1987) The effects of magnesium upon adenosine triphosphate-sensitive potassium channels in a rat insulin-secreting cell line. *J. Physiol. (London)* 391, 611-629.

Forsythe I.D., Westbrook G.L. (1988) Slow excitatory postsynaptic currents mediated by N-methyl-D-aspartate receptors on cultured mouse central neurones. *J. Physiol. (London)* 396, 515-533.

Fox A.P., Nowycky M.C., Tsien R.W. (1987) Single-channel recordings of three types of calcium channels in chick sensory neurones. *J. Physiol (London)* 394, 173-200.

Franciolini F. (1988) Calcium and voltage dependence of single  $\text{Ca}^{2+}$ -activated  $\text{K}^+$  channels from cultured hippocampal neurons of rat. *Biochim. Biophys. Acta* 943, 419-427.

Freedman J.E., Weight F.F. (1988) Single  $\text{K}^+$  channels activated by  $\text{D}_2$  dopamine receptors in acutely dissociated neurons from rat corpus striatum. *Proc. Natl. Acad. Sci. USA.* 85, 3618-3622.

Freedman J.E., Weight F.F. (1989) Quinine potently blocks single  $\text{K}^+$  channels activated by dopamine D-2 receptors in rat corpus striatum neurons. *Eur. J. Pharmacol.* 164, 341-346.

French C.R., Gage P.W. (1985) A threshold sodium current in pyramidal cells in rat hippocampus. *Neurosci. Lett.* 56, 289-293.

Freund T.F., Powell J., Smith A.D. (1984) Tyrosine hydroxylase-immunoreactive boutons in synaptic contact with identified striatonigral neurons, with particular reference to dendritic spines. *Neurosci.* 13, 1189-1215.

Frigyesi T.L., Purpura D.P. (1967) Electrophysiological analysis of reciprocal caudato-nigral relations. Brain Res. 6, 440-456.

Fry F.J., Cowan W.M. (1972) A study of retrograde cell degeneration in the lateral mammillary nucleus of the cat, with special reference to the role of axonal branching in the preservation of the cell. J. Comp. Neurol. 144, 1-24.

Fukushima Y. (1981) Single channel potassium currents of the anomalous rectifier. Nature (London) 294, 368-371.

Fuller D.R.G., Hull C.D., Buchwald N.A. (1975) Intracellular responses of caudate output neurons to orthodromic stimulation. Brain Res. 96, 337-341.

Galarraga E., Bargas J., Aceves J. (1985) Slow sodium and  $I_A$  currents in neostriatal neurons. Soc. Neurosci. Abstr. 11, 202.

Galarraga E., Bargas J., Sierra A., Aceves J. (1989) The role of calcium in the repetitive firing of neostriatal neurons. Exp. Brain Res. 75, 157-168.

Goldman D.E. (1943) Potential, impedance, and rectification in membranes. J. Gen. Physiol. 27, 37-60.

Groves P.M. (1983) A theory of the functional organization of the neostriatum and the neostriatal control of voluntary movement. Brain Res. Rev. 5, 109-132.

Gruol D.L., Jacquin T., Yool A.J. (1991) Single-channel  $K^+$  currents recorded from the somatic and dendritic regions of cerebellar Purkinje neurons in culture. J. Neurosci. 11, 1002-1015.

Grygorczyk R., Schwarz W. (1983) Properties of the  $Ca^{2+}$ -activated  $K^+$  conductance in human red cells as revealed by the patch-clamp technique. Cell Calcium 4, 499-510.

Guyton A.C. (1986) Textbook of medical physiology. Saunders, Philadelphia.

Hagiwara S., Kusano K., Saito N. (1961) Membrane changes of Onchidium nerve cells in potassium-rich media. J. Physiol (London) 155, 470-489.

Halliwel J.V. (1990) K<sup>+</sup> channels in the central nervous system. In "Potassium channels: structure, classification, function and therapeutic potential" (ed. Cook N.S.) pp. 348-381. Ellis Horwood Ltd., Chichester, UK.

Halliwel J.V., Adams P.R. (1982) Voltage-clamp analysis of muscarinic excitation in hippocampal neurones. Brain Res. 250, 71-92.

Halliwel J.V., Othman I.B., Pelchen-Matthews A., Dolley J.O. (1986) Central action of dendrotoxin: selective reduction of a transient K conductance in hippocampus and binding to localized acceptors. Proc. Natl. Acad. Sci. USA. 83, 493-497.

Hamill O.P., Marty A., Neher E., Sakmann B., Sigworth F.J. (1981) Improved patch-clamp techniques for high-resolution current recording from cells and cell-free membrane patches. Pflügers Arch. 391, 85-100.

Hamill O.P., Sakman B. (1981) A cell-free method for recording single channel currents from biological membranes. J. Physiol. (London) 312, 41-42P.

Haylett D.G., Jenkinson D.H. (1990) Calcium-activated potassium channels. In "Potassium channels: structure, classification, function and therapeutic potential" (ed. Cook N.S.) pp. 70-95. Ellis Horwood Ltd., Chichester, UK.

Hermann L. (1872) Grudriss der Physiologie, 4th Ed. Quoted in Hermann L. (1899) Zur Theorie der Erregungsleitung und der elektrischen Erregung. Pflügers Arch. 75, 574-590.

Hille B. (1984) Ionic channels of excitable membranes. Sinauer Associates, Sunderland, Mass., USA.

Hodgkin A.L. (1937) Evidence for electrical transmission in nerve. J. Physiol. (London). 90, 183-232.

Hodgkin A.L., Huxley A.F. (1952) Currents carried by sodium and potassium ions through the membrane of the giant axon of Loligo. J. Physiol. (London). 116, 449-472.

Hodgkin A.L., Katz B. (1949) The effect of sodium ions on the electrical activity of of the giant axon of the squid. J. Physiol. (London). 108, 37-77.

Hoehn K., Watson T.W.J., MacVicar B.A. (1993) A novel tetrodotoxin-insensitive, slow sodium current in striatal and hippocampal neurons. Neuron 10, 543-552.

Horie M., Irisawa H., Noma A. (1987) Voltage-dependent magnesium block of adenosine-triphosphate-sensitive potassium channel in guinea-pig ventricular cells. J. Physiol. (London) 387, 251-272.

Horn R., Patlak J.B. (1980) Single channel currents from excised patches of muscle membrane. Proc. Natl. Acad. Sci. USA. 77, 6930-6934.

Hornykiewicz O. (1966) Dopamine (3-hydroxytryptamine) and brain function. Pharmacol. Rev. 18, 925-964.

Hornykiewicz O. (1973) Dopamine in the basal ganglia. Its role and therapeutic implications (including the clinical use of L-DOPA). Br. Med. Bull. 29, 172-178.

Hull C.D., Bernardi G., Buchwald N.A. (1970a) Intracellular responses of caudate neurons to brain stem stimulation. Brain Res. 22, 163-179.

Hull C.D., Bernardi G., Price D.D., Buchwald N.A. (1973) Intracellular responses of caudate neurons to temporally and spatially combined stimuli. *Exp. Neurol.* 38, 324-336.

Hull C.D., Levine M.S., Buchwald N.A., Heller A., Browning R.A. (1970b) The spontaneous firing pattern of forebrain neurons. I. The effects of dopamine and non-dopamine depleting lesions on caudate firing patterns. *Brain Res.* 73, 241-262.

Inoue M., Nakajima S., Nakajima Y. (1988) Somatostatin induces an inward rectification in rat locus coeruleus neurones through a pertussis toxin-sensitive mechanism. *J. Physiol. (London)* 407, 177-198.

Israel J.M., Jaquet P., Vincent J.-D. (1985) The electrical properties of isolated human prolactin-secreting adenoma cells and their modification by dopamine. *Endocrinology*, 117, 1448-1455.

Izzo P.N., Bolam J.P. (1988) Cholinergic synaptic input to different parts of spiny striatonigral neurons in the rat. *J. Comp. Neurol.* 269, 219-234.

Jacquin T., Champagnat J., Madamba S., Denavit-Saubie M., Siggins G.R. (1988) Somatostatin depresses excitability in neurons of the solitary tract complex through hyperpolarization and augmentation of  $I_M$ , a non-inactivating voltage-dependent outward current blocked by muscarinic agonists. *Proc. Natl. Acad. Sci. USA.* 85, 948-952.

Jiang Z.-G., North R.A. (1991) Membrane properties and synaptic responses of rat striatal neurones *in vitro*. *J. Physiol (London)* 443, 533-553.

Jiang Z.G., North R.A. (1992) Pre- and post-synaptic inhibition by opioids in rat striatum. *J. Neurosci.* 12, 356-361.

Kasai H., Kameyam D., Yamaguchi K., Fukuda J. (1986) Single transient K channels in mammalian sensory neurons. *Biophys. J.* 49, 1243-1247.

Kawaguchi Y., Wilson C.J., Emson P.C. (1989) Intracellular recording of identified neostriatal patch and matrix spiny cells in a slice preparation preserving cortical inputs. *J. Neurophysiol.* 62, 1052-1068.

Kimura H., McGeer P.L., Peng J.H., McGeer E.G. (1980) The central cholinergic system studied by choline acetyltransferase immunohistochemistry in the cat. *J. Compar. Neurol.* 200, 151-201.

Kita H., Kita T., Kitai S.T. (1985a) Active membrane properties of rat neostriatal neurons in an *in vitro* slice preparation. *Exp. Brain Res* 60, 54-62.

Kita H., Kita T., Kitai S.T. (1985b) Regenerative potentials in rat neostriatal neurons in an *in vitro* slice preparation. *Exp. Brain Res* 60, 63-70.

Kita H., Kitai S.T. (1988) Glutamate decarboxylase immunoreactive neurons in rat neostriatum: their morphological types and populations. *Brain Res.* 447, 346-352.

Kita T., Kita H., Kitai S.T. (1984) Passive electrical membrane properties of rat neostriatal neurons in an *in vitro* slice preparation. *Brain Res* 300, 129-139.

Kitai S.T., Kocsis J.D., Preston R.J., Sugimori M. (1976) Monosynaptic inputs to caudate neurons identified by intracellular injection of horseradish peroxidase. *Brain Res.* 109, 601-606.

Kitai S.T., Surmeier D.J. (1993) Cholinergic and dopaminergic modulation of potassium conductances in neostriatal neurons. *Adv. Neurol.* 60, 40-52.

Kitai S.T., Wagner A., Precht W., Ohno T. (1975) Nigro-caudate and caudato-nigral relationship: an electrophysiological study. *Brain Res.* 85, 44-48.

Kitai S.T., Surmeier D.J., Stefani A. (1990) Dopaminergic modulation of voltage-dependent potassium conductances in rat neostriatal neurons. *Soc. Neurosci. Abstr.* 16, 418.

Kocsis J.D., Kitai S.T. (1977a) Dual excitatory inputs to caudate spiny neurons from substantia nigra stimulation. *Brain Res.* 138, 271-283.

Kocsis J.D., Sugimori M., Kitai S.T. (1977b) Convergence of excitatory synaptic inputs to caudate spiny neurons. *Brain Res.* 124, 403-413.

Koyano K., Tanaka K., Kuba K. (1992) A patch-clamp study on the muscarine-sensitive potassium channel in bullfrog sympathetic ganglion cells. *J. Physiol. (London)* 454, 231-246.

Kurachi Y., Nakajima T., Sugimoto T. (1986) On the mechanism of activation of muscarinic K<sup>+</sup> channels by adenosine in isolated atrial cells: involvement of GTP-binding proteins. *Pflügers Arch.* 407, 264-274.

Lacey M.G., Mercuri N.B., North R.A. (1987) Dopamine acts on D<sub>2</sub> receptors to increase potassium conductance in neurones of the rat substantia nigra zona compacta. *J. Physiol.* 392, 397-416.

Lancaster B., Nicoll R.A., Perkel D.J. (1991) Calcium activates two types of potassium channel in rat hippocampal neurones in culture. *J. Neurosci.* 11, 23-30.

Landis S.C. (1985) Environmental influences on the development of sympathetic neurons. In "Cell culture in the neurosciences" (Ed. Bottenstein J., Sato, G.). pp 170-192. Plenum, New York, USA.

Lang D.G., Ritchie A.K. (1988) Pharmacological sensitivities of large and small conductance  $\text{Ca}^{2+}$ -activated  $\text{K}^+$  channels. *Biophys. J.* 53, 144a.

Lang D.G., Ritchie A.K. (1990) Tetraethylammonium blockade of apamin-sensitive and insensitive  $\text{Ca}^{2+}$ -activated  $\text{K}^+$  channels in a pituitary cell line. *J. Physiol.* 425, 117-132.

Latorre R., Miller C. (1983) Conduction and selectivity in potassium channels. *J. Membrane Biol.* 71, 11-30.

Latorre R., Oberhauser A., Labarca P., Alvarez O. (1989) Varieties of calcium-activated potassium channels. *Ann. Rev. Physiol.* 51, 385-399.

Lehman J., Langer S.Z. (1983) The striatal cholinergic interneuron: synaptic target of dopaminergic terminals? *Neurosci.* 10, 1105-1120.

Lynch G., Smith R.L., Robertson R.T. (1973) Direct projections from brainstem to telencephalon. *Exp. Brain Res.* 17, 221-228.

Malenka R.C., Kocsis J.D. (1988) Presynaptic actions of carbachol and adenosine on corticostriatal synaptic transmission studied *in vitro*. *J. Neurosci.* 8, 3750-3756.

Marco L.A., Copack P., Edelson A.M. (1973) Intrinsic connections of caudate neurons. Locally evoked intracellular responses. *Exp. Neurol.* 40, 683-698.

Marty A. (1981) Ca-dependent potassium channels with large unitary conductance in chromaffin cell membranes. *Nature* 291, 497-500.

Marty A. (1983)  $\text{Ca}^{2+}$  dependent  $\text{K}^+$  channels with large unitary conductance. *TINS* 6, 262-265.

Marty A., Neher E. (1983) Tight-seal whole-cell recording. In "Single channel recording". (ed. Sakmann B., Neher E.) pp. 107-122. Plenum Press, New York, USA.

Masuko S., Nakajima Y., Nakajima S., Yamaguchi K. (1986) Noradrenergic neurons from the locus coeruleus in dissociated cell culture: culture methods, morphology and electrophysiology. J. Neurosci. 6, 3229-3241.

Matsuda H. (1988) Open-state substructure of inwardly rectifying potassium channels revealed by magnesium block in guinea-pig heart cells. J. Physiol. (London) 397, 237-258.

Maue R.A., Dionne V.E. (1987) Patch clamp studies of isolated mouse olfactory receptor neurons. J. Gen. Physiol. 90, 95-125.

McGeer P.L., Boulding J.E., Gibson W.C., Foulkes R.G. (1961) Drug-induced extrapyramidal reactions. J. Am. Med. Ass. 177, 665-670.

McGeer P.L., McGeer E.G., Fibiger H.C., Wickson V. (1971) Neostriatal choline acetylase and cholinesterase following selective lesions. Brain Res. 35, 308-314.

McLarnon J.G. (1989) Properties of single potassium channels in hypothalamic neurons. Pflügers Arch. 413, 604-609.

McLennan H., York D.H. (1966) Cholinergic mechanisms in the caudate nucleus. J. Physiol. (London) 187, 163-175.

McManus O.B., Magleby K.L. (1988) Kinetic states and modes of single large-conductance calcium-activated potassium channels in cultured rat skeletal muscle. J. Physiol. (London) 402, 79-120.

Mercuri N., Bernardi G., Calabresi P., Cotugno A., Levi G., Stanzione P. (1985) Dopamine decreases cell excitability in rat striatal neurones by pre- and post-synaptic mechanisms. *Brain Res.* 358, 110-121.

Miller C., Moczydlowski E., Latorre R., Phillips M. (1985) Charybdotoxin, a protein inhibitor of single  $\text{Ca}^{2+}$ -activated  $\text{K}^{+}$ -channels from mammalian skeletal muscle. *Nature (London)* 313, 316-318.

Miller J.J., Richardson T.L., Fibiger H.C., McLennan H. (1975) Anatomical and electrophysiological identification of a projection from the mesencephalic raphe to the caudate-putamen in the rat. *Brain Res.* 97, 133-138.

Misgeld U., Frotscher M., Wagner A. (1984) Identification of projecting neurons in rat neostriatal slices. *Brain Res.* 299, 367-370.

Miyake M., MacDonald J.C., North R.A. (1989) Single potassium channels opened by opioids in rat locus ceruleus neurons. *Proc. Natl. Acad. Sci. USA.* 86, 3419-3422.

Moore S.D., Madamba S.G., Joels M., Siggins G.R. (1988) Somatostatin augments the M-current in hippocampal neurons. *Science* 239, 278-280.

Nabatame H., Sasa M., Takaori S., Kameyama M. (1988) Muscarinic receptor-mediated inhibition of dopaminergic excitatory input to caudate neurons from the substantia nigra. *Jpn. J. Pharmacol.* 46, 387-395.

Narahashi T., Moore J.W., Scott W.R. (1964) Tetrodotoxin blockage of sodium conductance increase in lobster giant axons. *J. Gen. Physiol.* 47, 965-972.

Nauta W.J., Pritz M.B., Lasek R.J. (1974) Afferents to the caudato-putamen studied with horseradish peroxidase. An evaluation of a retrograde neuroanatomical research method. *Brain Res.* 67, 219-238.

Neher E. (1971) Two transient current components during voltage clamp in snail neurons. *J. Gen. Physiol.* 61, 385-399.

Neher E. (1981) Unit conductance studies in biological membranes. In "Techniques in cellular physiology" (Ed. Baker P.F.). Elsevier/North Holland, Amsterdam.

Neher E., Sakmann B. (1976) Single channel currents recorded from membrane of denervated frog muscle fibres. *Nature* 268, 799-802.

Neher E., Sakmann B., Steinbach J.H. (1978) The extracellular patch clamp: A method for resolving currents through individual open channels in biological membranes. *Pflügers Arch.* 375, 219-228.

Nernst W. (1888) Zur Kinetik der Lösung befindlichen Körper: Theorie der Diffusion. *Z. Phys. Chem.* 613-673.

Niki H., Sakai M., Kubota K. (1972) Delayed alternation performance and unit activity of the caudate head and medial orbitofrontal gyrus in the monkey. *Brain Res.* 38, 343-353.

Noma A. (1983) ATP-regulated K<sup>+</sup> channels in cardiac muscle. *Nature* 305, 147-148.

Numann R.E., Wadman W.J., Wong R.K.S. (1987) Outward currents of single hippocampal cells obtained from the adult guinea-pig. *J. Physiol (London)* 393, 331-353.

Ogata N., Tatebayashi H. (1990) Sodium current kinetics in freshly isolated neostriatal neurones of the adult guinea pig. *Pflügers Arch.* 416, 594-603.

Ohmori H., Yoshida S., Hagiwara S. (1981) Single K<sup>+</sup> channel currents of anomalous rectification in cultured rat myotubes. Proc. Natl. Acad. Sci. USA. 78, 4960-4964.

Pardo J.V., Creese I., Burt D.R., Snyder S.H. (1977) Ontogenesis of dopamine receptor binding in the corpus striatum of the rat. Brain Res. 125, 376-382.

Park M.R., Lighthall J.W., Kitai S.T. (1980) Recurrent inhibition in the rat neostriatum. Brain Res. 194, 359-369.

Patterson P. (1978) Environmental determination of autonomic neurotransmitter functions. Annu. Rev. Neurosci. 1, 1-17.

Phelps P.E., Houser C.R., Vaughn J.E. (1985) Immunocytochemical localization of choline acetyltransferase within the rat neostriatum: a correlated light and electron microscopic study of cholinergic neurons and synapses. J. Comp. Neurol. 238, 286-307.

Pineda J.C., Galarraga E., Bargas J., Cristancho M., Aceves J. (1992) Charybdotoxin and apamin sensitivity of the calcium-dependent repolarization and the afterhyperpolarization in neostriatal neurons. J. Neurophysiol. 68, 287-294.

Premkumar L.S., Chung S.H., Gage P.W. (1990) Coupled potassium channels induced by arachidonic acid in cultured neurons. Proc. R. Soc. London Ser. B. 241, 153-158.

Purpura P.D., Malliani A. (1967) Intracellular studies of the corpus striatum. I. Synaptic potentials and discharge characteristics of caudate neurons activated by thalamic stimulation. Brain Res. 6, 325-340.

Purves D., Lichtman J.W. (1985) Principles of neural development. Sinauer, Sunderland, Mass., USA.

Ramon y Cajal S. (1928) In "Degeneration and regeneration of the nervous system" (Ed. May R.M.). Haffner, New York, USA.

Richards C.D., Wann K.T. (1993) Single channel currents operating at the resting membrane potential of rat hippocampal neurones maintained in culture. J. Physiol. (London) 467, 248P.

Robertson R.T., Travers J.B. (1975) Brain stem projections to the striatum: experimental morphological studies in the rat. Exp. Neurol. 48, 447-459.

Roeper J., Hainsworth A.H., Ashcroft F.M. (1990) Tolbutamide reverses membrane hyperpolarisation induced by activation of D<sub>2</sub> receptors and GABA<sub>B</sub> receptors in isolated substantia nigra neurones. Pflügers Arch. 416, 473-475.

Rogawski M.A. (1985) The A-current: how ubiquitous a feature of excitable cells is it? TINS May, 214-219.

Rogawski M.A. (1986) Single voltage-dependent potassium channels in cultured rat hippocampal neurons. J. Neurophysiol. 56, 481-493.

Rudy B. (1988) Diversity and ubiquity of K channels. Neurosci. 25, 729-749.

Sakmann B., Neher E. (1983a) Single channel recording. Plenum Press, New York, USA.

Sakmann B., Neher E. (1983b) Geometric parameters of pipettes and membrane patches. In "Single channel recording". (ed. Sakmann B., Neher E.) pp. 37-51. Plenum Press, New York, USA.

Sakmann B., Noma A., Trautwein W. (1983) Acetylcholine activation of single muscarinic K<sup>+</sup> channels in isolated pacemaker cells of mammalian heart. Nature (London) 303, 250-253.

Sakmann B., Trube G. (1984) Conductance properties of single inwardly rectifying potassium channels in ventricular cells from guinea-pig heart. *J. Physiol. (London)* 347, 641-657.

Salkoff L., Wyman R. (1981) Genetic modification of potassium channels in *Drosophila* Shaker mutants. *Nature (London)* 293, 228-230.

Siegelbaum S.A., Camardo J.S., Kandel E.R. (1982) Serotonin and cyclic AMP close single K<sup>+</sup> channels in *Aplysia* sensory neurones. *Nature* 299, 413-417.

Sigworth F.J., Neher E. (1980) Single Na<sup>+</sup> channel currents observed in cultured rat muscle cells. *Nature* 287, 447-449.

Simonneau M., Distasi C., Tauc L., Barbin G. (1987) Potassium channels in mouse neonate dorsal root ganglion cells: a patch-clamp study. *Brain Res.* 412, 224-232.

Smart T.G. (1987) Single calcium-activated potassium channels recorded from cultured rat sympathetic neurones. *J. Physiol. (London)* 389, 337-360.

Soejima M., Noma A. (1984) Mode of regulation of the ACh-sensitive K-channel by the muscarinic receptor in rabbit atrial cells. *Pflügers Arch.* 400, 424-431.

Sole C.K., Zagotta W.N., Aldrich R.W. (1987) Single-channel and genetic analyses reveal two distinct A-type potassium channels in *Drosophila*. *Science* 236, 1094-1098.

Spehlmann R. (1975) The effects of acetylcholine and dopamine on the caudate nucleus depleted of biogenic amines. *Brain Res.* 98, 219-230.

Spruce A.E., Standen N.B., Stanfield P.R. (1985) Voltage-dependent ATP-sensitive potassium channels of skeletal muscle membrane. *Nature* 316, 736-738.

Standen N.B., Quayle J.M., Davies N.W., Brayden J.E., Huang Y., Nelson M.T. (1989) Hyperpolarizing vasodilators activate ATP-sensitive K<sup>+</sup> channels in arterial smooth muscle. *Science* 245, 177-180.

Standen N.B., Stanfield P.R., Ward T.A. (1985) Properties of single potassium channels in vesicles formed from the sarcolemma of frog skeletal muscle. *J. Physiol. (London)* 364, 339-358.

Stanfield P.R., Nakajima Y., Yamaguchi K. (1985) Substance P raises neuronal excitability by reducing inward rectification. *Nature (London)* 315, 498-501.

Stefani A., Surmeier D.J., Kitai S.T. (1990a) Properties of a voltage-dependent chloride current in rat neostriatal neurons. *Soc. Neurosci. Abstr.* 16, 418.

Stefani A., Surmeier D.J., Kitai S.T. (1990b) Serotonin enhances excitability in neostriatal neurons by reducing voltage-dependent potassium currents. *Brain Res.* 529, 354-357.

Stoof J.C., Drukarch B., De Boer P., Westerink B.H.C., Groenewegen H.J. (1992) Regulation of the activity of striatal cholinergic neurons by dopamine. *Neurosci.* 47, 755-770.

Storm J.F. (1987) Action potential repolarization and fast after-hyperpolarization in rat hippocampal pyramidal cells. *J. Physiol (London)* 385, 733-759.

Storm J.F. (1988) Temporal integration by a slowly inactivating K<sup>+</sup> current in hippocampal neurons. *Nature* 336, 379-381.

Sturgess N.C., Ashford M.L.J., Cook D.L., Hales C.N. (1985) The sulphonylurea receptor may be an ATP-sensitive K<sup>+</sup> channel. *Lancet* ii, 474-475.

Sugimori M., Preston R.I., Kitai S.T. (1978) Response properties and electrical constants of caudate nucleus neurons in the cat. *J. Neurophysiol.* 41, 1662-1675.

Surmeier D.J., Bargas J., Kitai S.T. (1988a) Voltage-clamp analysis of a transient potassium current in rat neostriatal neurons. *Brain Res.* 437, 187-192.

Surmeier D.J., Eberwine J., Wilson C.J., Cao Y., Stefani A., Kitai S.T. (1992a) Dopamine receptor subtypes colocalize in rat striatonigral neurons. *Proc. Natl. Acad. Sci. USA.* 89, 10178-10182.

Surmeier D.J., Kita H., Kitai S.T. (1988b) The expression of  $\Gamma$ -aminobutyric acid and Leu-enkephalin immunoreactivity in primary monolayer cultures of rat striatum. *Dev. Brain Res.* 42, 265-282.

Surmeier D.J., Bargas J., Kitai S.T. (1989) Two types of A-current differing in voltage-dependence are expressed by neurons of the rat neostriatum. *Neurosci. Lett.* 103, 331-337.

Surmeier D.J., Stefani A., Foehring R.C., Kitai S.T. (1991a) Developmental regulation of a slowly-inactivating potassium conductance in rat neostriatal neurons. *Neurosci. Letts.* 122, 41-46.

Surmeier D.J., Stefani A., Wilson C., Kitai S.T. (1991b) Dopaminergic modulation of sodium currents in retrogradely identified strionigral neurons of the rat. *Soc. Neurosci. Abstr.* 17, 851.

Surmeier D.J., Xu Z.C., Wilson C.J., Stefani A., Kitai S.T. (1992b) Grafted neostriatal neurons express a late-developing transient potassium current. *Neurosci.* 48, 849-856.

Tagaki M., Yamamoto C. (1978) Suppressing action of cholinergic agents on synaptic transmissions in the corpus striatum of rats. *Exp. Neurol.* 62, 433-443.

Thompson S. (1982) Aminopyridine block of transient potassium current. *J. Gen. Physiol.* 80, 1-17.

Thompson S.H. (1977) Three pharmacologically distinct potassium channels in molluscan neurones. *J. Physiol. (London)* 265, 465-488.

Treherne J.M., Ashford M.L.J. (1991) Calcium-activated potassium channels in rat dissociated ventromedial hypothalamic neurones. *J. Neuroend.* 3, 323-329.

Trube G., Sakmann B., Trautwein W. (1981) Inwardly rectifying potassium currents recorded from isolated heart cells by the patch clamp method. *Pflügers Arch.* 391, R28.

Trube G., Rorsman P., Ohno-Shosaku T. (1986) Opposite effects of tolbutamide and diazoxide on the ATP-dependent K<sup>+</sup> channel in mouse pancreatic  $\beta$ -cells. *Pflügers Arch.* 407, 493-499.

Trussel L.O., Jackson M.B. (1985) Adenosine-activated potassium conductance in cultured striatal neurones. *Proc. Natl. Acad. Sci. USA.* 82, 4857-4861.

Uchimura N., Cherubini E., North R.A. (1989) Inward rectification in rat nucleus accumbens neurons. *J. Neurophysiol.* 62, 1280-1286.

Vandermaelen C.P., Kocsis J.D., Kitai S.T. (1978) Caudate afferents from the retrorubal nucleus and other midbrain areas in the cat.

Van Dongen A.M.J., Codina J., Olate J., Mattera R., Joho R., Birnbaumer L., Brown A.M. (1988) Newly identified brain potassium channels gated by the guanine nucleotide binding protein G<sub>o</sub>. *Science* 242, 1433-1437.

Walters J.R., Bergstrom D.A., Carlson J.H., Weick B.G., Pan H.S. (1987) Stimulation of D-1 and D-2 dopamine receptors: synergistic effects on single unit activity in basal ganglia output nuclei. In "Neurophysiology of dopaminergic systems-current status and perspectives" (ed. Chiodo L.A., Freedman A.S) pp. 285-316. Lakeshore Publishing Co., Grosse Pointe.

Wann K.T. (1993) Neuronal sodium and potassium channels: structure and function. *Br. J. Anaesth.* 71, 2-14.

Wann K.T., Richards C.D. (1992) Properties of a large conductance potassium channel in rat hippocampal neurones maintained in culture. *J. Physiol. (London)* 452, 192P.

Wann K.T., Richards C.D. (1993a) Properties of single calcium-activated potassium channels of large conductance in rat hippocampal neurones in culture. *Eu. J. Neurosci.* (in press).

Wann K.T., Richards C.D. (1993b) Patch clamp analysis of the properties of a small conductance channel open at the resting membrane potential of rat hippocampal neurones. *Eu. J. Neurosci.* (in press).

Williams J.T., Colmers W.F., Pan Z.Z. (1988) Voltage- and ligand-activated inwardly rectifying currents in dorsal raphe neurons *in vitro*. *J. Neurosci.* 8, 3499-3506.

Wilson C.J., Chang H.T., Kitai S.T. (1982) Origins of postsynaptic potentials evoked in identified rat neostriatal neurons by stimulation in substantia nigra. *Exp. Brain Res.* 51, 217-226.

Wilson C.J., Chang H.T., Kitai S.T. (1983a) Origins of postsynaptic potentials evoked in spiny neostriatal projection neurons by thalamic stimulation in the rat. *Exp. Brain Res.* 51, 217-226.

Wilson C.J., Chang H.T., Kitai S.T. (1983b) Disfacilitation and long-lasting inhibition of neostriatal neurons in the rat. *Exp. Brain Res.* 51, 227-253.

Wilson C.J., Chang H.T., Kitai S.T. (1990) Firing patterns and synaptic potentials of identified giant aspiny interneurons in the rat striatum. *J. Neurosci.* 10, 508-519.

Wilson C.J., Groves P.M. (1981) Spontaneous firing patterns of identified spiny neurons in the rat neostriatum. *Brain Res.* 220, 67-80.

Wong B.S., Lecar H, Adler M. (1982) Single calcium-dependent potassium channels in clonal anterior pituitary cells. *Biophys. J.* 39, 313-317.

Wolf N.J., Butcher, L.L. (1981) Cholinergic neurons in the caudate-putamen complex proper are intrinsically organized: a combined Evans blue and acetylcholinesterase analysis. *Brain Res. Bull.* 7, 487-507.

Yakel J.L., Trussel L.O., Jackson M.B. (1988) Three serotonin responses in cultured mouse hippocampal and striatal neurons. *J. Neurosci.* 8, 1273-1285.

Yatani A., Codina J., Sekura R.D., Birnbaumer L., Brown A.M. (1987) Reconstitution of somatostatin and muscarinic receptor mediated stimulation of K<sup>+</sup> channels by isolated GK protein in clonal rat anterior pituitary cell membranes. *Mol. Endocrinol.* 1, 283-289.

Yoshida A., Oda M., Ikemoto Y. (1991) Kinetics of the  $\text{Ca}^{2+}$ -activated  $\text{K}^+$  channel in rat hippocampal neurones. Jap. J. Physiol. 41, 297-315.

Zbicz K.L., Weight F.F. (1985) Transient voltage and calcium-dependent outward currents in hippocampal CA3 pyramidal neurons. J. Neurophysiol. 53, 1038-1058.

Zona C., Avoli M. (1989) Calcium-activated potassium channels recorded from rat neocortical neurons in cell culture. Neurosci. Lett. 102, 223-228.

MEDICAL LIBRARY  
ROYAL FREE HOSPITAL  
HAMPSTEAD.